Bio-based sustainable polymers and materials: from processing to biodegradation.

OKOLIE, O., KUMAR, A., EDWARDS, C., LAWTON, L.A., OKE, A., MCDONALD, S., THAKUR, V.K. and NJUGUNA, J.

2023

Journal of
Composites Science

MDPI

Review

Bio-Based Sustainable Polymers and Materials: From Processing to Biodegradation

Obinna Okolie [1], Anuj Kumar [2], Christine Edwards [3], Linda A. Lawton [3], Adekunle Oke [4], Seonaidh McDonald [5], Vijay Kumar Thakur [6] and James Njuguna [1,*]

[1] Advanced Materials Research Group, School of Engineering, Robert Gordon University, Sir Ian Wood Building, Aberdeen AB10 7GJ, UK
[2] School of Chemical Engineering and Department of Nano, Medical and Polymer Materials, Yeungnam University, Gyeongsan 38541, Republic of Korea
[3] School of Pharmacy and Life Sciences, Sir Ian Wood Building, Garthdee Road, Aberdeen AB10 7QB, UK
[4] Leeds Business School, Leeds Beckett University, 503 Rose Bowl, City Campus, Leeds LS1 3HL, UK
[5] Innovate UK, UK Research & Innovation, Polaris House, Swindon SN2 1FL, UK
[6] Biorefining and Advanced Materials Research Centre, Scotland's Rural College (SRUC), Peter Wilson Building, The King's Buildings, West Mains Road, Edinburgh EH9 3JG, UK
* Correspondence: j.njuguna@rgu.ac.uk; Tel.: +44-(0)-1224262304

Abstract: In the life cycle of a material, there will be either chemical or physical change due to varying environmental factors such as biological activity, light, heat, moisture, and chemical conditions. This process leads to polymer property change as pertains to functional deterioration because of the physical, biological, and chemical reactions that result in chemical transformations and bond scission and thus can be regarded as polymer degradation. Due to the present demand for sustainable polymers, bio-based polymers have been identified as a solution. There is therefore a need to compare the sustainability impacts of bio-based polymers, to maximize their use in functional use stage and still withhold the bio-degradation capability. This study focuses are poly (lactic acid) (PLA), Poly (ε-caprolactone) (PCL), polyhydroxyalkanoates (PHA), and polyamides (PA) as biopolymers of interest due to their potential in technological applications, stability, and biodegradability. For preparing bio-based value-added products, an appropriate selection of the fabrication or functional modification process is a very important factor for particular industrial or biomedical applications. The literature review indicates that in vivo is preferred to in vitro because it suits an overall study of the experiment's effects on a living subject. This study will explore these features in detail. In particular, the review will cover processing and biodegradation pathways for each of the biopolymers. In addition, thermal degredation and photodegradation are covered, and future trends and conclusions are drawn.

Keywords: bio-based polymers; biodegradation; environment; photodegradation; polymerization; thermal degradation

Citation: Okolie, O.; Kumar, A.; Edwards, C.; Lawton, L.A.; Oke, A.; McDonald, S.; Thakur, V.K.; Njuguna, J. Bio-Based Sustainable Polymers and Materials: From Processing to Biodegradation. *J. Compos. Sci.* **2023**, 7, 213. https://doi.org/10.3390/jcs7060213

Academic Editor: Francesco Tornabene

Received: 21 January 2023
Revised: 31 March 2023
Accepted: 7 April 2023
Published: 24 May 2023

1. Introduction

The proliferation and persistence of plastic waste in the environment have attracted the attention of many commentators [1], promoting innovations in the production of plastic materials many of which can be degraded biologically. Despite the ongoing innovations for the plastic industry to be green [2,3], consumers are more confused about the sustainability potential of plastic products, possibly due to the lack of clarity in terminology. Biopolymers, which are sourced from living organisms, have been identified as the solution in achieving sustainability, and biopolymers can be either natural or bio-based polymers. Herein, bio-based polymer pertains to the artificial synthesis of natural resources such as biomass while natural polymers refer to polymers that are obtained from nature. However, not all biopolymers undergo biodegradation, and they include polyphenols and polyisoprenoids. Studies and marketing strategies have used the terms bio-based and biodegradable interchangeably

without clarifying what constitutes each category [3]. It should be noted that bio-based and biodegradable plastics are distinct products with different sustainability pathways that are not necessarily known to ordinary consumers. According to Lambert and Wagner [3], bio-based polymers are from renewable sources contrary to biodegradable plastics, which can be from renewable or non-renewable feedstocks but can easily disintegrate and biodegrade in the environment. This clarity is necessary given that bio-based plastics may not necessarily disintegrate in the environment due to the presence of chemical additives to increase their life span [4].

While plastics from organic materials, either bio-based or biodegradable, are considered as a preferred alternative to conventional plastics, there is a need to compare the sustainability impacts of the two alternatives. This comparison is required considering that the production of bioplastics (bio-based or biodegradable) may exhibit marginal sustainability advantages over conventional polymers and vice versa due to some externalities that are inherent in their production processes. According to Geissdoerfer et al. [5], circular products may have negative effects on sustainability while Oke et al. [1] argued that pro-environmental policies and behaviour may not necessarily contribute positively to sustainability. Similarly, Lambert and Wagner [3] concluded that biodegradable plastics may not eventually degrade when emitted into the environment.

For this work, bio-based polymers here is described as a partial polymer material made up of renewable and sustainable source materials or feedstock. This differentiates it from biopolymers that are purely derived from living organisms. As indicated earlier, the production route for these bio-based polymers influences their degradation. These biopolymers have been selected based on the ease of their production from naturally derived polymers with or without depolymerization. It is worth noting that some of the polymers, such as bio-polyethylene terephthalate (PET) and bio-polyolefins, cannot be involved with natural biological cycles as they are mostly non-biodegradable at the moment. Herein, we attempt to identify the processes involved with their applicability based on a cradle-to-grave assessment and potentials. While bio-based polymers can be biodegradable [6], the biopolymers of interest in this study are poly (lactic acid) (PLA), Poly (ε-caprolactone) (PCL), polyhydroxyalkanoates (PHA) (including polyhydroxy butyrate (PHB)), and polyamides (PA) (PA4, PA6, PA66 and PA11). These bio-based polymers (Figure 1) are produced as either biomass or by-products during the formation cycle of the organisms.

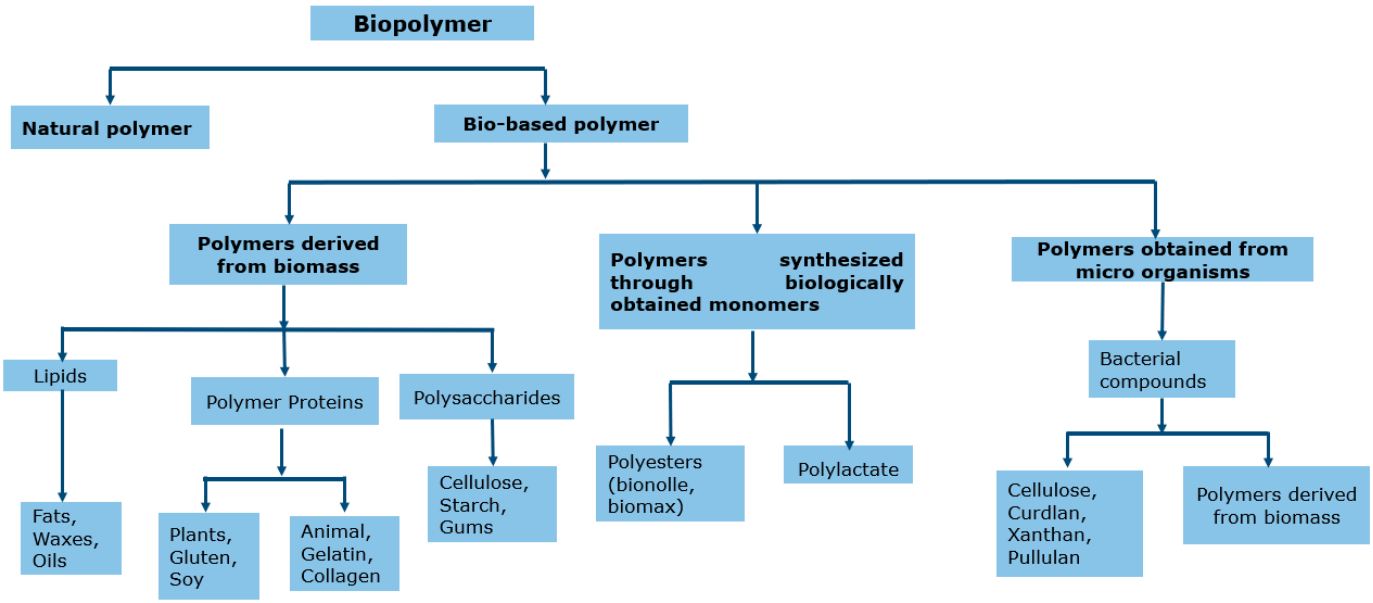

Figure 1. Basic classification of bio-based polymers.

To make informed decisions about the transition to bio-based plastic products, studies on whole lifecycle and life-costing assessment of plastics, from production to disposal,

should be conducted to establish the environmental, social, and economic impacts of bioplastics and conventional plastics. This will involve the analysis of material and energy balance at each stage of the plastic production process and across its entire supply chain. For instance, a material balance may reveal that using starch-rich products such as maize and wheat as the key constituents of bioplastics creates more negative socio-environmental impacts in the upstream supply chain, particularly during cultivation and transportations of feedstock. This is consistent with the work of Benavides et al. [7], who observed that the production pathways of biomass-derived PET are associated with increasing water extraction compared to the production of conventional plastics that consume less water.

Using the findings of different studies, Karamanlioglu et al. [4] reported that PLA has significant advantages over petroleum-based polymers. According to their study, the life cycle assessment (LCA) shows that PLA utilizes about 55% less fossil energy during production than conventional plastics and emits about 1600 kg CO_2/metric ton during decomposition compared to around 7150 kg CO_2/metric ton for petroleum-based polymers. However, there is a need to access the circularity and linearity potential of bio-based and biodegradable plastics for a better understanding of their impacts on the environment and socio-economic wellbeing. If microorganisms can be isolated to decompose polyester and polyurethane, efforts should focus on how conventional non-biodegradable plastics that are currently in circulation can be recovered while promoting the production of biodegradable plastics. Using potato, corn, and wheat starch as raw materials for bio-based plastics will not only have negative consequences on the environment through deforestation but will also impact the supply chain of agri-food production due to increasing demand. According to Karamanlioglu et al. [4], starch feedstocks in the production of bio-based plastics will cause land-use to change and exert pressure on agriculture. The consequences of the possible bioaccumulation of residues from bio-based or biodegradable plastic decomposition in living tissues, that may contaminate the food chain, are unknown and should be addressed in future research.

2. Processing and Synthesis of Bio-Based Polymers

As stated earlier, the evolving trend is the soaring demand for polymers that are naturally benign with low toxicity to human health and that will subsequently become more sustainable than their petroleum-derived counterparts. However, processing the bio-based feedstock, especially through environmentally friendly refining and manufacturing processes, as well as the potential for recycling, are still at infancy stage. Feedstock complexity provides an avenue for the innate chemical and biological characteristics that should be explored, but this complexity will require extra considerations depending on the polymer. This section involves exploring these characteristics as well as their synthesis, material behaviour, and in-use performance.

2.1. Processing of PLA-Based Materials

Among bio-based polymers, PLA has shown great potential and commercial value in different areas. PLA is a compostable and transparent synthetic polymer that can be obtained from natural resources such as rice, corn starch, potatoes, sugar beet, or sugarcane through ring-opening polymerization using a preparation of lactide or the condensation polymerization of lactic acid [8,9]. Although PLA can be produced chemically, microbial fermentation accounts for a majority of produced PLA worldwide while the remaining part is produced chemically by hydrolysis of lactonitrile. This is followed with purification of the lactic acid and the generation of cyclic dimer (lactide). The synthesis ends with the ring-opening polymerization of the lactide. In addition, it has thermoplastic properties and possesses good mechanical strength, biocompatibility, non-toxicity, easy availability, environment-friendly nature, good processability, and broad application range commercially compared to conventional thermoplastics [10,11]. Furthermore, PLA is the most produced bio-based polymer because of the compatibility with varying processing techniques. PLA has a relatively high glass transition, which makes the final product brittle

and shows brittle fracture behaviour at room temperature. However, in comparison to other bio-based polymers, i.e., PHB, PLA has better mechanical properties. It is worth noting that the other limitations of PLA are its inadequate thermal stability and low heat resistance. Therefore, researchers have proposed the blending of PLA with suitable materials as a strategy to improve the insufficient properties and inadequate characteristics of the virgin polymer [12].

In terms of end products, PLA, including other biopolymers, has a low oxygen barrier and poor resistance to heat. The barrier properties can be enhanced by coating it with materials, lamination of two or more biopolymers, blending, physical and/or chemical modification, and making micro-/nano-composites. Genovese et al. [13] designed bio-based PLA triblock copolymers for sustainable food packaging and showed better barrier and mechanical properties as compared to only PLA [13]. In another study, a twin-screw extrusion of PLA/carbon nanotubes (CNTs) was performed to prepare nanocomposites, and the crystallinity, mechanical, and electrical properties of the PLA/CNTs nanocomposites was enhanced with the increased content of CNTs due to nucleation and good dispersion of CNTs [14]. Further, compatibilized PLA was blended with natural rubber (NR)/CNTs and prepared nanocomposites by using melt-blending. Then, the effect of CNTs with different loadings (1–8 phr) was also investigated on rheological properties of PLA/NR nanocomposites. The results showed improved storage and loss modulus as compared to blends without CNTs. The increased content of CNTs exhibited no frequency-dependent behaviour [15].

Therefore, it is worth noting that the modified CNTs and PLA can provide an improvement in desired properties of PLA-based nanocomposites. In this regard, Zhou et al. [16] prepared PLA/oxidized-carbon nanotubes (OCNTs) nanocomposites by using a melt-blending process, where poly (butylene adipate-co-terephthalate) (PBAT) and ethylene-butyl acrylate-glycidyl methacrylate (E-BA-GMA) were applied as toughening resin and compatibilizer, respectively. In this study, 0.5% OCNTs showed a good combination of strength and toughness and higher thermal stability than that of only PLA [16]. The blending of the polymeric systems can also be beneficial based on the application. In this case, the electrospun PLA/CNTs/chitosan (CS) nanocomposite fibers showed good preservation behaviour for strawberries and demonstrated the best results with fiber having 7 wt% CS. In this study, these fibers delayed physiological changes in strawberries and extend their shelf life [17].

Apart from CNTs for nanocomposites, the use of nanocellulose as a renewable resource has shown potential in fabricating polymeric nanocomposites for industrial and biomedical applications. In this case, various (from various sources) nano-cellulose-reinforced PLA-based nanocomposites have been fabricated using different processing methods [18]. For example, Li et al. [19] prepared novel PLA/TEMPO-oxidized bacterial cellulose (TOBC) composites by using the Pickering emulsion approach, and screw extrusion was used to prepare PLA/TOBC filaments for fused deposition moulding (FDM). In this study, low content of TOBC showed effective enhancement in mechanical and crystallization properties of PLA due to uniform dispersion and was optimized up to 1.5 wt% of TOBC. Further, the increased amount of TOBC reduced the mechanical and crystallization properties of PLA nanocomposites [19]. Further, PLA and cellulose nanocrystals (CNCs) have been used for making bio-based, ultra-strong nanocomposites with an aligned structure and can be prepared at a large scale via surface functionalization of CNCs, liquid-assisted extrusion, and solid-state drawing. The nanocomposites can achieve high ultimate strength (353 MPa) and toughness (107 MJ/m^3) that are superior to those of other thermoplastic materials. Moreover, a relatively high glass temperature and strain-responsive birefringence behaviour were observed in these nanocomposites, and they have potential structural and optical strain-sensing applications [20]. In another study, electrically conductive and environment-friendly nanocomposites composed of PLA/polyaniline (PANI)/nanocrystalline cellulose (NCC) were prepared using the solvent-casting process. The incorporation of 1% NCC showed electrical conductivity up to 2.16 $S.m^{-1}$. Further, enhanced dispersion stability and reduced viscosity/viscoelasticity of PLA/PANI/NCC suspensions were observed. In

addition, the incorporation of NCC showed significant improvement in the mechanical properties of PLA/PANI/NCC nanocomposites [21].

UV-shielding and biodegradation abilities were significantly enhanced by incorporating 15% hybrids of CNC-zinc oxide (ZnO) into a PLA matrix [22] as shown in Figure 2. The transmittance of PLA-based nanocomposite films was slightly decreased with the increased content of CNC-ZnO hybrids (up to 15 wt%) as compared to pure PLA (see Figure 2Aa). Pure PLA film showed poor UV-shielding ability with utmost low absorbance in UVB and UVA regions (200–400 nm), whereas the incorporation of CNC-ZnO hybrids enhanced the absorption of UVB and UVA regions (200–400 nm), and the transmittance was reduced at the wavelength range of 320–400 nm (see Figure 2Ab). Therefore, the synergistic UV-shielding effects of CNC-ZnO hybrids into the PLA matrix showed excellent UV-shielding activity as compared to pure PLA matrix. Furthermore, apparent changes occurred on the surfaces of PLA/CNC-ZnO nanocomposite films before and after hydrolytic degradation (see Figure 2Ba) including after soil degradation (see Figure 2Bb).

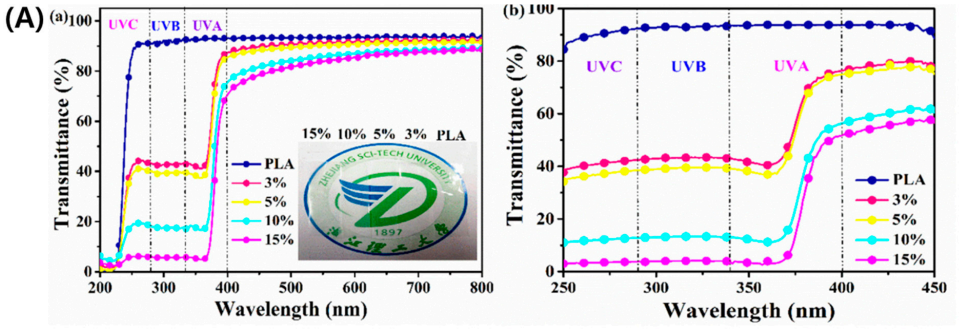

(c) Sample	UV shielding at 360 nm (%)	Transmittance at 550 nm(%)	Reference
PLA/CNC-ZnO 5%	62.8	90.6	This work
PLA/ZnO 5%	85.2	90	[34]

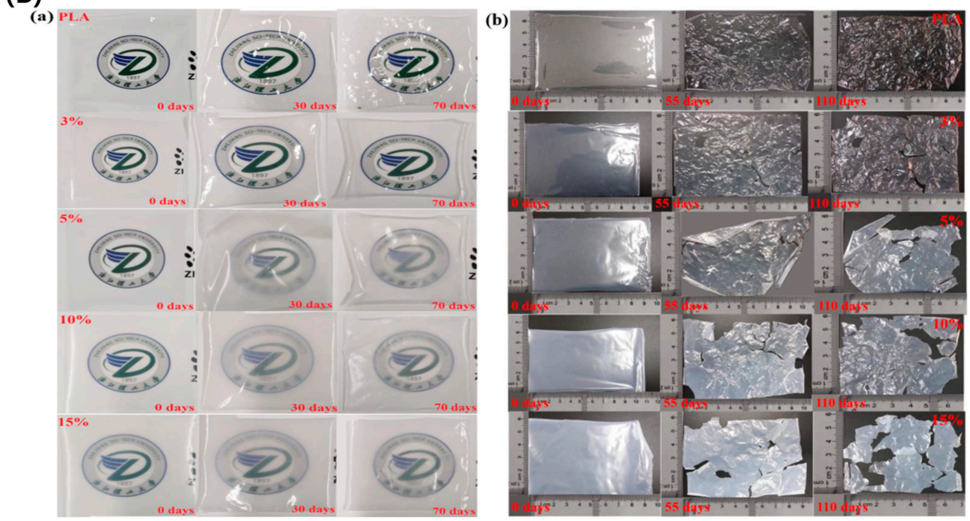

Figure 2. (**A**) Transmittance variation in pure PLA and PLA/CNCs-ZnO nanocomposite films (**a**) and their UV-vis diffuse reflectance spectra (**b**) magnification of the spectra between 250–450 nm to emphasise on the incorporation of CNC-ZnO hybrids and (**c**) a comparative data of UV-shielding and transparency of PLA/CNCs-ZnO and PLA/ZnO nanocomposite films. (**B**) Digital images of PLA-based nanocomposite films with apparent changes before and after (**a**) hydrolytic degradation and (**b**) after soil degradation [22], copyright 2023, Elsevier.

In addition, the incorporation of cellulose nanowhiskers (CNWs, 1–9 phr) along with montmorillonite (MMT, 5 phr) into PLA matrix improved the crystallinity, biodegradability, and thermal stability of the nanocomposite system. By incorporating 1 phr CNWs, highest tensile strength (~36 MPa) and ductility by 87% were significantly enhanced. However, Young's modulus was linearly increased with increasing CNWs content [23]. Furthermore, compared to CNCs or CNWs, cellulose nanofibres (CNFs) were used to enhance the properties. The effect of foaming method on shape-memory behaviour of cellulose nanofibr (CNF)-reinforced PLA/thermoplastic polyurethane (TPU) nanocomposites in the form of cylindrical shapes and sheets was analysed. The forming process resulted in a tangible increase in force recovery ratio (up to 40%) and an extensive reduction in actuation force (up to 10 times). Statistically, the existence of CNFs in the foamed nanocomposite showed a significant increase in actuation force and reduction in force recovery ratio. Additionally, a significant deviation between shape-memory properties was observed between experimental and analytical evaluation [24].

Similar to work performed with CNCs/CNWs, Herrera et al. [25] used chitin nanocrystals (ChNCs) and prepared modified blown films of plasticized PLA/ChNCs nanocomposite using melt-compounding and film blowing for packaging applications. The incorporation of 1 wt% ChNCs enhanced 175% tear strength, 300% puncture strength, and 4 °C glass transition temperature (Tg), as well as slightly improved the degree of crystallinity of films as compared to PLA films without ChNCs. Additionally, nanocomposite blown films showed lower fungal behaviour and exhibited lower electrostatic attraction between film surfaces that led to the easy opening of the plastic bags. However, barrier, optical, and thermal degradation of the films were not improved significantly with the incorporation of ChNCs [25].

In terms of processing sustainability and large-scale production, for blown films (Figure 3a–f) for food packaging, magnesium oxide (MgO)-reinforced PLA nanocomposite films have been fabricated using melt-processing through an industrial-level blown film extrusion setup. In this study, up to 1–2% incorporation of nano-MgO in PLA matrix enhanced the UV shielding (optical), barrier, mechanical, and antibacterial properties significantly [26]. For other industrial applications, linear low-density polyethylene (LLDPE)-toughened PLA nanocomposites were prepared by incorporating organophilic modified MMT. In this study, the increased content of MMT exhibited improved Young's and the flexural modulus. LLDPE enhanced the impact strength with a reduced tensile and flexural strength of the PLA nanocomposites. Furthermore, the increased content of MMT also decreased the tensile and flexural strength of the PLA/LLDPE nanocomposites, including the elongation at break and the impact strength. However, the thermal stability of PLA/LLDPE nanocomposites was improved with increased content of MMT. Below glass transition temperature, the storage modulus of PLA/LLDPE nanocomposites enhanced with increased content of MMT [27]. To promote a sustainable and green economy, PLA/organoclays nanocomposites have been developed for use in cosmetic packaging. The level of overall migration in a range of stimulants (maximum 0.88 ± 0.44 mg/dm^2) from all PLA/organoclays nanocomposites was well below the total established legislative migration limit (10 mg/dm^2). In addition, the migration extracts from nanocomposites encouraged minimal toxicity to the skin [28]. Furthermore, Nam et al. demonstrated the effect of organoclays on PLA/cellulose acetate butyrate (CAB) nanocomposites and found that thermal stability and mechanical properties were improved with the incorporation of organoclays [29].

Selective additives with special characteristics such as lotader AX8900 (impact modifier), triethyl citrate (TEC; plasticizer), and halloysite nanotubes (HNTs; a reinforcement) have been extruded with PLA in different compositions. PLA/HNTs nanocomposites exhibited 20 times higher storage modulus after rubbery state. The incorporation of lotader in PLA/HNTs decreased the crystallinity from 21% to 2% without affecting glass-transition temperature (Tg), whereas the addition of TEC resulted in the opposite effect. Further, the incorporation of HNTs along with lotader and TEC enhanced elongation 19 times, where

lotader and TEC synergistically improved the ductility of PLA while maintaining similar tensile properties [30]. An effective process has been presented for improved interfacial compatibility between matrix (PLA) and modified graphene via an elastomer modifier for better properties [31]. The reduction of graphene oxide (GO) by using glucose (rGO-g) shows high electrical conductivity and high efficiency in enhancing the electrical conductivity of PLA. Therefore, 1.25% rGO-g in the composite showed a high conductivity (2.2 S/m) due to chemical reduction (by glucose) and thermal reduction (during the compression moulding process) [32].

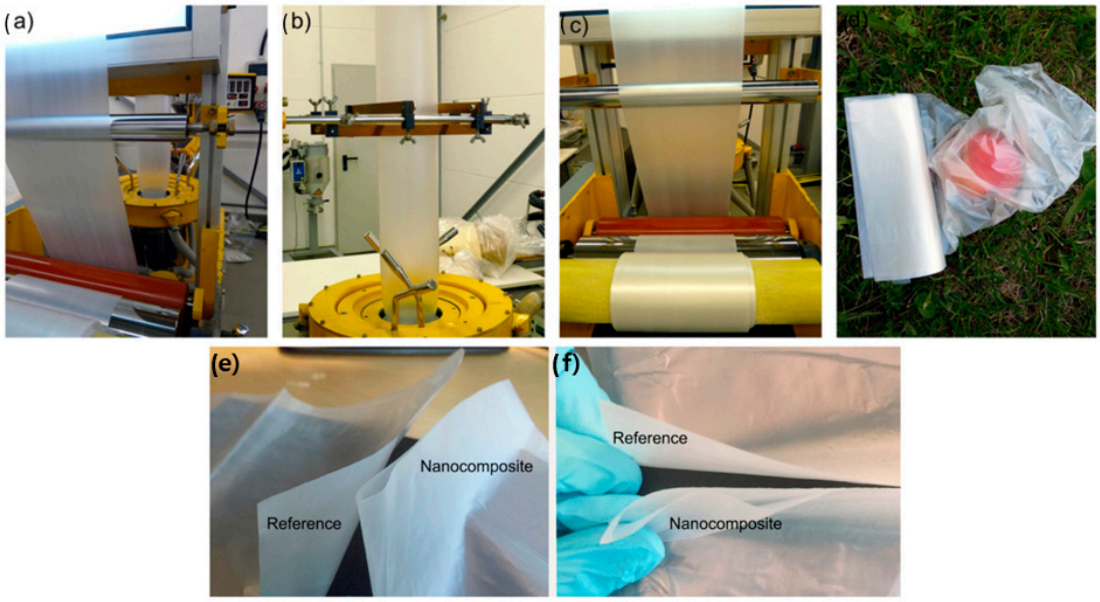

Figure 3. Film-blowing process: (**a**) reference, (**b**) nanocomposite undergoing film blowing (**c**) the nanocomposite, (**d**) final nanocomposite bags, (**e**) digital images of the reference and the nanocomposite bags with antistatic properties of the ChNCs and (f) magnified digital image of the reference and nanocomposite bag [25], copyright 2023, Elsevier.

PLA also has shown good potential in tissue engineering and drug delivery applications. The addition of PLA in nanocomposite scaffolds composed of hydroxyapatite (nHA) and CS provided a homogenous composite network that significantly resists high stress and showed enhanced elastic modulus (in situ precipitation process) [33]. Further, nHA was blended with PLA/starch/Poly (ε-caprolactone) (PCL) via melt-blending and produced antibacterial nanocomposites with an encapsulated drug. The increased nHA content improved hydrophilicity, antibacterial, and drug-release behaviour. In this case, 3% nHA exhibited good compromise between hydrolytic degradation and release profile (see Figure 4). Additionally, electrospun fibres of the optimum blend exhibited an enhanced fibroblast cell attachment [34].

For bone tissue engineering, Alam et al. [35] produced antibacterial metal/alloy nanocomposite scaffolds composed of PLA, copper (Cu), bronze (Br), and silver (Ag) particles using additive manufacturing (FFF, fused filament fabrication) for bone tissue engineering applications (see Figure 5a,b). In this study, metal/alloy particles increased the elastic modulus from 10% (0%, PLA-Br) to 27% (90%, PLA-Br) and effected a significant increase in antibacterial properties (~20–25%). The stiffness was increased up to 103% for PLA-Ag. In addition, the scaffolds treated with acid improved the bioactivity (~18–100%) for all samples, and maximum enhancement was observed for PLA-Cu (~100%) [35]. Further, PLA scaffolds have been prepared by reinforcing magnetic (iron oxide, Fe_2O_3) and conductive (carbon structures, CNF) nanofillers using FFF (additive manufacturing), and their biodegradation and bioactivity properties were evaluated for promising use for bone regeneration or replacement. Both nanofillers enhanced the water absorption capacity,

bioactivity, and biodegradation response. In vitro bioactivity exhibited improvement from ~2.9% (PLA) to ~5.32% and ~3.12% for PLA/CNF and PLA/Fe_2O_3 nanocomposites, respectively. However, stiffness values were decreased from ~680 MPa (PLA) to ~533 MPa and ~425 MPa for PLA/CNF and PLA/Fe_2O_3 nanocomposites, respectively [36].

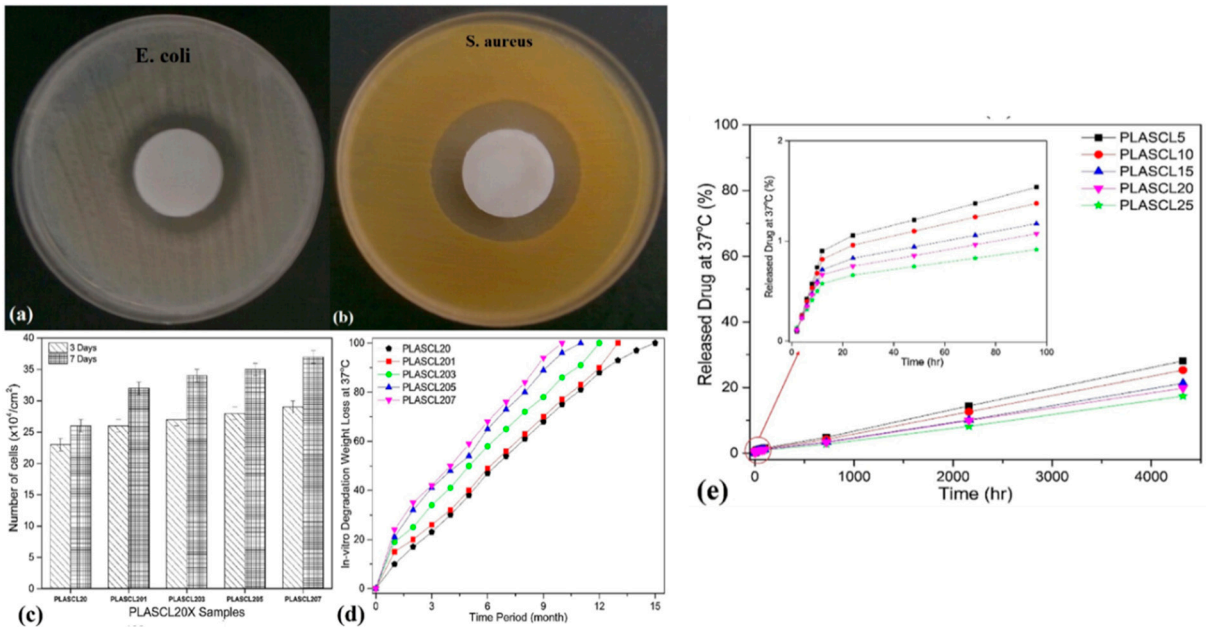

Figure 4. (**a**) PLASCL20X nanocomposite blends: antibacterial behavior against *E. coli* (**a**) and *S. aureus* (**b**), MTT assay after 3 and 7 days of incubation (**c**) and hydrolytic degradation 37 °C (**d**). Accumulative release behavior of PLASCL-based nanocomposite blends in 6 months based on weight loss and (**e**) Accumulative release behavior of PLASCL-based nanocomposite blends at 37 °C [34], copyright 2023, Elsevier.

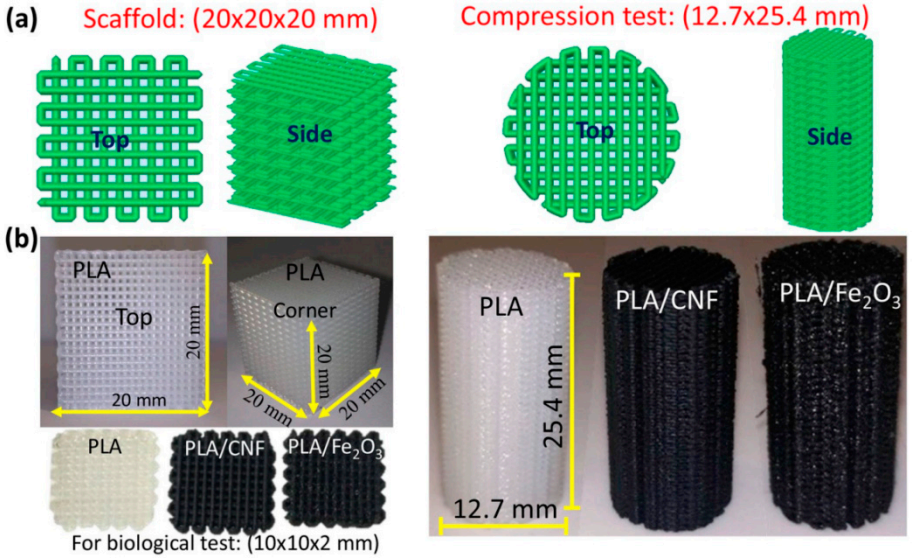

Figure 5. (**a**) CAD model and (**b**) 3D printed scaffold structures used for various tests [35], copyright 2023, Elsevier.

2.2. Processing of PCL-Based Materials

PCLs are synthesised through the ring-opening polymerization of ε-caprolactone (ε-CL) ions in the presence of diethylene glycol (DEG). PCL is a semi-crystalline polymer with sustained biodegradability, more flexibility, intrinsic hydrophobic nature, and ease of processing, but they do not possess good mechanical properties [37,38]. However, their

properties can be enhanced by incorporation of blends and fillers to form composites. An example is the composite of organic NPs (CNFs) and PCL introduced into the polypropylene (PP) matrix, where the elastic modulus of the hybrid composite was enhanced by the incorporation of 1% CNF only. In addition, crystallization of blend polymers in hybrid composites started at a higher temperature compared to single polymers [39]. Furthermore, the incorporation of ZnO NPs initiated an accelerated degradation in PLA/PCL blends prepared by using the melt-mixing method, whereas complex viscosity and elastic modulus were reduced with an increased amount of ZnO NPs, and this is correlated to the degradation and polymeric chain scission introduced by the ZnO NPs [40]. The higher loading of ZnO NPs resulted in a substantial decrease in pH (i.e., acidic pH) and thereby increased the extent of degradation (see Figure 6A). After 8 days of PBS incubation, higher physical degradation with smaller pieces was observed, and it was possibly due to the advanced molecular degradation of the nanocomposites with high ZnO content (see Figure 6B,C). Moreover, an elevated degradation rate was observed due to the synergistic effect of the higher content of ZnO NPs and acidic compounds. Furthermore, the PLA/PCL blend and nanocomposites exhibited a rapid weight loss pattern with different rates through the mechanism of degradation of ester bond caused by NaOH, and an advanced degradation rate was observed with increased content of ZnO NPs (see Figure 6D).

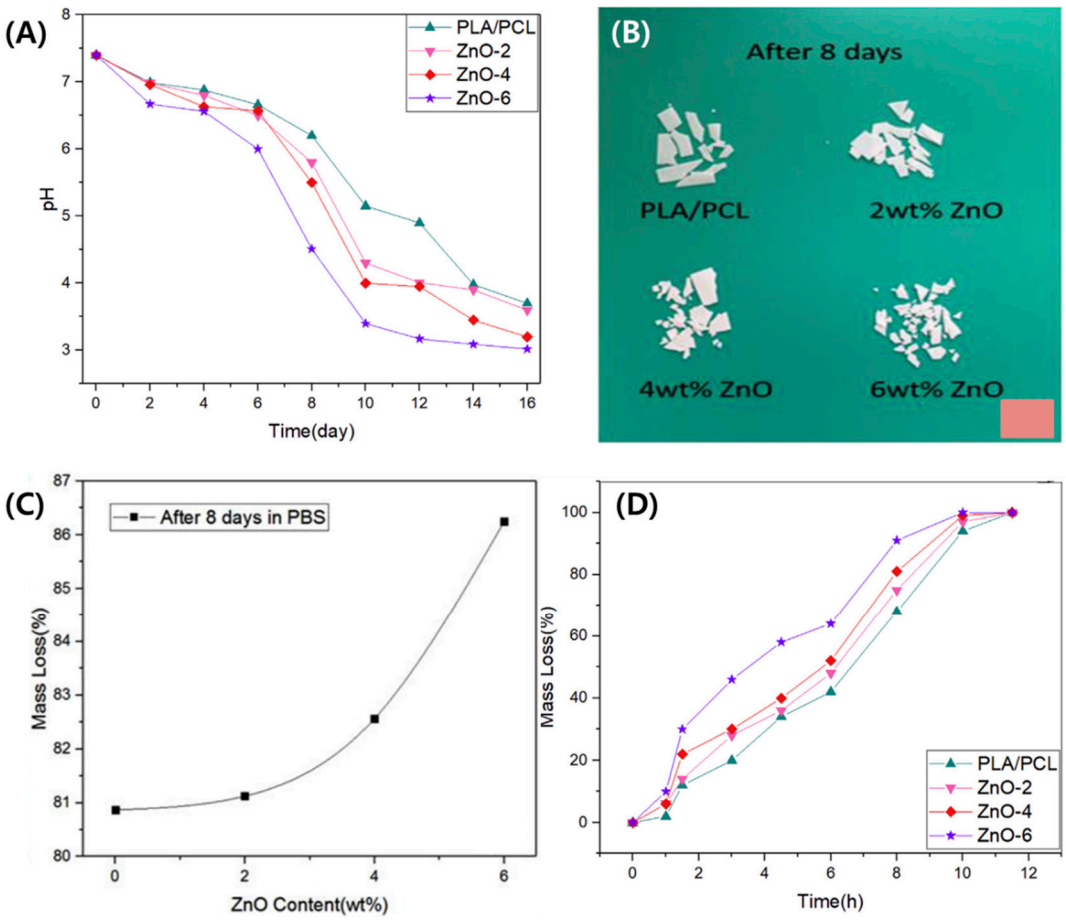

Figure 6. (**A**) pH values of PLA/PCL blend and PLA/PCL/ZnO nanocomposites in PBS at 80 °C after 16 days, (**B**) physical degradation of PLA/PCL blend and PLA/PCL/ZnO nanocomposites, (**C**) weight loss (%) vs. ZnO content in PBS at 80 °C after 8 days (**B**), and (**D**) weight loss (%) of PLA/PCL/ZnO nanocomposites in NaOH at 25 °C after 12 h [40], copyright 2023, Elsevier.

Recently, PCL has shown great potential in different applications, especially biomedical applications. For example, in the treatment of cancerous tumours, Guadangno et al. [41] developed antitumor electrospun PCL/functionalized-Fe_3O_4 (Fe_3O_4 from citric acid (CA))

hybrid membranes. In this study, the anticancer activity of the produced membranes was analysed against two different melanoma cell lines (low metastatic A375 and high metastatic A2058) and found a dose-dependent reduction against both cells' viability without affecting activity as compared to non-functionalized Fe_3O_4. In addition, the promising antitumour activity of membranes against uterine HeLa cells was also observed [41]. Similarly, PCL/ZnO from CA nanocomposite films has been prepared using the solvent-casting and evaporation method, in which enhanced elastic modulus and tensile strength of the nanocomposite films was observed, including good in vitro bioactive behaviour (the formation of HAp) in simulated body fluid (SBF) [42]. For guided bone regeneration, a silicon and magnesium co-doped fluorapatite (Si-Mg-FA) nanoparticles (NPs)s reinforced PCL fumarate (PCLF)/gelatin electrospun nanocomposite was prepared. In this study, PCLF with 5 wt% Si-Mg-FA NPs showed significant improvement in mechanical strength, whereas 10 wt% Si-Mg-FA NPs exhibited significant improvement in biodegradation of PCLF/gelatin in phosphate buffer saline (PBS), and no cytotoxicity was observed. However, PCLF/gelatin electrospun membranes with 5 wt% Si-Mg-FA NPs demonstrated appropriate mechanical and biological performances with good biodegradation rates [43]. In another study, bioresorbable magnesium hydroxide (MH) NPs were blended with PCL at 5 and 20 wt%, and the composite scaffold was fabricated using 3D printing technology. A significant improvement was observed in tensile modulus, while accelerating the weight loss of the composite scaffolds and reducing the molecular weight of PCL over a prolonged immersion time (150 days) in PBS at 37 $\pm$ 0.5 °C (pH 7.4). Furthermore, the composite scaffold was shown to be nontoxic and promoted osteoblast metabolic activity compared to only the PCL. Moreover, 3D-printed PCL/MH composite scaffolds could improve osteoblastic behaviour and moderate accelerated degradation behaviour [44]. Furthermore, for bone tissue regeneration, hydroxyapatite (Hap) (20 wt%) and HNTs (different amounts) incorporated in the PCL matrix showed considerable enhancement in mechanical properties and an improvement in degradation temperature [45]. In addition to this, precise and orderly complex porous PCL/HAp-based, composite, 3D, fibrous structures were manufactured using melt-electrospinning writing (MEW; as a direct additive manufacturing) for better infiltration and growth of cells compared to random 3D fibrous structures. The results showed faster degradation of PCL/HAp scaffolds in an alkaline environment (37 °C) than only PCL and facilitated a favourable environment for human osteoblast cell infiltration and growth, including HAp-induced bioactivity [46].

In another study, the addition of functionalized bioactive glass (BG) NPs improved the mechanical properties of PLA/PCL (80/20) nanocomposites. The values of maximum tensile (38 MPa) and flexural (94 MPa) strength were obtained using 3 wt% BGNPs, and it showed better human osteoblastic cell attachment and growth compared to only the polymer blend [47]. In addition, PCL/GO-based microporous scaffolds were prepared by using porogen leaching and an SC-CO_2-assisted solvent removal process (see Figure 7). The results exhibited a microporous interconnected network of scaffolds, and no cytotoxicity was observed towards L-929 mouse fibroblast cells, while triggered cell spreading was observed in the presence of GO [48].

Another thriving area of PCL application is their incorporation into membrane technology. Sadeghi et al. [49] investigated the gas permeation properties of PCL-based polyurethane-silica nanocomposite membranes and found a reduction in gas permeability but improvement in O_2/N_2, CO_2/N_2, and CO_2/CH_4 ideal selectivity [49]. A salient potential for PCL is the extraction of heavy metals and removal of lead (Pb) from aqueous waste; to this end, a bio-nanocomposite based on cyclodextrin-PCL-titanium oxide (TiO_2) was prepared using a solution blending method, and it found maximum Pb adsorption as 98% (pH 9.7), 10 ppm with 0.005 g dosage. In this case, Pb(II) followed pseudo-second-order kinetics, and the adsorption data fit the Langmuir isotherm [50]. Similarly, silver (Ag) and TiO_2 NPs-incorporated PCL electrospun mats were fabricated for possible use as a reusable SERS substrate for trace pollutants (quantitative analysis), photocatalyst for organic pollutant degradation, and antibacterial agent. In this study, the produced nanocomposite

exhibited highly effective detection of 10 mM for methylene blue (MB) as reusable analysis, complete photocatalytic degradation of MB and ibuprofen (Ibu) under UV irradiation for 180 min, and high bactericidal activity against *E. coli* (Gram-negative) and *S. aureus* (Gram-positive) bacteria [51].

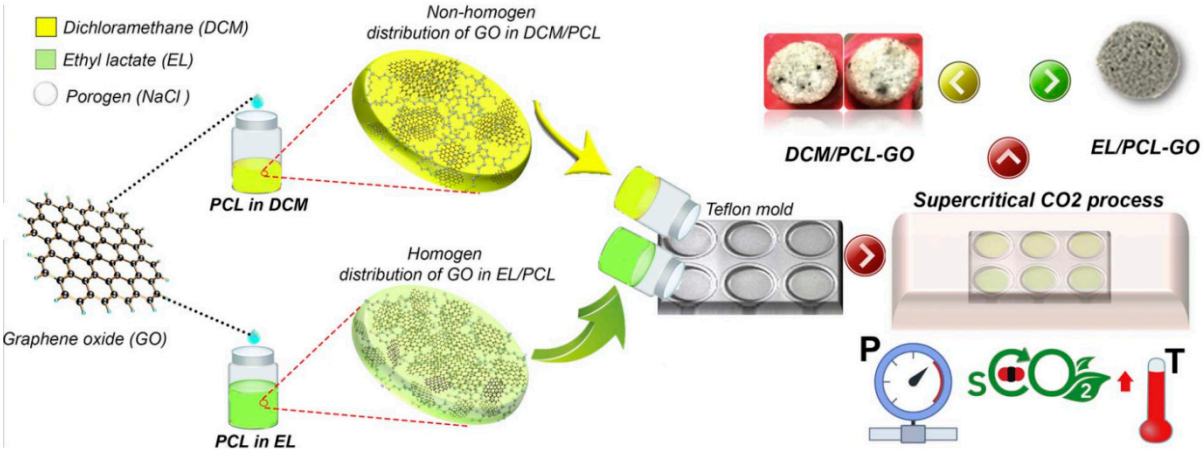

Figure 7. Schematic representation of the fabrication of PCL/GO scaffolds using a supercritical CO_2-assisted solvent removal process with two different solvents as dichloromethane (DCM) and ethyl lactate (EL) [48], copyright 2023, Elsevier.

2.3. Processing of PHA-Based Materials

PHAs are considered potential alternatives for conventional plastics from fossil sources and are derived in the form of intracellular granules from different bacteria [52]. PHA was first discovered in 1925 by Lemoigne during an investigation of Bacillus megaterium. It is produced by several bacteria through various renewable sources of waste feedstocks and mostly by fermentation. Generally, this fermentation process involves fermentation, isolation, and purification from a fermented broth. Usually, mineral materials are treated with a culture of seed that possesses bacteria. The feedstock ranges from bio-oils and biowaste, to cellulosic and fatty acids based on the PHA needed. The vessel is continuously sourced with carbon to encourage cell growth and increase PHA accumulation. The simplest and most common form of PHA is PHB, which was discovered by Lemoigne in 1926 as a component of bacteria Bacillus megaterium [53].

At present, over 150 PHA monomers have been identified that make up PHAs, and this range of diversity enables the production of bio-based polymers to suit specific applications. The PHA currently developed by several companies is the PHA copolymer with usually 80 to 90% (R)—3- hydroxybutyric acid monomer and 10 to 20% of a completing monomer to improve PHA properties. Examples of PHAs include:

- (PHA): Polyhydroxyalkanoates
- (PHB): Polyhydroxy butyrate
- Poly(3HB): Poly(3-hydroxybutyrate)
- Poly(3-HB-co-4HB): Poly(3-hydroxybutyrate-co-4-hydroxybutyrate)
- Poly(3HB-co-3HH): Poly(3-hydroxyoctanoate-co-hydroxyhexanoate)
- Poly(3HO-co-3HH): Poly(3-hydroxyoctanoate-co-hydroxyhexanoate)
- Poly (4-HB): Poly(4-hydroxybutyrate)

Generally, most of the bacteria for PHA biodegradation has been evaluated to generate just one PHA degradation but produce a minimum of varying extracellular PHA-depolymerases with the differences being their biochemical properties. In 1990, Imperial Chemical Industries (ICI) created biopol using PHBV as source material that can be degraded by microorganisms within months of being disposed in the environment. Subsequently, other companies such as Procter & Gamble and Du Pont showed interest in producing various PHAs; Batelle who produced PHA completely from vegetable oils.

Other sources of production from high-glucose intensity materials include potato scraps, corn, molasses, and beets [54,55].

Similar to other bio-based polymers, PHA composites or nanocomposites have shown great potential for various biomedical applications, catalysis, biosensors, and adsorbents [56–58]. PHAs are bio-based polymer with non-toxicity and belong to the polyester family. Poly (3-hydroxybutyrate) (PHB) is a form of PHA and possesses a limited processing temperature range with high crystallinity and high brittleness [59]. In this case, the melt-processing of PHB is a challenge due to chain scission during the melting process (i.e., thermal decomposition) [60]. Therefore, various approaches have been used to reduce its crystallinity, melting point, and broad processing range compared to only PHB [61,62]. In addition, to improve the mechanical performance of PHB, various forms of studies have been performed with nano reinforcements and polymers [63]. Among the family of PHAs, PHB and poly (3-hydroxybutyrate-co-3-hydroxy valerate) (PHBV) copolymers are the most often studied bio-based polymers for various applications, especially the biomedical field. Furthermore, PHB degrades at a higher rate than PHBV [64–66].

Focusing on their application, it is worth noting that PLA foams are mainly used as packing materials; high expansion and fine cells are difficult to achieve by using injection foam moulding (FIM) due to intrinsically low melt strength. Therefore, Lee et al. [67] added nanofibrils of polytetrafluoroethylene (PTFE) to improve entanglements of molecular chains and PHA to improve the impact strength of PLA foams processed using high-pressure FIM combined with a mould-opening technique, where a constant amount of supercritical nitrogen (0.6 wt%) was injected into FIM to obtain uniform mixtures and further injected into the mould cavity to make highly expanded foamed PLA specimens [67]. It is also known that PHAs suffer from poor oxygen barrier, poor strength and heat resistance, and severe bacterial contamination that limit their wide applications, especially in food packaging. In this case, tailor-made long alkyl chain quaternary sat (LAQ) modified-GO (GO-g-LAQ) was blended with PHA, which prepared PHA/GO-g-LAQ nanocomposites with significantly improved heat resistance, oxygen barrier, mechanical properties, and antibacterial properties (99.9%) against Gram-negative and Gram-positive bacteria [68]. In polarized optical microscopy (POM) analysis, PHA exhibited large sized spherulites due to inferior crystallization behavior, whereas GO nanosheets agglomerated in the PHA matrix and acted as nucleators in PHA/GO in improving overall crystallization rate of PHA. Further, a smaller size of spherulites with no aggregation was observed within 5 min in the case of PHA/GO-g-LAQ, and it crystalized completely in 20 min (see Figure 8A(a–c)). In a mechanical analysis, GO-g-LAQ significantly enhanced the tensile strength, but it restricted the deformation of PHA in PHA/GO-g-LAQ nanocomposite films, especially after 1 wt% of GO-g-LAQ (see Figure 8B(a,b)). Oxygen permeation was found to be enhanced significantly with increasing GO-g-LAQ content. The gas barrier mechanism of the nanocomposite can be seen in Figure 8C(a,b). Furthermore, no leaching of LAQ from the nanocomposite films was observed (see Figure 8D(a,b)).

Furthermore, Jayakumar et al. [69] biologically synthesised PHB/Ag nanocomposite films using a dairy-industry by-product (cheese whey) for food packaging applications and found it to be stable hydrophobically and significantly antimicrobial against common food pathogens. Further, it exhibited good mechanical properties and less migration of food stimulants than the overall migration limit accepted for food contact materials [69]. In another study, PHB/biosynthesized-Ag nanocomposite films were prepared, and Ag NPs did not show any effect on thermal properties, but they showed a slight reduction in crystallinity. In addition, nanocomposite films exhibited significant antimicrobial activity towards food-borne pathogens, and complete bio-disintegration occurred within composting conditions during the first 40 days, not affected by the presence of AgNPs [70].

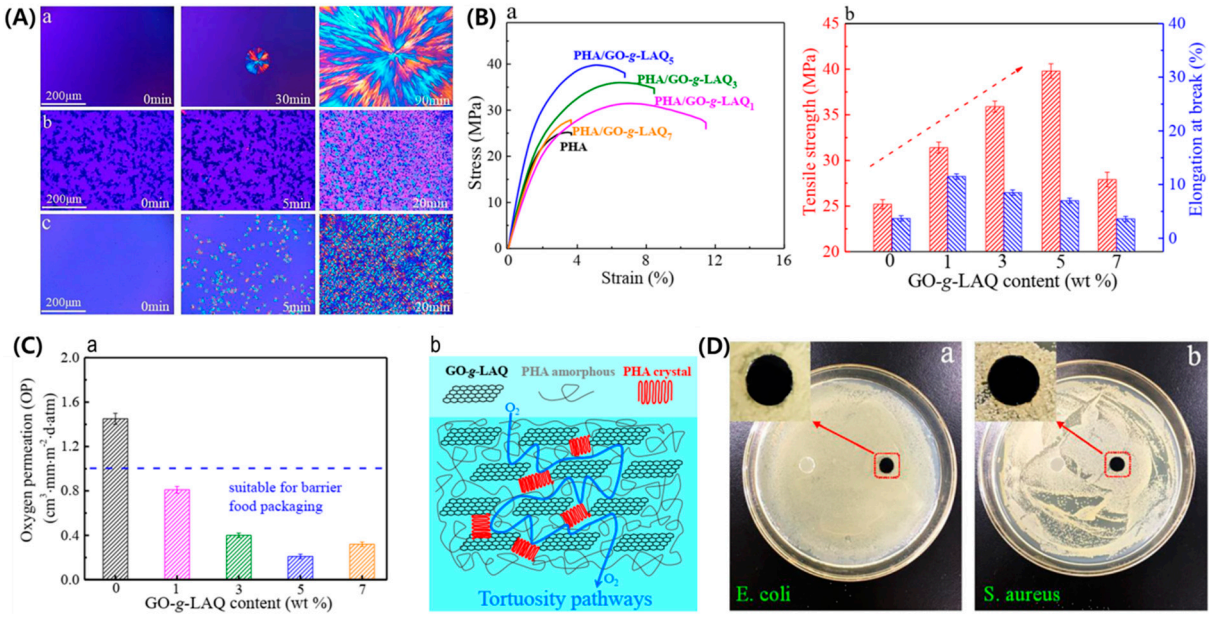

Figure 8. (**A**) POM images of (**a**) PHA (**b**), PHA/GO5, and (**c**) PHA/GO−g−LAQ5 nanocomposite films crystallized isothermally at 90 °C for various crystallization periods. (**B**) (**a**) Stress-strain curves and (**b**) tensile strength and elongation at break (%) of PHA/GO−g−LAQ nanocomposite films. (**C**) Oxygen permeation of PHA and PHA/GO−g−LAQ nanocomposite films (**a**) and gas barrier mechanism of PHA/GO−g−LAQ nanocomposite films (**b**). (**D**) Antibacterial activity through inhibition zone analyses of PHA and PHA/GO−g−LAQ5 nanocomposite (black sample) for (**a**) *E. coli* and (**b**) *S. aureus* [68], copyright 2023, Elsevier.

For biomedical applications, different nanofillers such as GO and CNF in PHBV and prepared films, where PHBV/GO showed higher cell proliferation towards time, as well as cell attachment and antibacterial activity, than the PHBV/CNF composite [71]. The nanocomposite coatings on bioceramic materials have shown great potential for bone tissue regeneration. In this advancement, a PHB-CS-multi-walled CNT-based nanocomposite coating was deposited on nano-bioglass/TiO_2-based scaffolds prepared using a foam replication method. The obtained scaffolds showed improved interconnected porosity and surface roughness, increased pH and degradation rate, enhanced apatite-forming ability, significant viability of cells, and high secretion of alkaline phosphatase [72]. Furthermore, gamma radiation-induced grafting of CS onto PHB was performed, and polyurethane composite scaffolds composed of PHB-g-CS and silica NPs were prepared by the salt-leaching method, and composite scaffolds showed good cytocompatibility [73]. Similarly, for skin tissue engineering, PHB-g-n-hydroxyethyl acrylamide (PHB-g-HEAA) as novel polyurethane scaffold showed good potential for wound dressing [74]. Furthermore, antioxidant and antimicrobial maleic anhydride-grafted PHBV (PHBV-g-MA)/fish scales (FSs) composites were prepared and processed in 3D printing filaments (as shown in Figure 9). Herein, improved adhesion between PHBV-g-MA and FSs and enhanced mechanical properties of the composite were demonstrated as compared to PHBV/FSs. However, human foreskin fibroblast cell viability was lower with PHBV-g-MA/FSs composites than PHBV/FSs composites [75].

In addition, biomaterials with bioactivity and sustained release of drugs are very promising in the treatment and prophylaxis of bone infection. Hence, injection-moulded nanocomposite composed of PHBV, nanodiamond, and nHAp loaded with vancomycin (VC) was prepared using a rotatory evaporator or spray-dryer. The nanocomposites showed improved flexural elastic modulus by 34% (similar to human bone) with the addition of NPs and exhibited a sustained release of VC for 22 days. Furthermore, VC provided antibacterial behaviour even after processing at 178 °C in an injection-moulding machine. In addition,

good cell attachment and growth on the nanocomposite was observed [76]. To improve properties, aminated-bacterial cellulose (BCA)-reinforced PHBV nanocomposite sponges were prepared using the impregnation method. Compared to only PHBV or PHBV/BC, enhanced thermal stability, reduced degradation, and improved compressive mechanical properties were observed with PHB/BCA nanocomposites, including good stability in simulated physiological environment and high swelling behaviour [77]. Pal et al. [62] prepared organically modified, nanoclay-reinforced PHBV/poly (butylene adipate-co-terephthalate) (PBAT) nanocomposite films processed through compression moulding and cast film extrusion. In this study, a pelletized nanoclay masterbatch was prepared by blending 20% nanoclay with PBAT using melt-extrusion and then was reinforced with PHBV/PBAT blend matrix to create nanocomposite pellets using a melt-extrusion process. The cast-extruded PHBV/PBAT/nanoclay (1.2%) nanocomposite films showed enhanced oxygen and water vapour barrier properties and % elongation at break (567.6 $\pm$ 0.1) as compared to compression-moulded films, due to better dispersion of the nanoclay and interaction between the nanofiller and matrix [63].

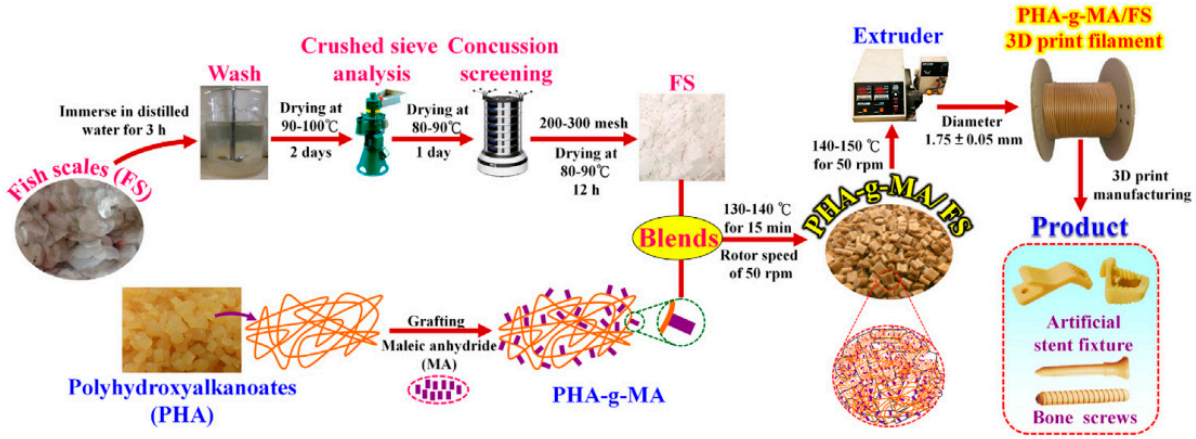

Figure 9. Schematic of the preparation of 3D printing filaments from a PHBV−g−MA/FSs composite [75], copyright 2023, Elsevier.

To enhance the mechanical performance of PHA in biomaterials such as scaffolds, PCL pellets were blended with PHA-based pellets. When the mixing ratio of PCL increased to 50%, the elongation at break of the blend was enhanced, and the gauge area of tensile-test specimens whitened and became porous, and this behaviour was understood using a rheo-optical technique based on near-infrared (NIR) spectroscopy while observing mechanical deformation of the blends during static tensile-tests. In this test, two-dimensional correlation spectra show the predominant deformation of the PCL phase. Figure 10 exhibits the digital images just after the break of specimens, and it demonstrates a flat fracture surface of PCL 0% specimen in Run 1 showing a brittle fracture. When the mixing ratio of PCL was increased, stringy fracture surfaces were observed in the specimens of Runs 2 and 3, in which the Run 3 specimen became partially white and looked porous. In addition, the specimen of Run 4 showed whitening and necking after maximum stress, but porous and stringy areas were decreased with an increased mixing ratio of PCL. Whereas, after maximum stress, Run 5 of only PCL showed a translucent necking area, and the necking area became thin and finally led to the break of the specimen [78].

Biocomposites composed of plasticized-PHB and defibrillated wood waste fibres (CF) were prepared, and the obtained biocomposite exhibited enhanced thermal and mechanical properties compared to only PHB. This is possibly due to the presence of lignin on the CF surface, which facilitated the interaction between PHB and CF. Furthermore, the doubling of plasticizer amount in PHB led to more flexible biocomposites [79]. In addition, different amounts of CNCs were reinforced in PHB/PCL (75/25) blends, and films were prepared using solvent-casting followed by melt-compounding and then were subjected to a thermo-

compression process. In this study, 3 wt% CNCs in PHB/PCL (75/25) blend provided good wettability and optical, thermal, and mechanical properties [80].

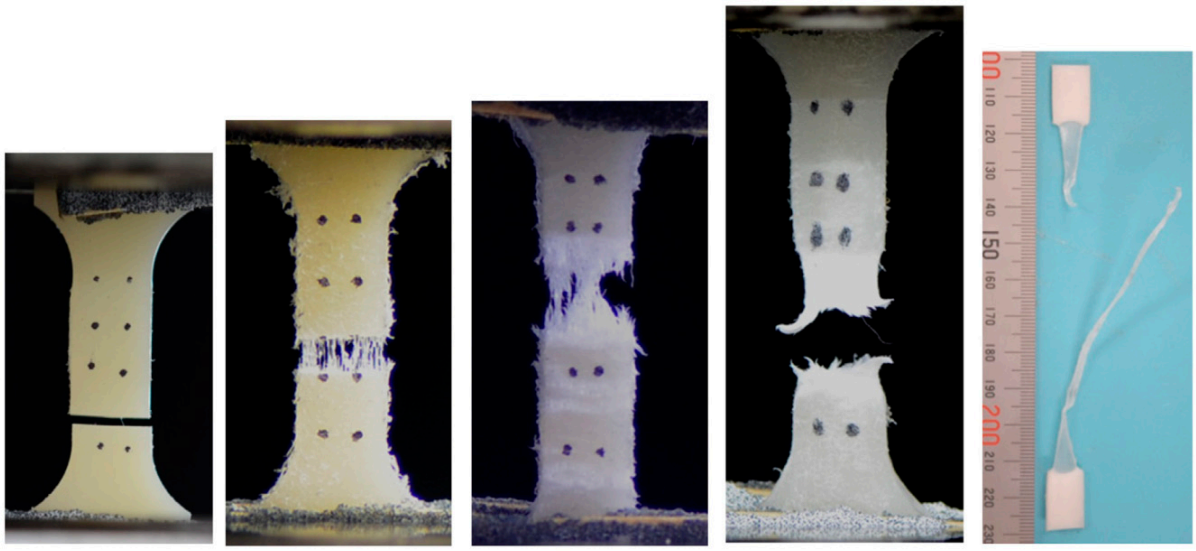

Figure 10. Digital images of the fracture behavior of the static tensile-test specimens just after the break of Run 1 (PCL0%), Run 2 (PCL30%), Run 3 (PCL50%), Run 4 (PCL70%), and Run 5 (PCL100%) [78], copyright 2023, Elsevier.

High transparency in all developed films was observed (see Figure 11a). Visually, no significant variations between loaded or unloaded nanocomposite films were observed, while only a slight change in tones (i.e., dark) were observed as the content of CNCs was increased. Further, the highest transmittance was noticeably observed with 3 wt% CNCs in PHB75/PCL25/CNCs 3 wt% as compared to PHB75/PCL25, and this is due to good dispersion of CNCs and the interaction between matrix and CNCs (see Figure 11b). The disintegration or brittleness of nanocomposite films was enhanced with the incorporation of CNCs in the PHB75/PCL25 matrix, and the level of disintegration was improved with increasing the content of CNCs and/or time period (see Figure 11c). Figure 11d shows the resulting weight loss during disintegration analysis towards incubation/disintegration time. Similarly, the compatibility between PHB and PCL by reactive extrusion with di cumyl peroxide (DCP) has been successfully explored, while in another study the effect of surface-modified HNTs on the properties of the PHB/PCL (75/25) blend improved the thermal and mechanical properties [80–82].

2.4. Processing of PA-Based Materials

Polyamides (PAs), which consist of varying forms, are commonly used thermoplastics for textiles, automotive industries, sports, textile filaments, and packaging due to their ease of processing, chemical resistance, high strength, stiffness, and durability [83–85]. Polyamides are linked by amide bonds, which form hydrogen bonds to the closest polymer chain. There are various PA6 prefix examples, PA4, PA6, PA10, PA11, and PA12, with the number describing the number of carbon atoms connecting amide bonds, and with the best-known forms being PA6 and PA66. Sustainable manufacturing of PA and PA blends in green chemistry is the basic principle.

Generally, bio-polyamides are niche products due to them being increasingly high performing polymers, and they account for 5% of the present biopolymer market. Although most bio-based PAs are quite recent achievements, PA11 (rilsan) obtained from castor oil has been synthesised and applied since the 1940s. Winnacker and Rieger [86] classified the bio-based PA to match its synthesis routes (ROP and polycondensation) with the initial materials needed to evaluate the possibility of this novel perspective. In addition, several

forms of diamines and dicarboxylic acids ease the tuning of PA properties, and PA can also be altered in the nitrogen atom. In polyamide chemistry, the task of investigating crystallinity through x-ray diffraction is a major factor. Figure 12 below shows a generic synthesis of PA.

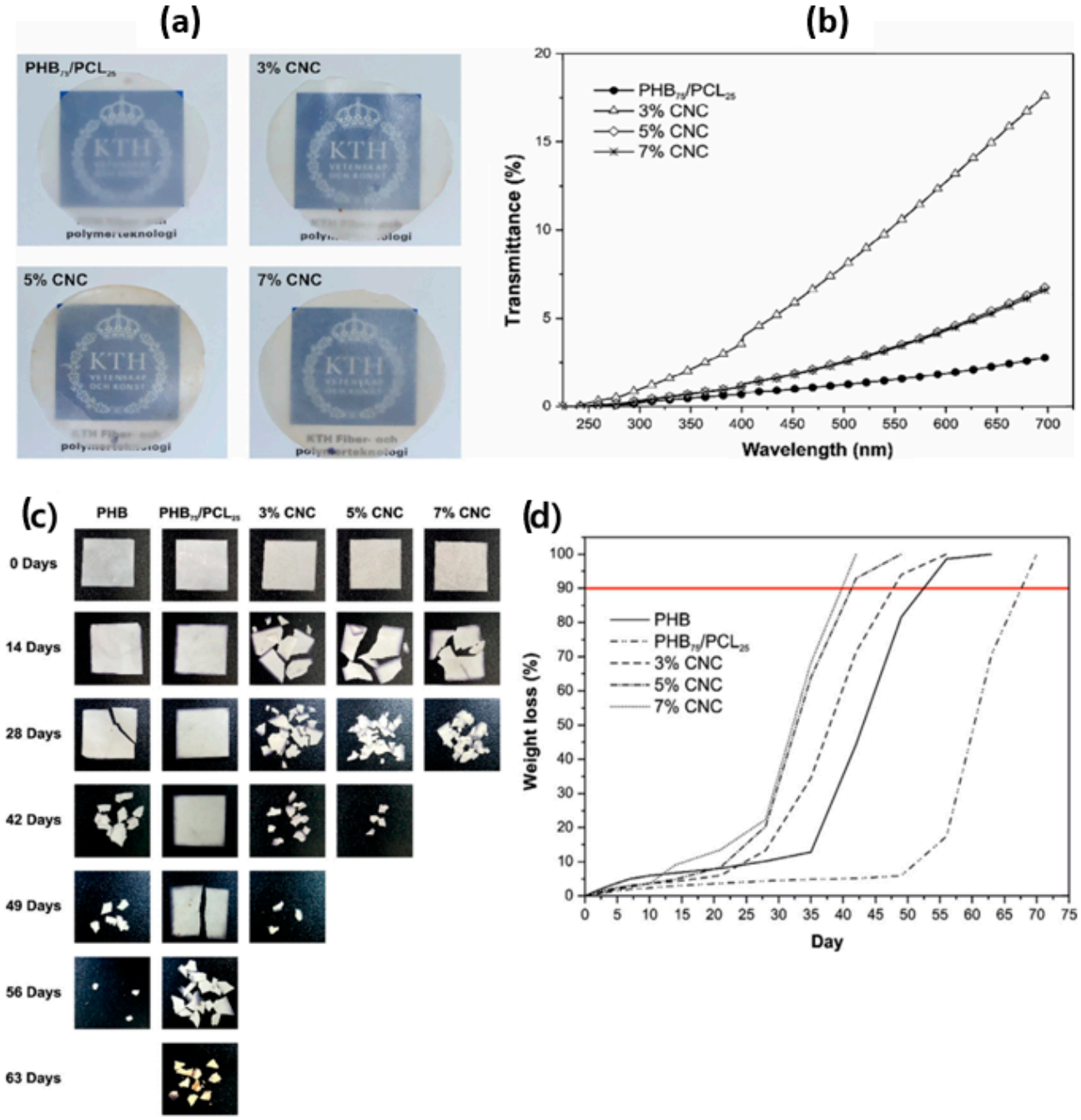

Figure 11. (**a**) Digital images of visual appearance, (**b**) UV-vis spectra of PHB/PCL (75/25) with various contents of CNCs, (**c**) qualitative visual appearance, and (**d**) weight loss of aged films during the disintegration process in controlled compost soil in terms of the incubation period [81], copyright 2023, Elsevier.

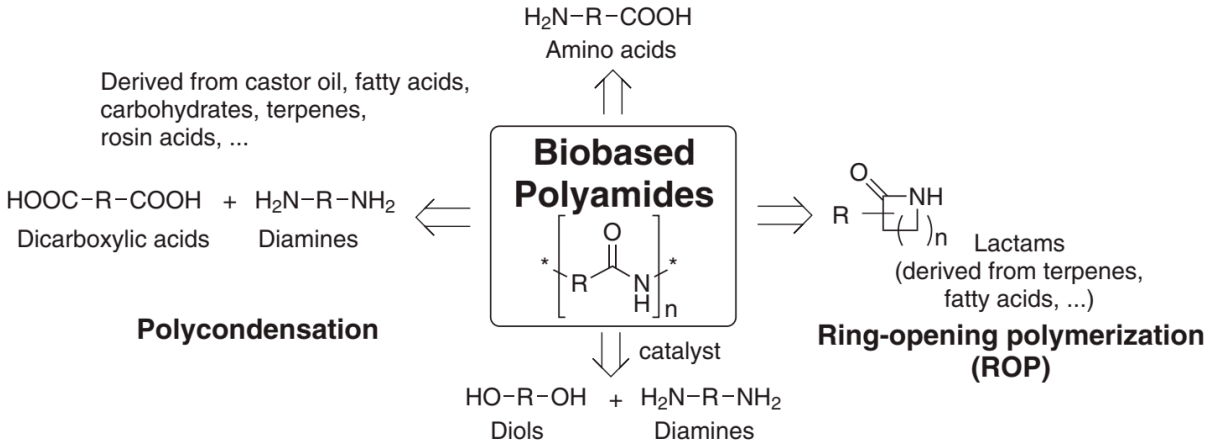

Figure 12. General structures and approaches for the synthesis of sustainable polyamides [86], copyright 2023, Elsevier.

There are generally two broad methods of developing bio-PA, i.e., bio-based polyamides through polycondensation reactions and bio-based polyamides through ring-opening polymerization of lactams, which includes the polycondensation of diamines, dicarboxylic acids, and bio-based ω, α—amino acids. The major source for building blocks of bio-based PA is castor oil from Ricinus commis [87] due to castor beans having an unusually high oil content (45–60%) that mostly contains C18 fatty acid (80–90%) and is available in the form of triglyceride ester, which is a reliable source of producing bio-PA in commercial amounts [88]. The castor beans are separated from their shells and pressed mechanically to obtain triglycerides (oil) (Table 1 provides the differences in properties).

Table 1. Selected properties of SA/DAII and SA/DAB copolymers [86], copyright 2023, Elsevier.

Poly Amide	Monomer Feed, mol Ratio [a] (DAB/DAII)	Built-in Composition (DAB/DAII) [b]	Mn [c] [g mol^{-1}] Pre-Polymer	Mn [d] after SSP	$T_{5\%}$ [°C]	Tm [°C]	Tc [°C]
PA1	1.0/0	1.0/0	9600	21,900	424	246	221
coPA2	0.91/0.09	0.89/0.11	6500	21,300	388	242	209
coPA3	0.83/0.17	0.86/0.14	5000	18,700	379	236	201
coPA4	0.78/0.22	0.80/0.20	5500	20,400	377	232	198
coPA5	0.55/0.45	0.57/0.43	2500	3900	321	198	156
PA6	0/1.0	0/1.0	4200	-	300	152	96

[a] Determined via weighed-in monomers; [b] Determined via NMR; [c] Determined for polyamides before solid state polymerization by SEC; [d] After solid-state polymerization.

This undergoes either the saponification step or transesterification step (with both steps being effective for splitting the ester bonds) to obtain ribonucleic acid or any corresponding methyl ester, respectively. Sebacic acid is derived from the alkali fission of ribonucleic acid and NaOH (Figure 13 depicts the synthesis of PA 11).

For the bio-polyamides obtained from carbohydrates, rosin and terpene acids through polycondensation, bio-based sebacic acid (SA), and carbohydrate derived from alcohol are used to prepare total bio-based semi-crystalline polyamides, and diamino butane is used to produce copolyamides with varying monomer feeds used [89]. The prepolymers are synthesised through polycondensation and subsequently passed to a solid-state polymerization process, which leads to an increment in molecular weight to provide varying polyamides (Milstein catalyst) [90]. The DSC and XRD study images on PA 11 are shown in Figure 14.

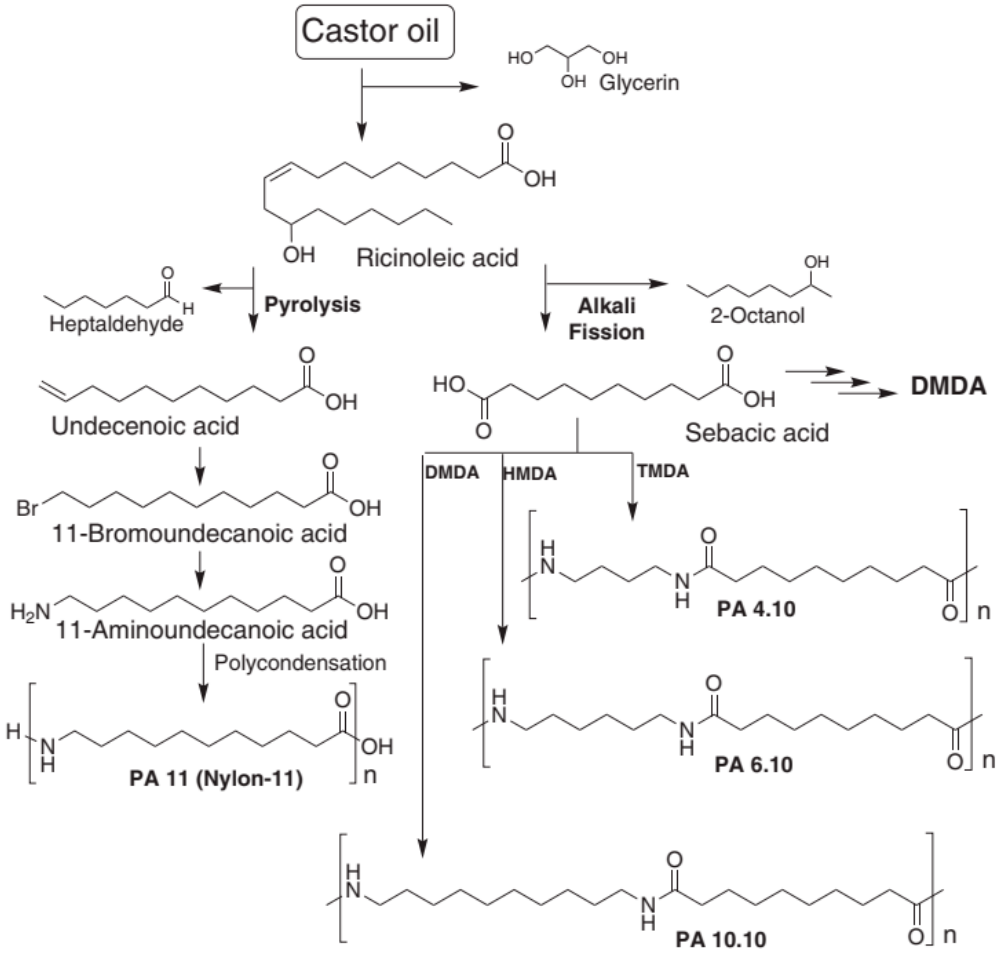

Figure 13. Monomers and polyamides from castor oil. (**Left**) synthesis of Nylon-11 via polycondensation of 11-aminoundecanoic acid. (**Right**) cleavage of ricinoleic acid to sebacic acid and its transformation with different diamines to the corresponding polyamides [86], copyright 2023, Elsevier.

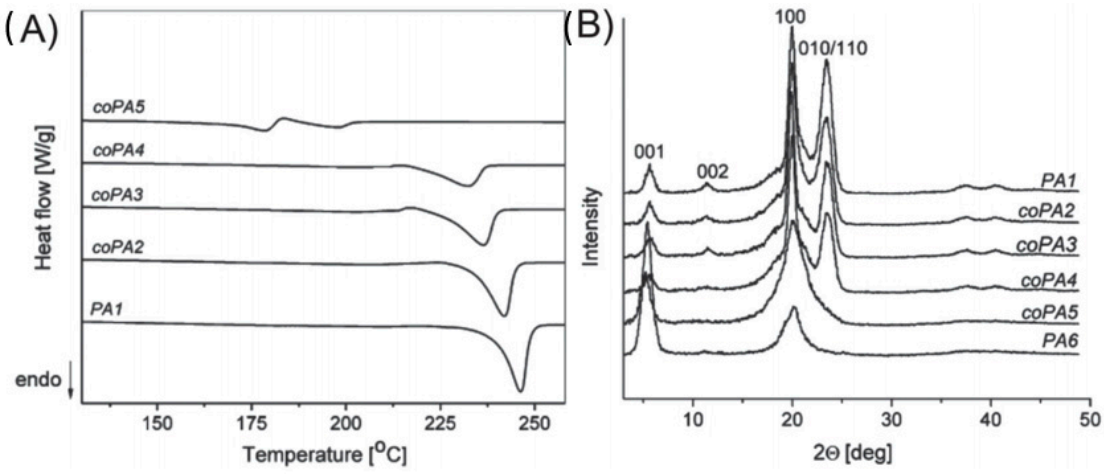

Figure 14. (**A**) DSC traces of polyamides from Table 1; (**B**) Corresponding X-ray reflections [86], copyright 2023, Elsevier.

In the bio-based PA through ring-opening, polymerization of lactam lysine derived from glucose is cyclized and undergoes deamination to produce CL. This approach is more sustainable although the stereo information is annihilated. Bio-based ϵ-caprolactam can be derived from 5-hydroxymethylfurfural (fructose), which takes two steps to be transformed

and then must be treated with ammonia obtain CL. When lactam is heated in a vacuum or when argon has a low HCL amount, PA with high molar masses in thousands are obtained. The specific chain length plays a crucial role, with PA showing high melting points of around 289 °C, which creates a scenario for use in high-performance applications. The derivation of lactam from camphor and nopinone is schematically represented in Figure 15.

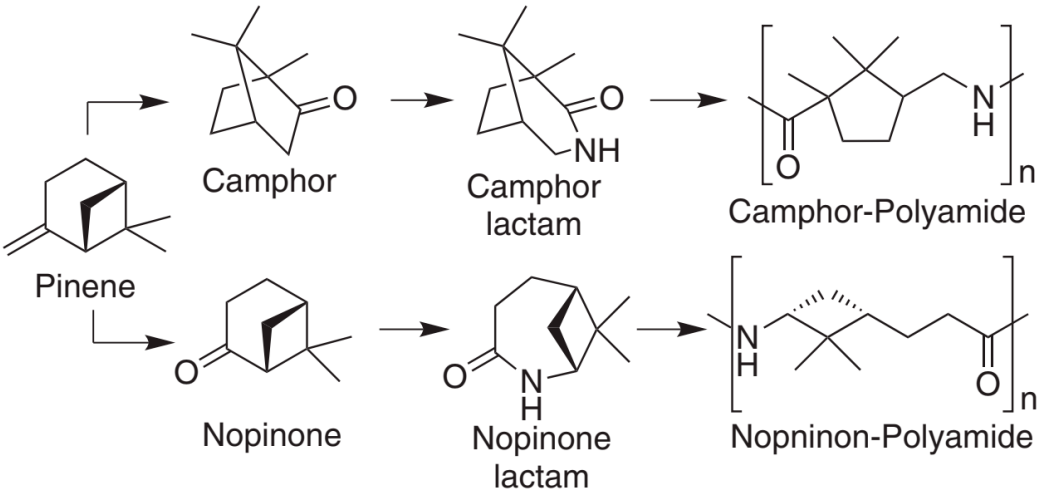

Figure 15. Lactams from camphor and nopinone as building blocks for sustainable, structurally significant polyamides [86], copyright 2023, Elsevier.

Similar to the previous bio-based polymers, further improvement in their properties (including mechanical) is required of PAs, and this has been obtained by incorporating fillers or nanofillers depending on the filler dispersibility. Moreover, PAs have been applied in diverse applications based on their performance in areas such as anticorrosive coatings [91], tissue engineering [92], flame retardant materials [93], and antifouling properties [94]. To this end, several methods have been explored to improve PA performance.

Touchaleaume et al. [95] developed a facile method to prepare PA6/pristine or organo-modified MMT clay nanocomposites using a water-assisted extrusion method, which improves the clay dispersion and reduces melting temperature of PA6 by 66 °C, leading to the prevention of polymer matrix degradation during processing. It is worth noting that the dispersion state and the thermal and mechanical properties of pristine MMT clay were found to be similar to that of organo-modified MMT clay [95]. By using melt-extrusion and injection moulding, a PA6/combined ratio of biocarbon/nanoclay-based nanocomposites was prepared, and fillers did not affect the degree of crystallization, while there was a strong influence on crystallite orientation. In this study, a small fraction of nanoclays in hybrid fliers exhibited improved coefficient of thermal expansion and mechanical properties. Furthermore, the obtained injection-moulded nanocomposites with ~28.5 wt% bio-based amounts showed excellent mechanical properties as well as enhanced dimensional stability suitable for use in sustainable automotive parts [96]. Further, the incorporation of rice husk ash (10–20 wt%) in fully (PA10,10) and partially (PA6,10) bio-based composites showed significant improvement in young's modulus, a slight reduction in tensile strength, and a large reduction in the deformation at the break. Both PAs showed similar matrix-filler stress transfer with rice husk ash, while exhibiting better properties than those of PLA. In addition, the addition of modified clay (Cloisite 30B) with 10 wt% rice husk ash in the composites exhibited the best thermo-mechanical properties [97]. In another study, a newly synthesised semi-aromatic PA and organo-modified-MMT-based nanocomposite were developed to improve flammability and thermal properties as compared to only a semi-aromatic PA matrix [98]. Further, semi-aromatic PA was reinforced with MWCNTs and prepared nanocomposites using a solution-mixing method, and improvements were observed in flame retardancy of semi-aromatic PA/MWCNT nanocomposites as compared to only PA [99].

In terms of thermal performance, to prevent excessive thermal degradation during high-temperature processing (i.e., compression moulding and injection moulding), thermally stable PA11/sulfated-CNC nanocomposites were prepared using the industrially viable method of ball milling followed by a compounding process. This industrially viable method of milling and compounding can be seen in Figure 16. The results showed enhanced storage modulus (in rubbery plateau) and Young's modulus while maintaining the toughness of PA11. In this study, the surface charge density of the CNCs exhibited good dispersion and improved mechanical performances. In addition, ball-milled nanocomposite samples exhibited higher stiffness compared to compounded nanocomposite samples [100].

Figure 16. Schematic representation of the premixing process of milling (Mi) and compounding (Co) to develop homogeneously dispersed PA11/CNC-based composites [100], copyright 2023, Elsevier.

In another study, the effect of nonmodified or aminosilane-modified CNCs on the isothermal and non-isothermal crystallization behaviour of PA6/CNC nanocomposites was investigated. In this study, nanocomposites were prepared using in situ anionic ring-opening polymerization and subsequent melt-extrusion. Morphological analysis showed a network-like fibrillar structure for nonmodified CNCs, while fine dispersion (mostly as individual whiskers) was observed for modified CNCs. The morphology and surface functionality of CNCs control the crystallization activity of PA6 composites. In this case, nonmodified CNCs hindered the polymer crystal growth, and modified CNCs improved the nucleation rate of the crystal [101]. Further, modified CNCs led to significant improvements in solid-state mechanical properties of the PA6/modified CNC nanocomposites due to fine dispersion and rigid interfacial layer, and they significantly enhanced melt elasticity and strength in shear and elongational flow in the nanocomposite systems [102]. PA11/dried CNF nanocomposites were prepared using direct melt-mixing, and the obtained nanocomposites exhibited good thermal and mechanical stability and melt processing behaviour. Peak force-quantitative nanomechanical mapping (PF-QNM) of nanocomposites showed higher structural order with 3 and 5 wt% CNFs and lower with 8 wt% CNFs as compared to the PA11, demonstrating good mechanical properties [103].

Another aspect to consider for PA processing is that due to the antifouling properties PA possesses, biofouling causes degradation of membrane properties such as permeability, selectivity, and long-term stability when utilized in membrane technology. To prevent this

biofouling, Ali et al. [94] used Ag-doped GO (GO-Ag) as nano reinforcement in PA thin-frame membrane and prepared PA/GO-Ag-based thin films via interfacial polymerization. The results exhibited a high-water flux recovery ratio (89%) and low irreversible resistance (10%) after hydraulic washing of PA/GO-Ag (80 ppm) nanocomposite membrane. Further, good antifouling properties of PA/GO-Ag (80 ppm) were observed with 86% reduction in viable *E. coli* cells in bacterial suspensions, with slight bacterial adherence only on the surface of nanocomposite membranes [94]. Further, nanofibrous scaffolds from PA66 and CS blends were fabricated using a one-step co-electrospinning method, and PA66/CS20% exhibited enhanced hydrophilicity and mechanical properties as well as osteogenic properties, including a high apatite-forming ability compared to only PA66 nanofibrous mats and other sample groups [104].

As a result of the biofouling, the biodegradation control function for this polymer is crucial. Therefore, Masui et al. [105] prepared visible light-sensitive PA4-TiO2 nanocomposite films (using the solvent-casting method) with antibacterial activity upon fluorescent light irradiation, and they improved it with increased concentration of TiO_2 under fluorescent light irradiation. Nanocomposite films showed high antibacterial activity with increased illumination intensity and irradiation time. Furthermore, biodegradation of PA4 was controlled by incorporating visible-light-sensitive TiO_2, where biodegradation is activated in the dark and suppressed when exposed to fluorescent light irradiation [106]. In addition, layered double hydroxides (LDH) as an alternative to silicate crystals were used to prepare PA6/LDH nanocomposite from organo-modified LDH using melt-processing. In this case, exfoliated nanocomposites were prepared with a low exchange capacity LDH, and residue tactoids were found with a high exchange capacity LDH [106]. In another study, flame retardant PA6/bridged 9,10-dihydro-9-oxa-10-phosphaphenanthrene-10-oxide (DOPO)-derivative (PHED) nanocomposite filament yarns were prepared through melt-spinning, and they produced knitted fabrics. The PA6/PHED (15 wt%) nanocomposite filament yarns showed enhanced thermos-oxidative stability and self-extinguishment of fibre strands and knitted samples within 1s followed by the significant reduction of melt-dripping and melt-drop flammability [85].

3. Bio-Based Polymer Degradation

In the life cycle of material, there will be either chemical or physical change due to varying environmental factors such as biological activity, light, heat, moisture, and chemical conditions, which is referred to as aging. This process leads to polymer property change as pertains to functional deterioration because of the physical, biological, and chemical reactions, which result in chemical transformations and bond scission, and thus, this can be regarded as polymer degradation. Degradation is noticeable when a material property changes in regard to mechanical, electrical/optical characteristics, erosion, delamination/phase separation, discolouration, cracking, and crazing. The degradation changes include new functional group formations, both bond scission and chemical [107]. Examples of the various polymer degradation routes are biological, photo, or thermal as shown in Table 2.

Table 2. Various polymer degradation routes.

Factors (Requirement/Activity)	Photo-Degradation	Thermo-Oxidative Degradation	Biodegradation
Active agent	UV-light or high-energy radiation	Heat and oxygen	Microbial agents
Requirement of heat	Not required	Higher than ambient temperature required	Not required
Rate of degradation	Initiation is slow; ut propagation is fast	Fast	Moderate
Other consideration	Environment friendly if high-energy radiation is not used	Environmentally not acceptable	Environment friendly
Overall acceptance	Acceptable but costly	Not acceptable	Cheap and very much acceptable

There is an increasing trend of polymer consumption in both industrial and domestic applications, which is inherently coupled with the substantial environmental threat the generated waste poses because of the lack of efficient waste management control. Degradation techniques, which include biodegradation as well as thermal and photo degradation, have been devised as a strategy for curtailing the effect of polymer disposal. For a bio-based polymer to be biodegradable, it should be hydrolysable at decomposition temperature (~50 °C) for a defined duration (usually 6 to 12 months). Due to hydrolysis, the polymer degrades in physiological environments through macromolecular chain scission into smaller parts and subsequently into a simpler end product with stability. Therefore, the hydrolysable linkages serve a vital role in the degradation of the polymer molecules through energy interactions. Basically, biodegradation of biopolymers can be categorized into two types, which are extracellular and intracellular depolymerases [108,109]. Biodegradation occurs when organic substances break down from the actions of living or unliving organisms. This is mostly used in the context of waste management, environmental remediation, and polymeric material because of its longevity. Organic materials degrade through either anaerobic (no oxygen) and aerobic (with oxygen) processes. Another related term is biomineralization, which is when organic materials are transferred to minerals [110]. Polymers undergo aerobic biodegradation in nature and anaerobic degradation in landfills and sediments, also breaking down partially aerobically and anaerobically within soil and composts. Overall, large polymers break down to carbon dioxide with the aid of a variety of several organisms, while parts of the polymer break down to their constituent monomers, and other constituents use monomers which excrete waste compounds in the form of usable by-products. Table 3 summarizes the various microorganisms that degrade polymers.

Table 3. List of different microorganisms reported to degrade different types of polymers [99], copyright 2023, Elsevier.

Polymer	Micro-Organism	Incubation Time	Reference
Poly(3-hydroxybutyrate-*co*-3-mercaptopropionate)	*Schlegelella thermodepolymerans*	18 h	[111]
Poly(3-hydroxybutyrate)	*Pseudomonas lemoignei*	60 h	[112]
Poly(3-hydroxybutyrate-*co*-3-mercaptopropionate)	*Pseudomonas indica*K2	18 h	[111]
Poly(3-hydroxybutyrate) Poly(3-hydroxybutyrate-*co*-3-hydroxyvalerate)	*Streptomyces* sp. SNG9	30 days	[113]
Poly(3-hydroxybutyrate-*co*-3-hydroxypropionate)	*Ralstonia pikettii*T1	18 h	[111]
Poly(3-hydroxybutyrate-*co*-3-hydroxypropionate)	*Acidovorax* sp. TP4	100 h	[114]
Poly(3-hydroxybutyrate) Poly(3-hydroxypropionate) Poly(4-hydroxybutyrate) Poly(ethylene succinate) Poly(ethylene adipate)	*Alcaligenes faecalis* *Pseudomonas stutzeri* *Comamonas acidovorans*	120 days	[115]
Poly(3-hydroxybutyrate)	*Alcaligenes faecalis*	20 h	[116]
Poly(3-hydroxybutyrate)	*Schlegelella thermodepolymerans* *Caenibacterium thermophilum*	2–3 days	[117]
Poly(3-hydroxybutyrate-*co*-3-hydroxyvalerate)	*Clostridium botulinum* *Clostridium acetobutylicum*	14 weeks	[118]
Poly (ε-caprolactone)	*Clostridium botulinum* *Clostridium acetobutylicum*	14 weeks	[118]
	Fusarium solani	60 days	[119]

Table 3. *Cont.*

Polymer	Micro-Organism	Incubation Time	Reference
Poly (lactic acid)	*Fusarium moniliforme*	40 weeks	[120]
	Penicillium roquefort *Amycolatopsis* sp.	14 days, 7 days	[121,122]
	Bacillus brevis	-	[123]
	Rhizopus delemer	-	[124]
Polymer Blends			
Starch/polyethylene	*Aspergillus niger* *Penicillium funiculosm* *Phanerochaete chrysosporium*	8 weeks	[125]
Starch/polyester	*Streptomyces* *Phanerochaete* *chyrsosporium*	8 weeks	[125]

Biodegradation research on polymers is carried out both in vitro and in vivo studies. In vitro techniques refer to when the procedure is carried out in controllable conditions, outside of a living cell. Most cellular biological experiments are performed outside of organisms. The downside of in vitro techniques is the failure to reproduce the exact conditions of the cell (Marshall protocol), notably a microbe. In vivo techniques refer to the use of living organisms instead of a partially or totally dead organism. In vivo techniques exist in two forms, which are clinical trials and animal studies. In vivo is preferred to in vitro because it suits an overall study of the experimental effects on a living subject [126].

3.1. PLA Biodegradation

Lactic acid is a chiral molecule that has two known enantiomers as L and D (lactic acid) and has the molecular formula $CH_3CH(OH)COH$ and organic acid. When in the solid-state, it is extremely soluble in water and white in colour. The solubility of lactic acid is extremely high, i.e., 1 unit of lactic acid dissolves in 12 units of water [127]. In liquid state, lactic acid is a colourless solution. Lactic acid is based on an aliphatic—hydroxy acid (AHA) because of the carbonyl group adjacent to the hydroxyl group, and its conjugate base is termed lactate [128,129]. PLA production is depicted in Figure 17a.

PLA single monomer is the lactic acid that is produced through either chemical synthesis or fermentation. Both optical active configurations D (−) and L (+) stereoisomers via fermentation are produced with bacterial fermentation (heterofermentative and homofermentative) of carbohydrates [127]. For industrial production of lactic acid, the lactic fermentation process is utilized instead of synthetic production of PLA due to major limitations such as capacity limitation, because of huge dependence on another process by-products, high cost of manufacturing, and lack of ability to produce the much desirable L—lactic acid stereoisomer. These stereo forms are pictorially represented in Figure 17b.

The degradation of PLA and PLA-based bio-composites involves the hydrolysis of the ester groups into either carboxyl or hydroxyl groups. This phase further enhances the autocatalytic action of the PLA composites that enable hydrolytic degradation. The oligomers and any fillers diffuse within the PLA matrix to a buffer solution that encourages autocatalytic activity. The degradation at the environmental level of PLA occurs through a two-step process. At the initial degradation phase, the large polyester chains are hydrolysed to create a smaller molecular weight oligomer. This reaction is boosted with either bases or acids and is heavily affected by moisture and temperature levels. Polymer embrittlement occurs at this step at certain stages where molar weight (Mn) reduces to less than 50,000 Da. In addition, at similar Mn, the degradation process of microorganisms in the environment is not interrupted through the conversion of smaller molecular weight part to humus, carbon dioxide, and water [130,131]. Vert et al. [132] and Li et al. [133] studied

the degradation of the mechanism of parallelepiped material comprising various PLA/GA polymers, copolymers, and stereo copolymers [124,125]. It was concluded that a greater size of PLA/GA polymers degraded heterogeneously, with the internal part degrading faster than the surfaces where degraded materials formed, and this is attainable for both in vivo and in vitro techniques [134].

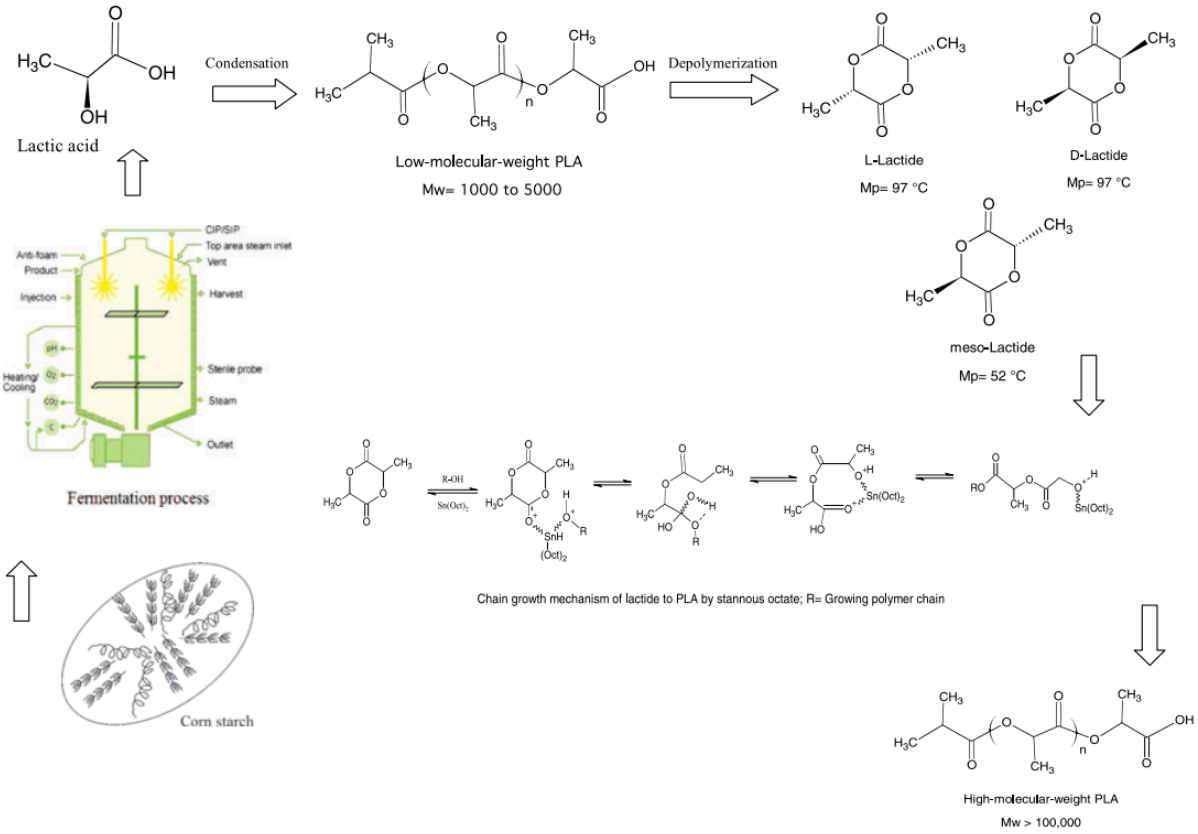

(**a**)

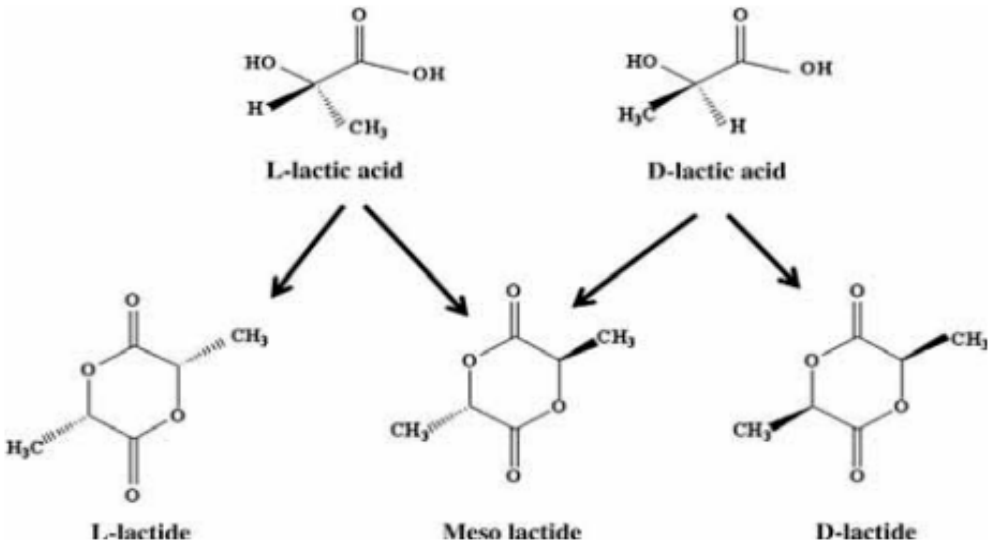

(**b**)

Figure 17. (**a**) Production stages for biobased PLA [127] copyright 2023, Elsevier. (**b**) Stereo forms of lactides [130], copyright 2023, Elsevier.

For moulded PLA components, the structural integrity reduces with molecular weight reduction and finally the material decomposing. On this note, Shimpi et al. [135] investigated the polymer composites of isotactic polypropylene (iPP) and PLA (iPP/PLA) and iPP/PLA packed with calcium carbonate nanoparticles ($nCaCO_3$). The biodegradable experiment was an in vitro study with a submerged culture of fungus P. chrysosporium for the microbial degradation of iPP/PLA and iPP/PLA/$nCaCO_3$ composites. The suspension (1%: 105 spores per ml) was inoculated into a sterilized basic method with varying preweight composites. These samples were incubated for varying days (7, 14, 21, and 28 days) at ambient temperature. The extracellular protein was excreted, and biomass produced from the fungus (reacting metabolically when degrading) was obtained and analysed at the incubation stage. A noticeable change occurred in the growth of fungus due to culture density changes. In addition, from the turbidity of the solution, it was observed that there was fungi growth (as seen in Figure 18a,b).

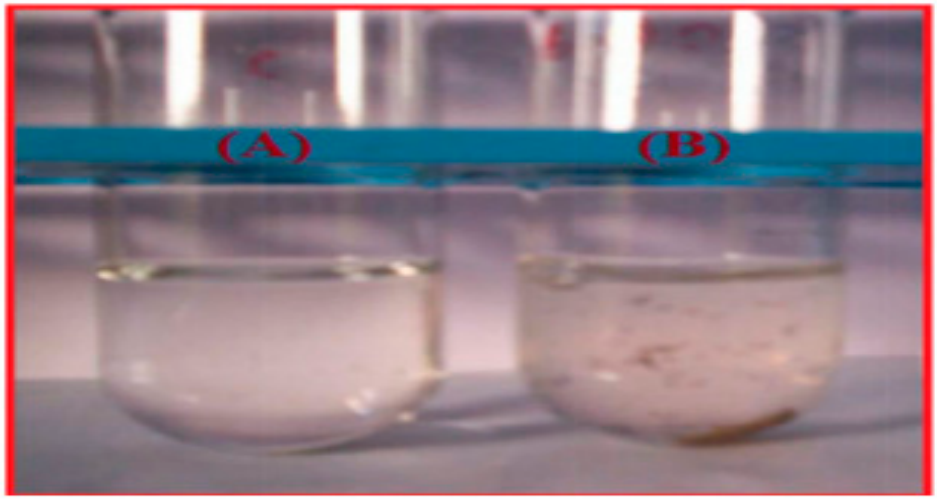

(**a**)

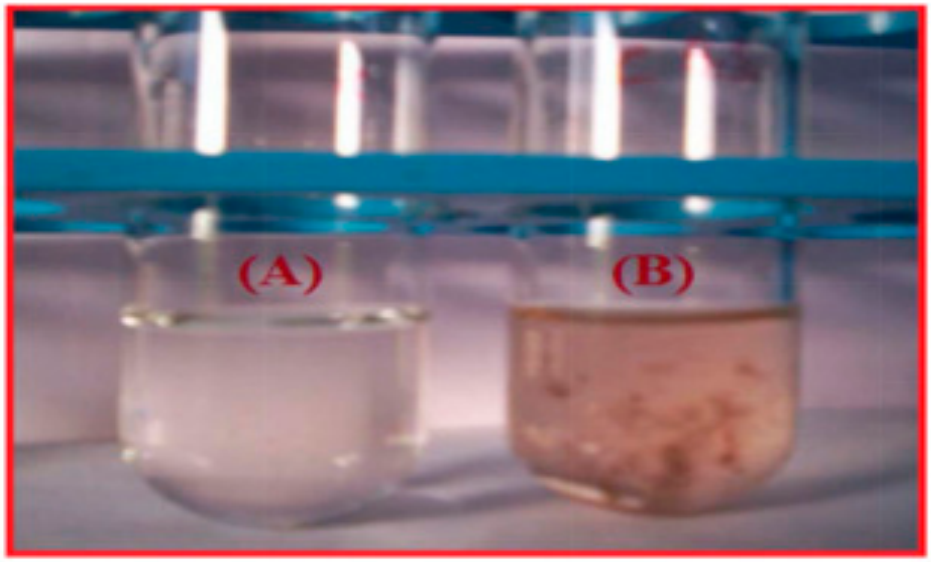

(**b**)

Figure 18. (**a**) 30% of degradation for IPP/PLA composites (**aA**) before and (**aB**) after 28 days of degradation; (**b**) 5 PHR IPP/PLA/$nCaCO_3$ nanocomposites (**bA**) before and (**bB**) after 28 days of degradation [135], copyright, 2023, Wiley online library.

In the Shimpi et al. [135] study, all the compositions exhibited fungal growth between 7 to 28 days. Maximum turbidity was noticed at the 28th day because of the stationary phase and lyses fungal biomass. Figure 19 shows that the *P. chrysoporium* aided the maximum growth process of biomass production iPP/PLA composites and iPP/PLA/$nCaCO_3$ nanocomposites. The study concluded that both iPP/PLA composites and iPP/PLA/$nCaCO_3$ nanocomposites support fungal growth of *P. chrysoporium*, which leads to degradation and is revealed through the production of biomass, excretion of extracellular protein, and reshaping of the matrix structure with a proportion transformation in degradation.

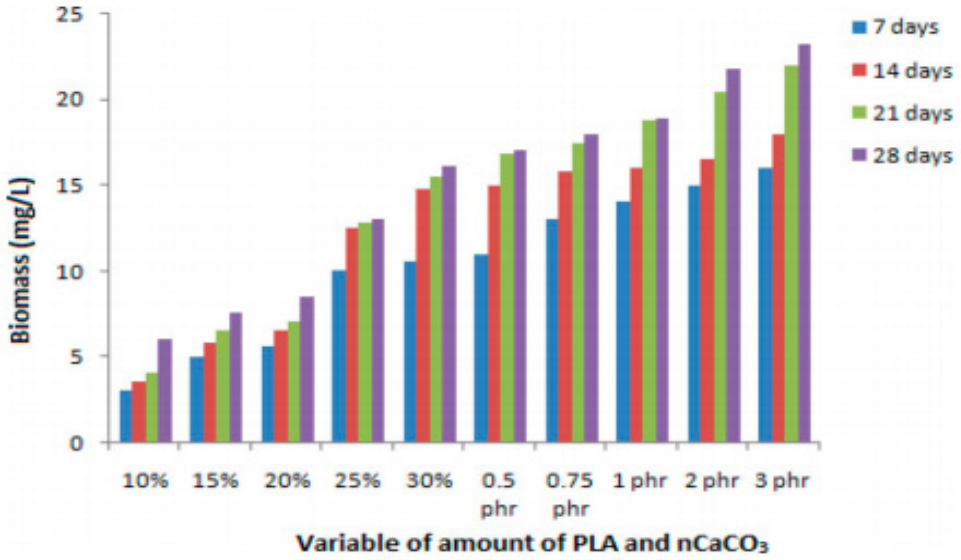

Figure 19. Biomass production density observed for iPP/PLA composites and iPP/PLA/$nCaCO_3$ nanocomposites [135], copyright, 2023, Wiley online library.

In a previous study, it was ascertained that with the secretion of protein, an increase in degradation of both iPP/PLA/$nCaCO_3$ and iPP/PLA composites occurred due to the addition of $nCaCO_3$ [136]. In addition, the better spacing of the treated montmorillonite (MMT) allowed for easier water absorption into the polymer chains which triggered the degradation rate with fungal growth within the polymeric matrix. Due to this microbial attack, the mechanical properties of both composites after degradation were observed to reduce, owing to the maximum fungal growth associated with segregation of the reinforcement and polymeric chains. Generally, PLA is highly resistant to degradation when subjected to regular environmental conditions compared to any other type of aliphatic bio-based polymers, which makes PLA not readily available for degradation. However, in comparison to P(3HB,4HB) blends, they both biodegrade in varying conditions (i.e., soil depth), with PHA degrading faster with the sequence of its increasing weight content in a composite, as well as faster than the PLA alone. Although PLA will hydrolytically degrade through bulk hydrolysis (decrease of carbon content while oxygen content increased), PHA biodegradation is the result of bacteria-catalyzed erosion initiated at the surface that spreads inwards. For PLA, this hydrolysis cleaves the ester bonds that generates oligomers and monomers of lactic acid. Therefore, microbial strains and humidity conditions are key parameters for PLA biodegradation. In addition, the introduction of nanoclays into PLA has been established as a method of enhancing the PLA degradation rate due to the presence of hydroxyl groups related to the silicate layers in the clay. However, this depends on the affinity of the microbial strain to the nanoclay.

3.2. PA Biodegradation

Polyamides are a useful class of polymers due to their exhibition of electrical insulation, abrasion resistance, tensile strength, high impact and tunability, and biocompatibility, depending on the structure of the PA. This positions PAs for a variety of industrial applications [136].

PA6 biodegradation was studied in intrauterine devices (IUD), with an in vivo technique, by Hudson and Crugnola [137] over two years. The results were obtained with the aid of synthesised 14C, labelled PA66, exposed in vitro to varying enzymatic solutions. PA66 was noticed to be unaltered by esterase but degraded when in contact with trypsin, papain, and chrymtpysin although this degradation is minute [138]. From biochemical studies carried out on the biodegradation of PA66 with lignin-degrading fungi [139,140], the presence of polyamide degradation from enzymes was noticed in the culture medium of a white decayed fungus strain. A polyamide degradation scheme does not rely on external hydrogen peroxide (H_2O_2), but catalase inhibits it. A nuclear magnetic resonance (NMR) study suggested that there was an attack by the enzyme on the methylene group adjoined to the nitrogen atom on the polymer chain, and the subsequent reaction occurred oxidatively, as shown in Figure 20.

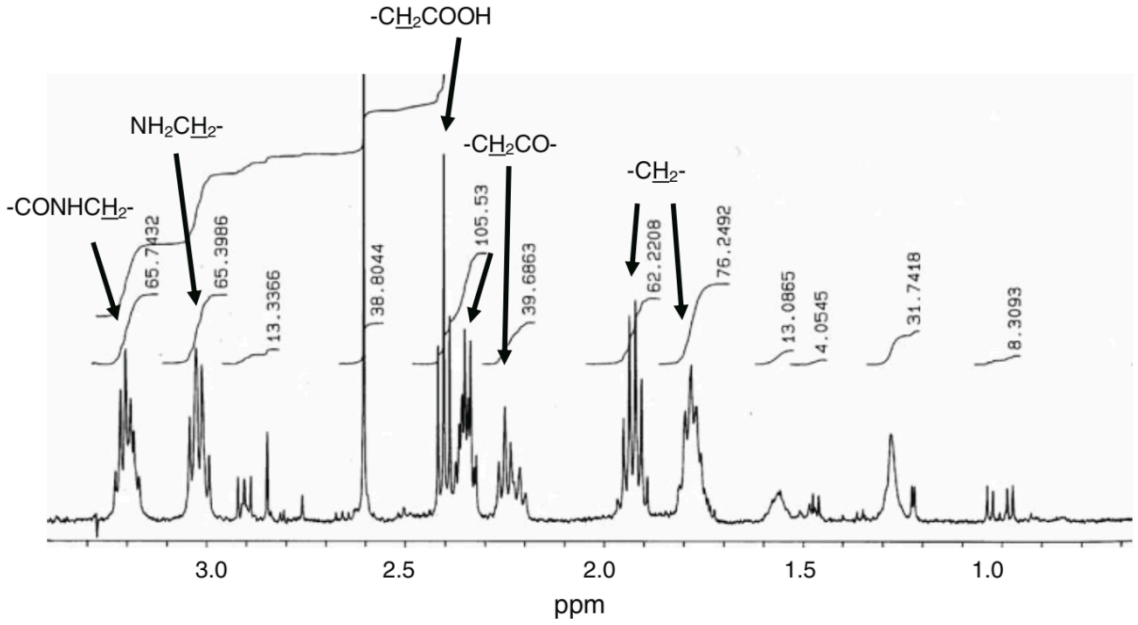

Figure 20. NMR spectra of soluble intermediates [141], Copyright © 2008, Springer, LLC.

Yamano et al. [141] researched the mechanism and characterization of PA4 using Pseudomonas sp. It was deduced that polyamide hardly degrades naturally in the environment, although protein possesses an amide bond, which easily degrades when applying proteolytic activity. However, some microorganisms are known for degrading polyamides; for example, flavobacterium sp. K127 can degrade PA6 oligomers hydrolytically [142], but PA6 polymers cannot be degraded by it. Deguchi et al. [139] observed that white decayed fungi strain IZU -154, Trametes Versicolor, Phanerochaete, and chrysosporium exhibit PA6 and PA66 biodegradation activity via a process of oxidation.

Yamano et al. [141] also reported on the biodegradation mechanism of PA4 and described the seclusion of PA4-degrading bacteria from an initiated slurry. NMR analysis showed that Pseudomonas sp. caused degradation of PA4, with the ND-11 strain having higher degradation than the ND-10 strain. The CO_2 gas increased within the trap, and NO_3^- ions were observed in the culture broth, which indicates that the end products of PA4 degradation by ND-10 and ND-11 were NO_3^- and CO_2.

Figure 21 shows the PA4 degradation by ND-11 strains after 14 days in aerobic conditions. The PA4 degraded by 0.5% (wt/vol) due to the ND-11 strain, whereas there was an increase in the total organic carbon (TOC). This result suggests that there was a conversion of PA4 into water-soluble minute molecules. The difference in PA4 and PA6 degradation based on the microorganisms used is due to the varying biodegrading mechanisms between the two polymers despite the fact that they possess identical amide bonds in their molecular structure. From the culture supernatants analysed (as seen in Figure 21b), measurement of the enzymatic actives of the supernatants was carried out, and there was a degradation of PA4 emulsion by the supernatant. Both the supernatant protein concentration and PA4 degrading activities had increments with time; there was no increase in the protease activity. Based on the results, it was suggested that the degrading enzyme for PA4 varies with proteases measured, with azocasein being a substrate. This calls for future study on the characterization of degrading enzymes [141]. In terms of molecular weight measurements, Figure 21 depicts the changing polymer residue amount. The reduction of polymer residue intensity with changing time shows the degradation of the polymer; however, there was no reduction in molecular weight. This indicates that for PA4 degradation, it started from the polymer surface, and the lower molecular weight dissolved was removed quickly by the aqueous phase solution. Due to this, there was no change in the molecular weight of the remaining polymer. The results suggest that the use of degrading bacteria on PA4 produces extracellular enzymes and converts PA4 to GABA (gamma-aminobutyric acid). With the use of this enzyme, continuous production through a chemical recycling system can generate PA4.

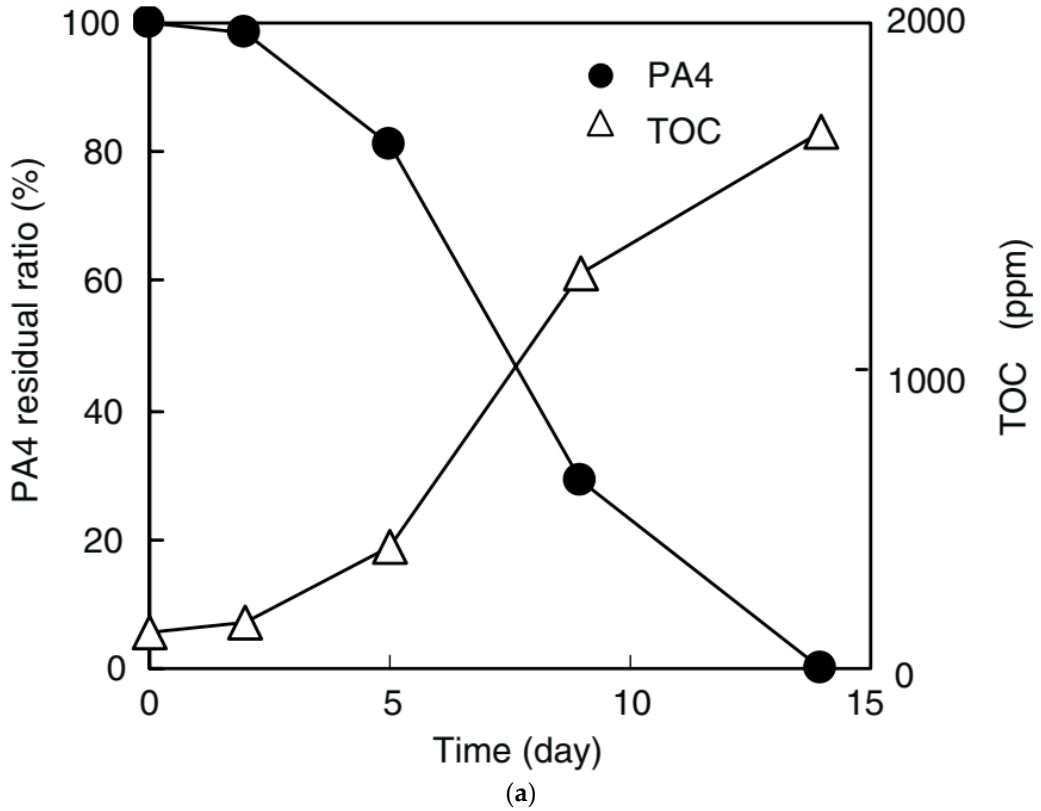

(**a**)

Figure 21. *Cont.*

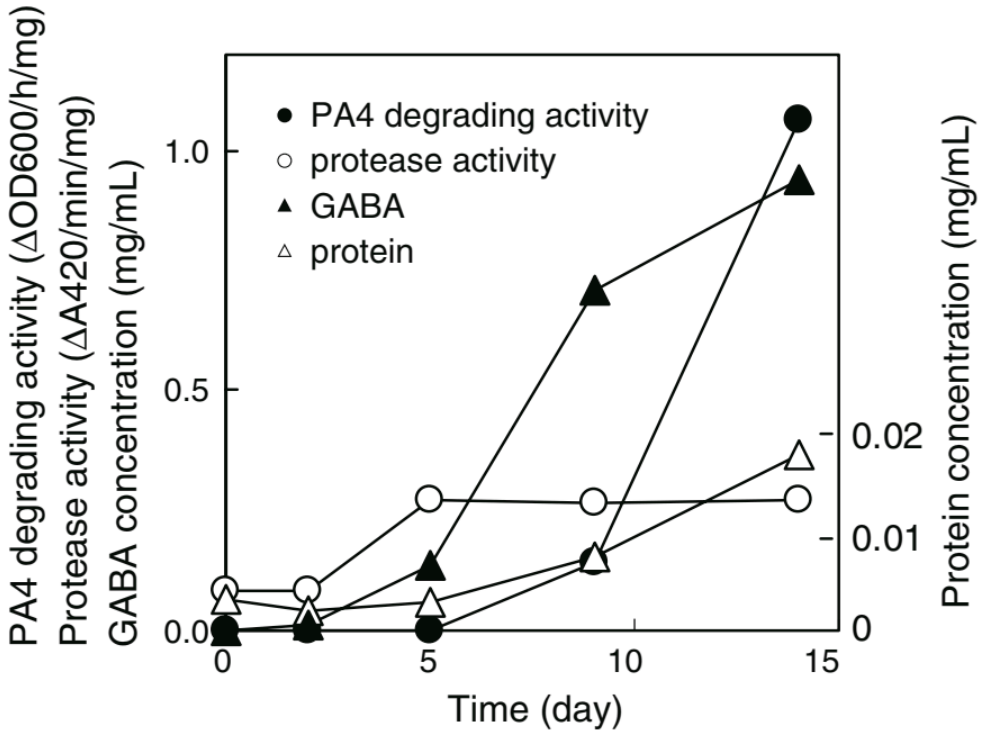

(**b**)

Figure 21. (**a**) Weight loss of PA4 and increase of TOC in PA4 biodegradation process; (**b**) Enzymatic activities of culture supernatant and GABA concentration [141], Copyright © 2008, Springer, LLC.

Essentially, PA is hydrolysable and more susceptible to biodegradation because of the presence of extracellular hydrolases involved in protein and cellulose degradation. However, polyamides such as PA6 are highly resistant to microbial interaction. Although their amide linkages are similar to peptide bonds of protein, they differ in that the alkyl component of the PA is less polar than the proteins, and the proteins have no presence of varying side chains. In addition to hydrolase, there are other hydrolysis enzymes for PA (i.e., protease, amidase, and cutinase) that can bolster microbial activities. Besides hydrolysis, enzymatic oxidation also contributes to the oxidative degradation of PA.

In addition, PAs have strong cohesive intermolecular force created from the hydrogen bonds between the molecular chains of the PA, which makes them have poor degradation in comparison to other polyesters. Through the use of these extracellular enzymes, hydrolytic and oxidative degradation of the PA occurs from chain scission of the chains, which results in short-chain polymers and small molecular bits such as oligomers, monomers, and dimers. From this review, it was observed that the level of biodegradation for PAs is mainly noticed from the reduction in molecular weight. Other observations are the oxidative discolouration of the PA, with possible degradation into the production of linear and cyclic monomers, as well as oligomers based on the result of enzymatic hydrolysis.

3.3. PCL Biodegradation

Poly (ε-caprolactone) (PCL) belongs to the biodegradable polyester family. Natural polyesters are known by the general formula (R-OCO-R) nx majority of the aliphatic polyesters and are derived from lactone ring polymerization. The most prominent polyesters are Poly (ε-caprolactone), which are industrially synthesised through ring-opening polymerization of ε-caprolactone (Figure 22) with the aid of a catalyst (metal oxides).

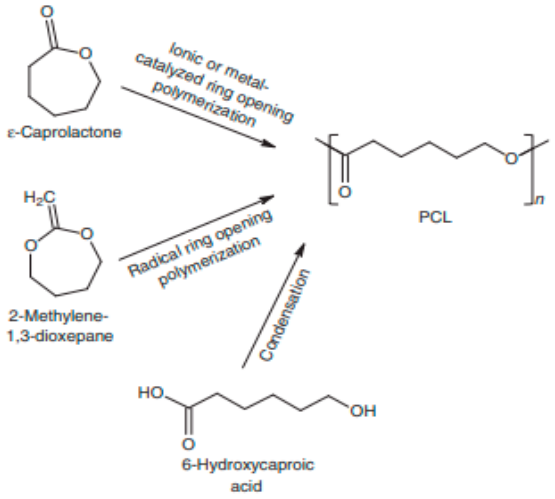

Figure 22. Synthetic routes to PCL by ionic or metal-catalyzed ROP of ϵ-caprolactone, by RROP of MDO, and by condensation of 6-hydroxycaproic acid [143], Copyright 2023, Hindawi Publishing Corporation.

Most early known reports on aliphatic polyester biodegradability were based on PCL; it is also a biocompatible polymer with the ability to be degraded by a wide range of cell types. PCLs exhibit an intrinsic hydrophobic nature, due to their poor wetting surface and interaction with biofluids, hence avoiding cell proliferation and adhesion [144]. This relatively high hydrophobicity and crystallinity is responsible for the seemingly slow degradation of PCL. Due to the nature of toxicity of polycaprolactam, it is mostly included as an unreactive monomer in the wastewater of PA6 industries, and therefore extraction of PCL from the waste stream is critical. Successive metabolism stages of caprolactam using nitrogen and carbon as the sole sources were studied [145]. Pseudomonas aerugiosastrain, mcm B-407 was secluded from the activated slurry that treats waste from industry-produced PA6 [146]. This microorganism can extract poly-caprolactam with a subsequent decrease in chemical oxygen demand (COD).

Lam et al. [147] characterized the PCL degradation mechanism through in vitro studies by DSC, GPC, and SEM and suggested that HO- radical is a noteworthy cause of the degradation of PCL implants. Woodward et al. [148] also carried out an in vitro degradation and concluded that PCL shape plays no role in degradation rate; rather, it is a homogenous degradation that dominates this procedure. Diaz et al. [143] carried out the studies on in vitro degradation of PCL/nanohydroxyapatite (nHA) composite scaffolds. The technique of fabrication for this research was thermally induced phase separation (lyophilization) and the addition of nHA before fabrication of the composite scaffold; this procedure allowed for the proper homogenous dispersion of the nHA particles. From the analysis, the degradation kinetics relied highly on the molecular weight of the polymer. Materials with large molecular weight take more time to degrade and are added through the polymer chain length. The number of ester bonds to be cleared is determined depending on the increase in chain length from higher molecular weight, and this is necessary for the generation of water-soluble oligomers/monomers that allow for erosion, with subsequent degradation taking longer. The PCL polymer is hydrophobic semi-crystalline, with its crystallinity continuously reducing with increasing molecular weight.

From Figure 23, based on SEM imaging, the nHA particle present in the PCL scaffold tends not to have any impact on pore size. However, nHA presence leads to an irregular morphology, as there is no disturbance of the solvent crystallization and pattern changes in crystal growth by the nHA particle. Mechanical properties are an aspect of the research due to the scaffolds acting as conveyors of growth and protein factors.

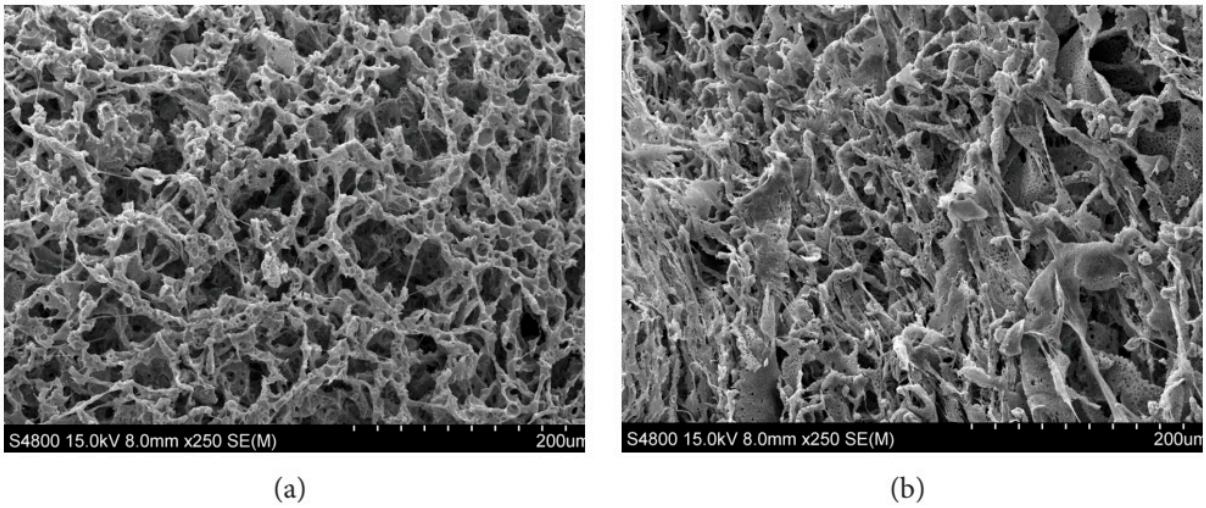

Figure 23. SEM observation of surface morphology of PCL × 250; (**a**) PCL before degradation; (**b**) PCL/10 wt% nHA before degradation [143], Copyright 2023, Hindawi Publishing Corporation.

From Figure 24, the mechanical properties (yield strength and compressive modulus), which are a function of degradation time, linearly increase with an increase in nHA particles added to the scaffold, with a variation when there is a higher nHA content but constant sample size. This can be attributed to the immediate shift in the scaffold morphology, which is due to high nHA concentrations assuming a fibrous appearance.

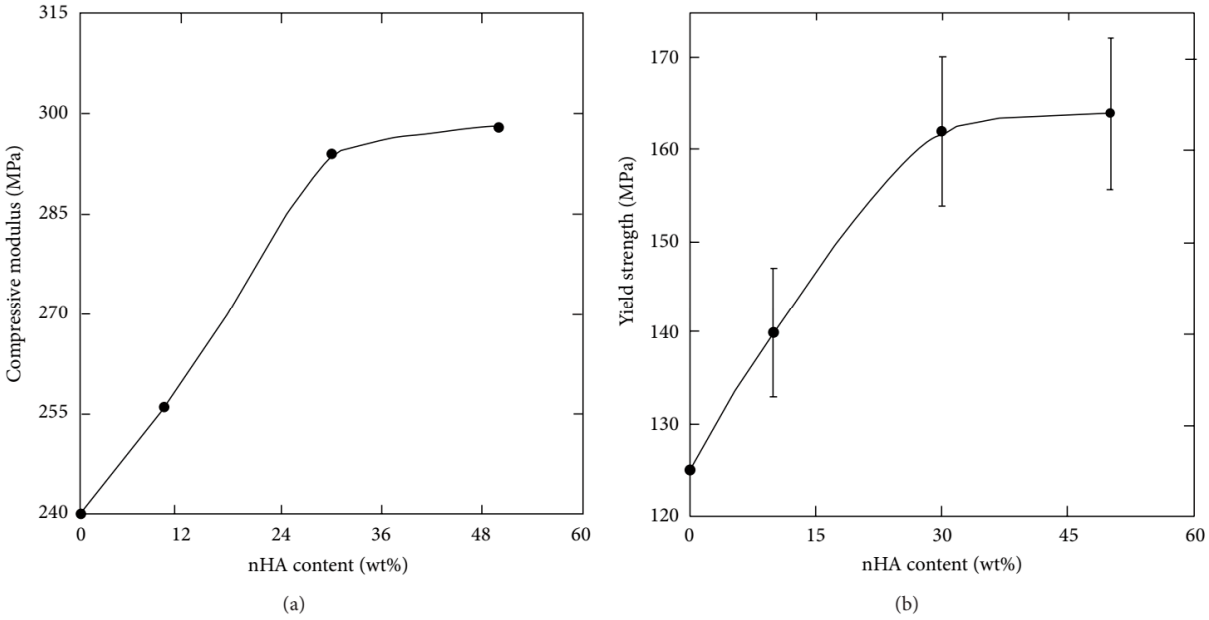

Figure 24. (**a**) Compressive modulus and (**b**) yield strength of PCL/nHA composite scaffolds as a function of nHA content (wt%) [143], Copyright 2023, Hindawi Publishing Corporation.

The degradation behaviour relies on the hydrolytic cleavage of ester bonds, which leads to scission of the random chains. Although the mechanical properties of PCL were retained in Diaz et al. [143], PCL/nHA composite properties reduced during the degradation process; the samples with the higher nHA concentration were more affected. The incorporation of nHA particles to PCL accelerated the degradation; depending on the purpose of use, variation in nanoparticle sizes might increase or reduce degradation.

Sun et al. [149] conducted an in vivo study to grasp the adsorption, degradation, and excretion of a PCL-based implant device. This was observed for 3 years in rats. For this

study, radiolabeling was used to trace to the adsorption, excretion, and distribution of PCL. The device was a 2-year contraceptive implant, which used composites of PCL/pluronic F68 compound and levonorgestrel solvent (LNG) powder as a filler; this implant is both organic acid water-soluble and pharmaceutically applied as an emulsifier. The change in molecular weight of the PCL capsules at changing time intervals were evaluated.

As shown in Figure 25, the PCL matrix tends to decline with time after implanting the rats. There was a noticeable relationship between time and the logarithm of molecular weight, which affirms the earlier stated mechanism of the ester linkages undergoing random hydrolytic chain scission. Figure 25b graphically shows the degradation of the implants at changing times within 3 years. In brief, the in vivo degradation in the PCL study indicates a two-stage pattern. At the first stage, there is molecular weight reduction but no mass deformation or loss. However, at the second stage, there is degradation when the molecular weight arrives at 5000 Da; at this stage, the material is shattered, and mass loss occurs.

Basically, PCL degrades due to hydrolytically unstable ester bonds. PCL degradation is a bulk process that can be divided into two stages, the first of which is the degradation of the amorphous phase, which increases PCL crystallinity, which is due to the reduction of chain scission and molecular weight as the cleavage occurs in the amorphous region. In the second stage, most of the amorphous region has degraded, which is followed by degradation at the crystalline phase. PCL is then susceptible to cleavage of the ester bond, and at that point the enzymatic surface erosion advances. This creates chain scission that reduces with the onset of weight loss. This reduction in the rate of chain scission is linked to crystallinity increase as cleavage occurs in the amorphous area of the polymer. The material weight loss is affiliated to the rise in chain scission of lower molecular weight and break up into the production of smaller particles. Essentially, PCL hydrolyzes through the bulk degradation mode from elevated kinetics at increased degradation temperatures and reduced molecular weights.

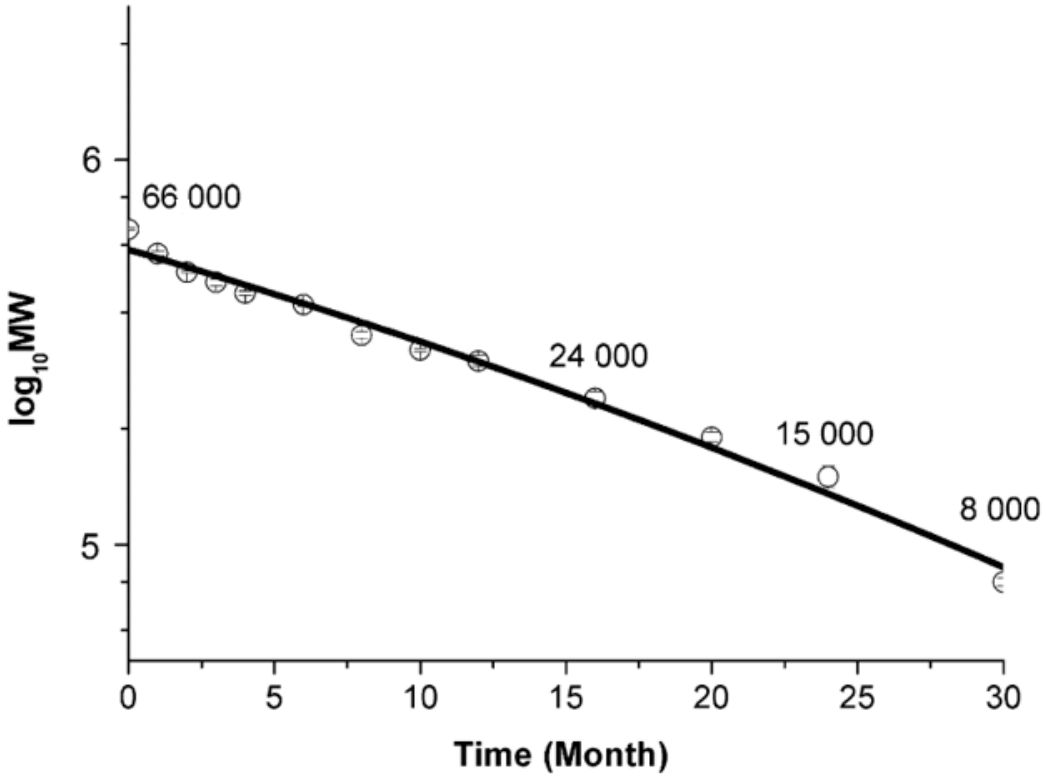

(**a**)

Figure 25. *Cont.*

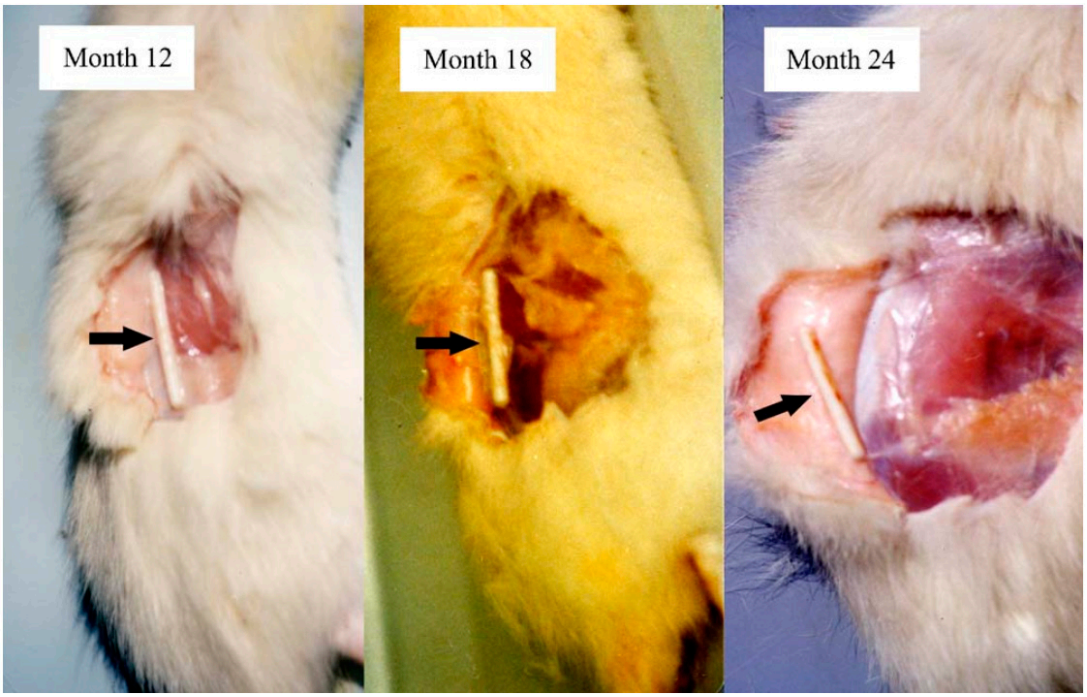

(**b**)

Figure 25. (**a**) Decrease in Mw of PCL/F68 capsules with time after implanted in rats. The results indicated a linear relationship between the logarithm of Mw and time; (**b**) Images of the PCL/F68 capsules in rats. The photographs were taken when the capsules were withdrawn from rats at different time points, showing the open site of the implantation and the appearance of the capsules. Black arrows indicate the PCL/F68 capsules [149], copyright 2023, Elsevier.

Biodegradation of PCL results in the fragmentation of the polymer until total decomposition into H_2O and CO_2 through microbial interactions. Enzymatic degradation occurs on the PCL surface from microorganism interaction while hydrolytic degradation occurs very slowly due to PCL's hydrophobic nature. Similar to the other bio-based polymers, PCL is sensitive to environmental conditions, and the observed weight loss is because of increased chain scission at a low molecular weight from degradation. In addition, it is obvious that PCL tends to degrade faster in compost than in aqueous conditions. From the review, it can be deduced that in natural conditions, enzymatic hydrolysis is common while in laboratory conditions there is more chemical hydrolysis. Therefore, PCL is significantly influenced by the enzymatic attack from microorganism interactions in natural conditions instead of chemical hydrolysis, which is resisted by PCL.

3.4. PHA Biodegradation

PHAs are hydrolyzable bio-polyesters with their composition being the determinant of thermal and mechanical properties. The glass transition temperature varies from 45 to 190 °C and is reliant on the chemical composition. PHA has similar properties to polypropylene and has an anion barrier and moisture resistance properties [150,151]. PHB acid derived from neat PHB is relatively stiff and brittle while PHB copolymers, which contain fatty acid (β—hydoxyvaluric acid), will probably be elastic.

When certain limitations are taken out, the microorganism that creates and stores PHAs, which are limited in nutrients, may undergo degradation and metabolize [152]. However, there is no guarantee that the ability of PHA to be stored will result in degradation in the environment [153]. Simple polymers can be too big to pass directly through the bacteria cell wall. Therefore, the bacteria release extracellular hydrolases that can convert the polymers to their matching hydroxyl acid monomers [151]. R-3 hydroxybutyric acid is produced from PHB hydrolysis [154,155] while both 3-hydroxyvalerate and

3-hydroxybutyrate are produced from PHBV [156]. These monomers are soluble in water but little enough for diffusion through the cell wall; in one study, tricarboxylic acid cycle and β—oxidation oxidized PHA for carbon dioxide production and water as by-products in aerobic conditions. Methane can also be obtained when under anaerobic conditions [157].

Generally, there is no harmful by-product or intermediate during PHA degradation. A variety of anaerobic and aerobic microorganisms which degrade PHA (fungi and bacteria) undergo isolation in several environments [158]. Acid Vorax faecicios, Variovoxax paradoxes are readily found in soil, while the activity slurry has Allengenes faecals and Pseudomonas being isolated. Moisture does not solely affect PHA, and it is always stable in the atmosphere.

Shah et al. [159] studied an isolated streptocytes strain (Streptoyerticillum kashmeriense AF1), which can degrade PHB and PHBV, while the bacteria strain bacillus megaterium AF3 degrades PHBV. This was achieved through soil containing active sewage slurries based on the production of clear zones during hydrolysis of PHB and PHBV that contain a mineral salt algae dish. The rate of microbial degradation for PHBV films present in soil was based on distribution of a population of the microbes and the capability of the production of the PHBV-degrading microorganism that occupied the incubated PHBV film surface [160]. From this team of researchers' previous study [161], the SEM imaging captured (Figure 26) the PHBV film deep in the soil containing sewage slurry for about 120 days, showing degradation accompanied by surface roughening, cavities, disintegration, pits, and grooves.

Subsequently, S. kashmirense AF1 obtained on a PHBV film surface showed that the degradation activity was a combining effect of a microbial occupation of the film surface, which includes antinyocetes, bacteria, and fungi. The study aligns with that of Molitoris et al. [162] who observed varying irregular erosion pits on the surface of PHA, caused by Comamonas [162]. The Sturm test is also widely used to study biopolymer biodegradation for aromatic and aliphatic compounds [163]. The CO_2 evolved was gravimetrically calculated based on PHB and PHBV degradation as a result of Bacillus megaterium AF3 via Sturm test; from the results obtained for all cases, the CO_2 amounts involved during this activity were higher than the control.

For extracellular PHB depolymerases, several microorganisms have a crucial role in PHB metabolism in the environment and have been widely studied in the literature, i.e., the use of isolated and purified microorganisms such as Alcaligenes [164], Comamonas [112,165], and Pseudomonas species [166–168]. This proves that extracellular PHB depolymerases are predominant in the environment. From these analyses, it was revealed that enzymes are made up of catalytic domains, a substrate body domain, and a linking region that contains the two domains.

Essentially, the degradation of PHAs is reliant on the chemical structure (i.e., monomeric composition and side chain) and physical structure, which includes the sample dimension, surface morphology, crystallinity, and molecular weight. Similar to PLA, other factors are the depolymerase, moisture content, temperature, and microbial strain availability. It can be concluded from this review that the degradation of PHA is initiated by bond cleaving. The blends with 3HV and 3HB (medium chain length monomers) enhance the hydrolytic stability of the PHBV copolymer due to the higher hydrophobicity of PHBV over the PHB. For PHA, the PHA depolymerases, which are sequenced from organisms with degrading capabilities, are vital enzymes for degradation. PHA depolymerases hydrolyze the long, water-insoluble PHAs into smaller water-soluble materials that can absorb microbes that metabolize the monomers as if they were nutrients. Although bio-based polymer biodegradation rate may be unpredictable, certain concepts such as functionalization can be beneficial. Polymer functionalization offers a broad range of robust and reproducible degradation activity that is suitable to meet the objectives of sustainable polymer materials.

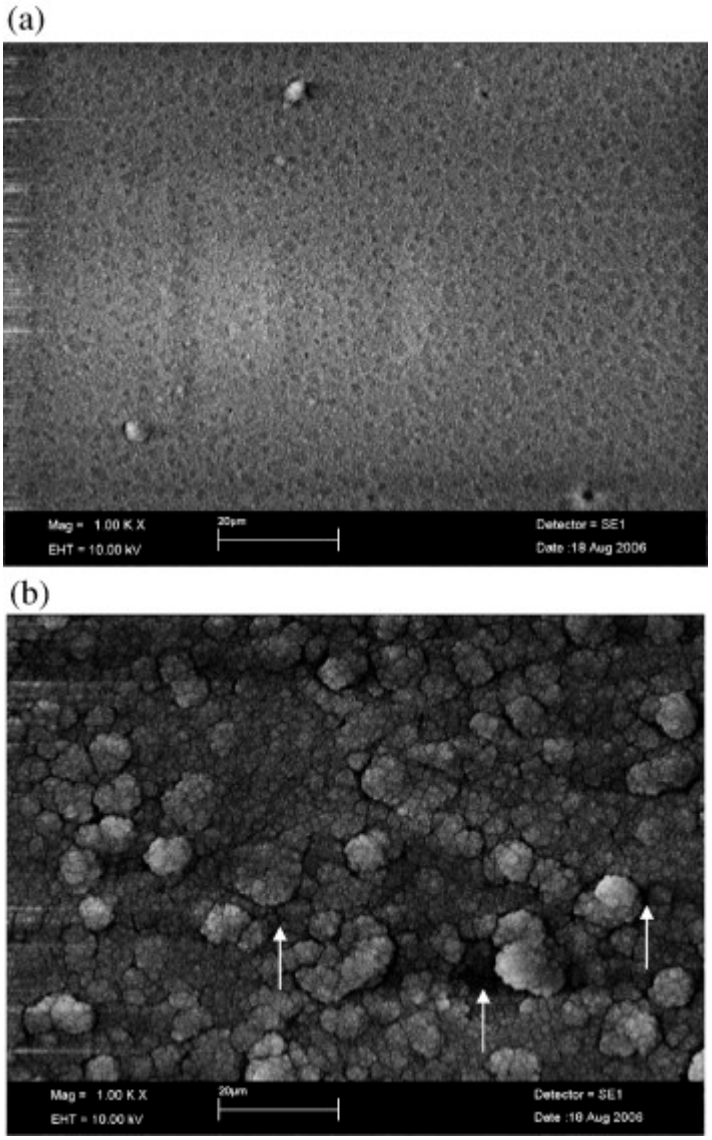

Figure 26. Scanning Electron Micrograph of poly(3-hydroxybutyrate-co-3-hydroxyvalerate) film (**a**) before soil burial and (**b**) after soil burial for 120 days [159], Copyright © 2008, Springer, LLC.

4. Other Influential Forms of Degradation

As stated earlier, degradation behaviour is an essential function of a biobased polymer and is dependent on the polymers' applications. Therefore, degradation can be either unwanted when it occurs during processing or needed in situations of biomedical utilizations. Degradation can either be biotic or abiotic, the former being involved with a biocatalytic process as described above [169] while in abiotic degradation, the biobased polymers go through certain changes over time when subjected to various environmental conditions such as heat (thermal) and light (photo), which are the inducers. These changes have a major impact on the properties and the service life of the polymers. Degradation because of heat is accelerated by exposure to reaction compounds such as ozone and stress [170].

4.1. Thermal Degradation

Thermal degradation is molecular deterioration as an outcome of overheating; this is an abiotic process that occurs mostly during manufacturing and thus is not wanted. At higher temperatures, the parts of the long-chain backbone disintegrate and react with each other to alter the properties of the polymer. The chemical reaction that occurs in

thermal degradation results in optical and physical changes with regards to the original specific properties.

As the material degrades, there will be a decline in mechanical properties such as composition, molecular weight, and molecular weight distribution of the polymers. Other molecular changes include chalking and cracking, colour changes, ductility, embrittlement (chain hardening), and softening (chain scission) [79].

A generic model for the mechanism path for thermal degradation is in the following paths:

(i) Initiation;
(ii) Propagation;
(iii) Termination.

An illustration of this degradation mechanism is shown in Figure 27 below, where the free radical is represented by R.

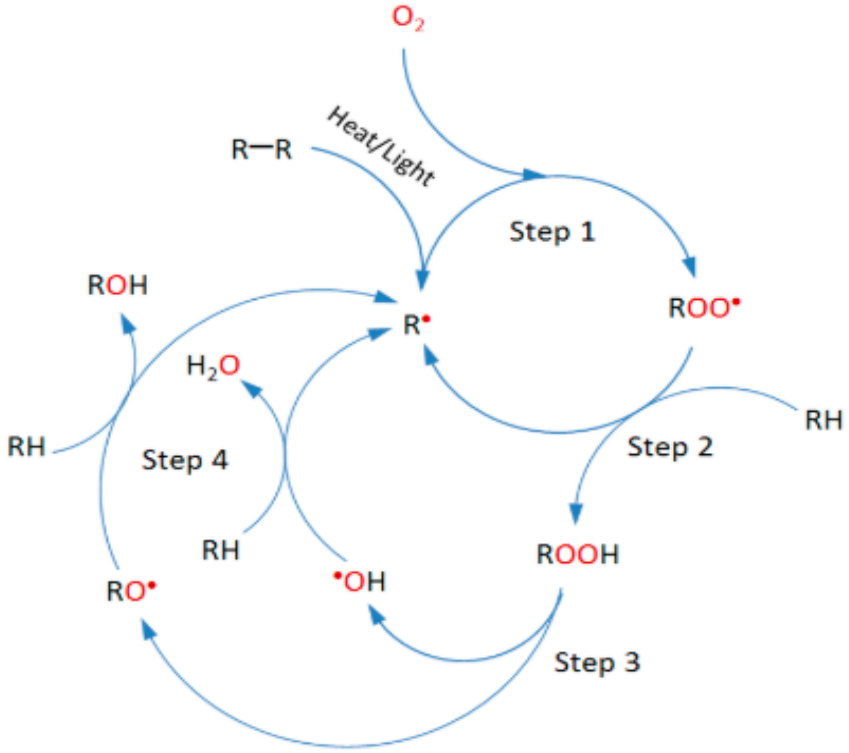

Figure 27. Generic thermal degradation mechanism [152], copyright 2023, Elsevier.

In general, an aliphatic polyester such as PLA has poor thermal stability. The degradation process can be initiated at lower temperatures such as 215 °C [171], whereas the main degradation can be derived from TGA to cover between 215–370 °C [171–173]. The peak of degradation falls at roughly 360 °C [171–173]. However, Carassco et al. [173] noticed that the thermal stability increases with the molecular weight increase. For the case of α—hydroxy ester PLA, it was finalized that the carbonyl-carbon-oxygen will probably break in heating with the reaction kinetics of the first order [172]. The thermal degradation mechanism seems to be complex, involving trace water amounts undergoing thermal hydrolysis, a zipper form of depolymerization, erratic oxidations of the central chain scission, and intra/intermolecular transesterification [168]. In addition, unreactive initiation monomer residual catalysts, reactive end groups [169–171], and impurities have been noticed to increase the thermal degradation of PLA [171,174]. PLA hydrolysis within processing is a key factor for molecular weight reduction as observed in some studies [169,175]. Therefore, efficient PLA granule drying is necessary for the extrusion process in order to reduce residence time and processing temperature.

Kopinke et al. [171] suggested that PLA can be degraded via inter and intrachain transesterification, which matches the outcome of the study by McNeill and Leiper [176]

via cis elimination, non-radical, and radical reactions, which provide CO_2, CO, acrylic acid, acyclic oligomers, and methyl ketone. Jamshidi et al. [177] and McNeill and Leiper [176] described the necessity of a non-radical destructive ester exchange, which involves terminal hydroxyl groups. Additives such as those produced by hydroxyl functional groups or deactivators of unused catalysts can enhance PLA melt stability [176–178]. Tsuji and Fukui [179] demonstrated an improvement of thermal stability lower than 260 °C from the formation of stereo complex PDLA/PLLA. Exceeding this temperature, there is a noticeable benefit of blended films, which can be attributed to stereo complex breakages and therefore the return to single PLA-chain properties. In addition, Ohkita and Lee [180] researched the thermal degradation of PLA/corn starch (CS) biocomposites; for all composites, a two-stage mass loss was noticed. The first stage of degradation was at 280–350 °C as a result of CS decomposition, which is similar to neat CS. For the second stage, the high temperature was within the range of 350–400 °C, matching the degradation of PLA. With an increasing weight % of CS, thermal degradation temperatures of the composite were reduced. It was concluded that the thermal stability reduced with CS addition, and the introduction of lysine diisocyanate (LDI) into the composite increased the thermal degradation temperature.

A two-stage degradation mechanism was proposed by Persenaire et al. [181]. It was finalized that the initial process showed a polyester chain rupture through an ester pyrolysis reaction. The evolved gas was recognized as CO_2, H_2O, and 5-hexenoic acid. The second stage resulted in the formation of ε-caprolactone (cyclic monomer) due to the unzipping depolymerization process. It is expected that the degradation rate would be massively reduced with PCL chain length. This behaviour can be attributed to the activation of the chain cleavage through pyrolysis reaction at the initial degradation stage. The acetylation of a hydroxyl end group has demonstrated an ability to mitigate the possibility of degradation from depolymerization. Although this is not the same for the second degradation mechanism where the initial obstruction of the terminal hydroxyl end group cannot prevent the degradation. In addition, the water molecules produced at the first stage can hydrolyse the polyester chains to produce a free hydroxyl end group and carboxylic acid. There was also a suggestion that the substitution of oxygen for helium could trigger an increase in degradation rate via thermoxidation.

The study by Rattanapan et al. [182] prepared and tested a bio-based polyurethane foam (PUF) from natural rubber and PCL diol. Based on the thermal degradation study obtained through TGA, the molar ratios between the four samples of the PUF with HTNR and PCL were 1/0 (PUF_1), 1/0.5 (PUF_2), 1/1 (PUF_3), and 0.5/1 (PUF_4), respectively. A two-step thermal degradation was noticed for the PUF1 sample while from the other sample there was a three-step thermal degradation. The first-stage degradation at 326–333 °C matched the methane bond breaking, the second stage of 352–370 °C matched the decomposition of HTNR [183,184], and the third stage of 437–465 °C matched the PCL diol decomposition. The maximum degradation temperature of the second and third stages relied on the PCL diol content.

PU thermal degradation can occur via various paths/methods such as cleavage of end chain, crosslinks, and random chain cleavage. Furthermore, a report by Chattopadhyay and Webster [185] emphasised that crosslink and random chain cleavage are the major decomposition paths, because PU crosslink cleavage requires higher thermal energy. Therefore, this decomposition begins with side-chain degradation.

PHB and Poly (3HB-co-HV) undergo thermal degradation at temperatures between 250–400 °C in nitrogen based on the study by Li et al. [186]. Poly (3HB-co-HV) seemed to have better thermal stability than PHB. The initiation for this degradation can be attributed to chain scission of the ester linkage. The PHB yield from this degradation is 2-butenoic acid, propane, and propenyl-2-butenoate, while that of poly (3HB-co-HV) are 2-butenoic acid, 2-pentanoic acid, CO_2, propenyl-2-butenoate, and butyl-2-butenoate.

Aoyagi et al. [187] experimented on the thermal degradation of PHB, PCL, and PLA. Through the activation energy for thermal degradation, PHB was proven to be greater

than PCL and matched PLA. However, there was a complexity in setting parameters for PHB thermal degradation solely through the TGA techniques, as PHB yields a less volatile product. Therefore, it was suggested that other techniques to analyse extensive parameters of this process in the melt phase be further researched.

Catalysts have proven to be influential in PLA and PHA thermal degradation by enhancing the depolymerization in a gentle condition and the yields formed [171,187–192]. Using a catalyst such as aqueous dibutyltin dimethoxide for thermal degradation of PHA leads to a cyclic ester, which can be easily repolymerized to the initial polymer, while an alkali earth compound catalyst produces vinyl monomers, which can be further reacted to yield higher Tg polymers [187] or can undergo microbial repolymerization to co- or homopolymers [189,190,192,193].

A major drawback for PHB has been its thermal instability during melt processing [191]. The study of the thermal degradation of PHB and other PHAs has gained increasing interest. Lately, it has been proven that PHB can be chemically recycled with final products such as cyclic trimer, linear oligomers (crotonate end group is present), [194] and crotonic acid [188]. Therefore, if materials sourced from renewable resources can be properly recycled, with specific controls of their thermal degradation (Figure 28), an efficient recycling process for these materials that minimizes production energy and resources should be provided.

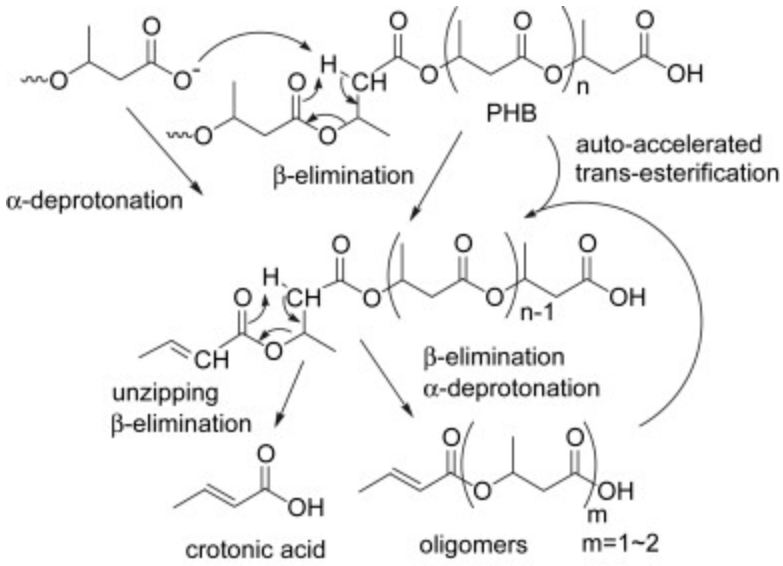

Figure 28. Expected thermal degradation pathways of PHB [191], copyright, 2023, Wiley online library.

Controlled thermal degradation with applicable catalysts is recommended for improved results. Other than biodegradability, the thermal degradation and stability characteristics of a bio-based polymer are necessary for their full application, processing, and thermal recycling [187].

4.2. Photodegradation

This form of degradation causes polymers to show a decrease in molecular weight and loss of mechanical property. This photochemical reactivity makes it a good fit for certain applications such as films that are exposed to sunlight and different weather situations, although this solution may not be sufficient for the initial problem of total degradation in a shorter span. Biodegradation will also be incorporated, although the potency relies on some factors such as the chemical and physical properties of the surface, inherent microbiota, and material composition [195–197]. The impact of these factors is massive to the extent that slight variation in the chemical structure may lead to significant changes as it relates to biodegradability. In the same way, other factors that hugely affect the progress

of biodegradation include the specific microorganisms to be used and environmental conditions [198].

In addition, some factors that could likely lead to photodegradation of biopolymers can be split into two parts [199,200]:

(1) Internal impurities—may possess chromophoric groups (acids, carbonyls, esters, etc.) that are being added to macromolecules in a polymerization process and storages, and they are:
   (a) Catalyst residue.
   (b) Carbonyl.
   (c) Charge-transfer complexes with oxygen.
   (d) Hydroperoxide.
   (e) Unsaturated bonds(-C=C-).

(2) External impurities—which possesses chromophoric groups are:
   (a) The compounds from polluted environments and smog (naphthalene and anthracene).
   (b) Traces of metals and metal oxides from machines and equipment (Cr, Fe, and Ni).
   (c) Traces of catalysts and solvents.
   (d) Additives (dyes, pigments, photo stabilizers, and thermal stabilizers).

Photodegradation specifically is a process whereby photons are absorbed, especially the wavelengths within the UV-visible spectrum, which leads to degradation of the molecules [201]. In this process, the molecules evolve and convert to new species. There are generally three types of photodegradation, which are:

1. Photooxidation—for the process there is a combination of UV lights and oxidants such as H_2O_2, Fenton or O_3 to enhance the degradation rather than solely UV [202].
2. Photolysis,—this process utilizes radiation and ultraviolet (UV) light to produce some reactive species, e.g., excited molecules, ions, and radicals [202,203]. The impact of radiation in the compound relies on the energy amount transferred through radiation and the compound's nature. The intensity can be increased in aqueous solutions via the formation of primary products from photolysis of water; this acts as an intermediate species and generates hydroxyl (OH^-), electrons (e^-_{aq}), and hydrogen radicals (H^-), which decompose the solutes.
3. Photocatalysis—this comprises a photoinduced reaction, which is enhanced through catalytic reactions. The process is initiated when the photon has the required energy (equal or greater than catalysts bandgap energy) to be absorbed. Consequently, there will be a separation of charges due to the movement of the excited electron (e^-) from the valence band to the conduction band of the catalysts; this produces a hole (h^+). The electron-charged holes can meander to the surface of the catalyst, which can move into other species that are spotted on the surface.

Certain semiconductors (such as TiO_2, CdS, Fe_2O_3, ZnS, and ZnO) can behave as catalysts because of the electronic structure of the metal atoms, which is known to have an empty conduction band (separated by the bandgap) and a filled valence band. The popular semiconductor is mostly used as a catalyst in TiO_2; this can be attributed to its biological and chemical inertness, ease of production and use, efficient catalytic reactions, and photocatalytic stability. It is also cost-effective and has a very low environmental impact [204]. ZnO can also be used as an efficient substitute.

Luo et al. [205] studied the effect of TiO_2 nanoparticles on PLA photodegradation. It was demonstrated from a sample preparation that was subjected to photodegradation through UV irradiation. There was an observation that the photodegradation was initiated at the interface of PLA/TiO_2 between the nanofiller and polymer matrix; there was also an indication of bulk erosion and heterogenous degradation mechanisms of all samples. The variations in FTIR structure with the degradation time showed that TiO_2 nanofillers modified the PLA's degradation when subjected to increased artificial UV radiation. An

increased degradation rate of PLA was observed with the introduction of TiO_2 nanofillers, and this impacted the level of dispersion for TiO_2 nanofillers. It was finalized that PLA photo degradability can be controlled by addition of TiO_2 nanofiller whereby the key factor is effective dispersion and distribution of TiO_2 nanoparticles. A depiction of a TiO_2-induced PLA photodegradation mechanism is presented in Figure 29.

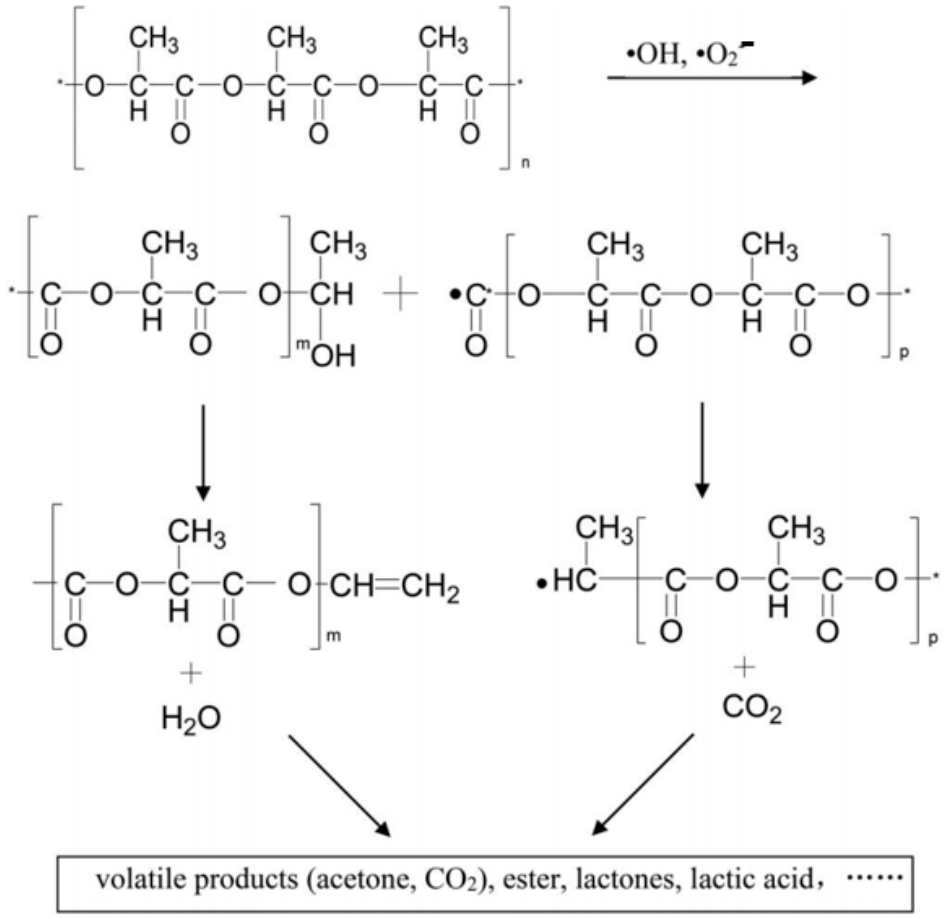

Figure 29. Photodegradation mechanism of PLA induced by TiO_2 under accelerating artificial irradiation conditions [205], copyright, 2023, Wiley online library.

Photodegradation mechanisms on PCL were studied by França et al. [206]; they were analysed by subjecting the samples to UV-B radiation for 9 weeks. From the results obtained, it was obvious that PCL was affected by radiation based on the alteration of the elongation at break and elastic modulus of the samples, which was linked to the obtained SEM images of fibrous and erosion morphologies. In addition, FTIR tests showed changes in the carbonyl group, which were verified from the appearance of microcracks in the microscopy results. There was also a noticeable increase in the degree of crystallinity with longer exposure time; this can be attributed to the result of chemi-crystallization.

The research conducted by Wellen et al. [207] on the photo stabilization and photodegradation of PHB within 12 weeks concluded that the extent of photodegradation relies on the *hv*/light (energy) content. This change is not solely based on the chemical structure but also on the colour of the samples. PHB with greater *hv* content is lighter than PHB of lesser *hv* content, and, as a result, the UV radiation penetrates at deeper lengths into the samples (test bars). Furthermore, fracture surface damage, molecular weight, mechanical properties, and whiteness were prominent on PHB with greater *hv* content. In terms of photostability, the addition of antioxidant additives and UV absorbers enhanced the UV stability of PHB and reduced the photodegradation rate as noticed from the degree of

crystallinity, mechanical properties, and molecular weight. This will be valuable for the design of materials with better stability during processing.

Han et al. [208] successfully prepared a free-standing, controllable visible light photodegradable PLA/chitosan (CTS)/molybdenum disulphide (MOS_2) film composite. The photodegradation mechanism of the PLA/CTS/MOS_2 film composite subjected to visible light was presented as follows:

$$MoS_2 + hv \rightarrow MoS_2(e^-, h^+) \quad (1)$$

$$e^- + O_2 \rightarrow O_2{}^- \quad (2)$$

$$h^+ + O_2{}^- \rightarrow {}^1O_2 \quad (3)$$

$$O_2{}^{0-} + H_2O \rightarrow HO^0{}_2 + OH^- \quad (4)$$

$$2HO_2{}^0 \rightarrow H_2O_2 + O_2 \quad (5)$$

$$H_2O_2 + hv \rightarrow 2HO^0 \quad (6)$$

$$h^+ + OH^- \rightarrow HO^0 \quad (7)$$

$$h^+ + H_2O_2 \rightarrow HO^0 + H^+ \quad (8)$$

The MOS_2 small bandgap was highly reactive to visible light and enhanced the absorption abilities of the visible light of the material. When exposed to visible light, MOS_2 in the composite absorbed photons, which resulted in the movement of the excited electrons from the valence band to the conduction band and generated a hole (h^+) on the valence band and an electron (e^-) on the collection band. These generated species reacted with environmental H_2O and O_2 to yield several free radicals (e.g., OH^-, H_2O_2, $O_2{}^-$, and $^1O_2$). These active radicals were moved to the surface of the material and attacked the close carbon chain, and a redox reaction with the materials occurred. These resulted in composite polymer chain breakage and degradation to oligomers and further degradation of H_2O and CO_2 [208].

The visible-light photodegradation of the PLA/CS and PLA/CS/MoS_2 composite films is shown in Figure 30. The photodegradation of PLA/CS/MoS_2 films was much faster as compared to PLA/CS films (see Figure 30A). Further, the photodegradation rate of PLA/CS/MoS_2 was reduced with increased irradiation time and prolonged exposure to visible light exhibited some wrinkles on the surface of the PLA/CS/MoS2 composite films (see Figure 30B).

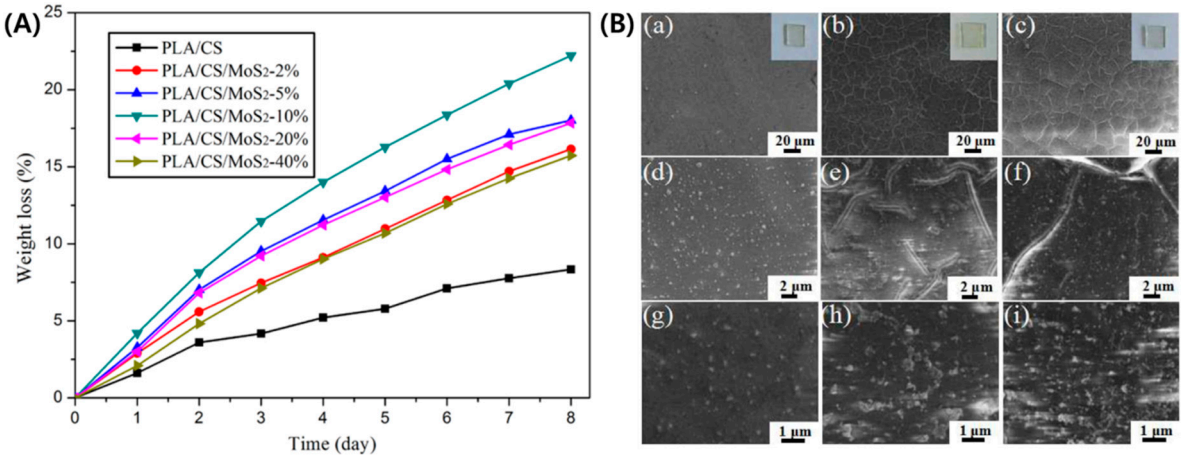

Figure 30. (**A**) Visible-light photodegradation analysis of PLA/CS and PLA/CS/MoS_2 composite films with various amounts of MoS_2 and SEM images of PLA/CS/MoS_2 composite films after exposure to visible light for 0 days (**B**(**a**,**d**,**g**)), 4 days (**B**(**b**,**e**,**h**)), and 8 days (**B**(**c**,**f**,**i**)). Inset: digital images of PLA/CS/MoS_2 composite films (**B**(**a**–**c**)) for 0, 4, and 8 days, respectively [208], copyright 2023, Elsevier.

This was also a similar mechanism for the research on bio-based PLA [203]. Natural additives are also potentials for photodegradation; the reviewed additives are quercetin (natural flavonoid antioxidants) [209], phoebe zhennan wood [210], and orontic acid, used as a nucleating agent on PLA and increasing the rate of degradation [211].

5. Potential Applications and Trends

Over the last few decades, there has been a rise in economic, environmental, and social demand for alternative materials, resources, and energy to replace existing fossil-fuel-based, nonrenewable sources. Bio-based polymeric materials derived from renewable feed sources are now a strategic avenue for sustainable development. A key advantage of bio-based polymers relies on biodegradability; however, from this review it has been deduced that not all bio-based polymers are inherently biodegradable. Other factors that influence their appeal are accessibility, low carbon footprint, economic efficiency, and low toxicity. Environmentally, bio-based polymers are beneficial to the earth and living organisms as they reduce the carbon footprint because they interact with microorganisms to degrade into constituent monomers with bi production of water, CO_2, and CH_4 without emitting toxic elements. Bio-based polymers are presently being applied industrially. Based on the ability of bio-based polymers to mitigate long-term economic and environmental threats from waste, they serve an integral role within the circular economy. For both economic and environmental considerations, aligning bio-based polymers with the current recycling network garners appealing propositions. However, they require a collegiately developed assessment of the life cycle and global incorporation of efficient organic waste management, as there is growth in specific feed material biowaste collection. It should be noted that not all bio-based polymers, including composites, are environmentally friendly, and hence, a polymer should be labelled as environmentally friendly only based on its lifecycle assessment rather than its origin. Bio-based polymers have the benefit of being capable of biological handling at the end of service life either through anaerobic digestion or composting.

To entirely adopt bio-based polymers into the circular economy, processing should be circular as well, which facilitates the use of waste streams and renewable sources. Hence, bio-based material can be repaired, reused, recycled, and remanufactured. The circular economy here is not solely restricted to resources but also includes the life cycle path, which may be based on economic, environmental, and technological cycles, especially for the future. There is a dire need for bio-based polymers produced from bio-based materials, and they can be processed through biological, chemical, or mechanical means. The combination of conventional and renewable raw materials facilitates bio-based polymer production. In terms of processing parameters, the multipronged approach is considered appropriate for the evaluation of processing viability. This implies that various techniques should be utilized in prioritizing, weighing, and ascertaining the sustainability parameters for assessing alternatives such as petroleum-based products against bio-based products. The key efficient processing methods for these polymers include extrusion (higher mixing efficiency, short processing time, and continuity), melt compounding, electrospinning, and extraction. A novel processing technique is the biorefining strategy, which uses biomass efficiently to prepare bio-based polymers. Industrially, the biorefinery process will need a highly efficient conversion rate of the feedstock to produce biopolymers. Furthermore, the pretreatment method serves a critical role in the processing of bio-based polymers regarding to any requirement in altering the chemical composition.

Recently, microwave-assisted synthesis is being championed industrially as it offers feasible alternatives to conventional heating techniques that enable benchmarking in terms of energy and time efficiency. They possess the capability of reducing heating duration and materials with superior homogeneity, which serve a central role in the optimization of the production processes, as heating is needed for chemical alterations, and polymer processing can improve in-service performance. Moreover, microwave irradiation is applicable in deriving bio-based polymers from natural biomass at an industrial scale. Another

disruptive processing technique is 3D printing, which manufactures tailor-made products in a layer-by-layer approach using computer-aided design, which is expected to some extent to replace the conventional polymer manufacturing technique. There is also the exploration of 4D printing, which has time as a dimension. Basically, the use of 3D printing of bio scaffolds with bio-based polymers is a growing area, and it is expected to witness exponential growth in the future. The key advantage is where a bio-based polymer such as PLA is applied as a bio scaffold that degrades into components viz, anhydrides, carbonates, esters, amides, etc., making it compatible with the human body. Consequently, the major application of bio-based polymers is the medical industry because of their biocompatibility and biodegradation with nontoxic effects. They are increasingly being used as elastomers, plastics, and adhesives. Regardless of current progress with bio-based polymers, further evaluations are required to establish the feasibility of bio-based polymers replacing their petroleum-based counterparts.

Despite the massive environmental impact bio-based polymers provide, the full utilization of bio-based polymers is hindered by their relatively poor barrier and mechanical properties in comparison to petroleum-sourced counterparts. This creates the need for reinforcing them with fillers and compounds that boost their properties and performance. In terms of the effect of UV irradiation on biodegradation, industries such as agriculture have recently been using biopolymers such as PLA for making films for mulching applications due to their biodegradability [212]. These mulching films, which enable moisture retention in the soil and the regulation of surface temperature, have their mechanical properties impacted by solar radiation. This is attributed to the crosslinking that occurs and tends to impede biodegradation due to the decrease in the ability of higher molecular weight polymers in absorbing microorganisms [213]. Hence, further investigation is needed on the effect of ultraviolet (UV) irradiation on the biodegradability of bio-based polymers. To improve the mechanical properties of the bio-based polymers in a reproducible approach at a commercial scale, the monomers undergo isolation, modification, or/and synthesis. The polymers can also be reinforced with organic and inorganic fillers, and processing factors can be optimised. These reinforcing agents or compatibilizers are introduced into the polymers to make them feasible for structural application. Whereby the properties of these bio-based polymers are bolstered by reinforcements to form composites, varying processing synthesis techniques are constantly investigated based on their applicability. The final properties of these biocomposites are dependent on several elements including viz, crystallinity, morphology, molecular weight, and processing technique. The various processing methods including the UV curing technique also emphasise the need to mainly use specific feedstock, when necessary, which enlarges the potential and scope for processing. Amongst the challenges in sourcing the feedstock for bio-based polymers, is the fact that they are prevalently in the form of food and drugs for consumption. Post consumption, biowaste material is generated, which can be harnessed. However, this circumstance has several issues, of which the main one is the necessity for real-time waste collection and processing. Researchers are enthusiastic that improving accessibility, ease, and supportability of bio-based polymers from every plausible source can rectify this challenge. Additionally, a long-term challenge for polymers based on feedstock is deforestation, and this will require improved strategies for the utilization of recovered cellulose as a source for bio-based polymers.

Unfortunately, the bio-based polymer market has not yet stabilized. Noticeably, the market for the consumption of bio-based polymers is to an extent unpredictable, and consequently, bio-PET is not viewed as sensationally as PLA. Apparently, a safe environment and awareness of health hazards are major factors for the popularity of polymers. However, unless the cost efficiency is improved by recycling using low-cost techniques, the cost will remain a limitation. This will serve as a distinct procedural improvement that does not have a negative effect on the ecosystem. Currently, bio-based polymers account for a small portion of the global thermoplastic market. In fact, according to Business Wire [214], the global application of bio-based polymers constituted roughly 0.25%

of total thermoplastic use. Nonetheless, they possess a significant potential for tremendous growth when considering the circular economy. Presently, bio-based polymers have reached a wide market, which comprises several applications that range from everyday use to highly sophisticated applications for advanced research development in varying fields such as (a) bio-based polymers and applications, (b) the global bio-based market growth of biopolymers, (c) bio-based polymers derived from renewable resources, and (d) biopolymer application in the marine industry. More investigations of bio-based polymer applications in varying fields are expected, with more focus on the biomedical flied. A multi-disciplinary research effort will be essential in fully determining technical and commercial success of utilizing bio-based polymers.

The several bio-processing techniques are deduced to be economically more expensive than petroleum-based counterparts due to the complexity involved. This serves as a major barrier to bio-based polymer adoption. The mitigation strategy has been identified as the application of good manufacturing practices, process monitoring, and quality control techniques. Hence, the future of bio-based polymer products is reliant on consumer affordability, preference, and government legislation. The difference in the constitutional framework also indicates how the bio-based products should be prioritized and favoured, through benefits such as Bio Preferred (United States), the UK Plastic Pact (United Kingdom), and the Lead Market Initiative (European Union). The universal appeal even adds more pressure on the need for replacing petroleum-based polymers with renewable sourced materials for producing environmentally friendly polymers. As already stated, that fact that the raw materials for bio-based polymers are wood impacts food and other agricultural resources. To avoid competition between biopolymer and agricultural resources, derivatives of renewable biomass are currently being investigated. In addition, sustainable processing is viewed to have the potential for complying with the concept set by the United Nations Sustainability Development Goals (UN SDGs). The positive attitude of government legislation and customer support are congruent in the development of bio-based products. At the moment, not all bio-based polymers are fully utilized. However, there is an expectation that future industrial growth will not be problematic because of general public awareness. Therefore, the socio-economic and physical factors should be frequently estimated with the tenets of sustainability, such as the economy, which includes production benefits and cost; social acceptance, which includes employment opportunities and public acceptance; and bio-physical considerations, which refers to the mass balance.

Improving bio-based processing technologies involves increasing mass production and direct cost reduction. Bio-based polymers have significant potential but are only limited to a select number of polymers that have been industrialized currently. Monomers are essential in the development of biopolymers, especially for high thermal stability. Procedures such as the microbial synthesis of these aromatic monomers by fermentation, which is important, remain a challenging research field as the aromatic monomers are complex to produce using fermentation. Although researchers are investigating extraction of the aromatic compounds from wood lignin, many aromatic compounds can be simultaneously synthesised from lignin, which hampers their use as raw materials for plastics. This process remains expensive and energy demanding [215]. Hence, appropriate processing techniques are greatly needed. The large-scale industrialization of these materials at this stage is challenging due to the lack of experience and skill transferability along with supply/demand balance estimation. The challenges faced by industry regarding the use of bio-based polymers are the dearth of composting infrastructure on an industrial scale; the incapability of certain anaerobic digestion plants to process compostable polymers; differences between actual and laboratory test conditions as the rate of biodegradation will vary, which affects the processing time; and lastly, sensitization to synthetic polymer recycling as a way of life for composting because biopolymer processing is at an early stage of adoption. Some of these challenges are to be addressed by achieving the vital technology economy through improved: (a) novel microbial enzymes, (b) efficiency of processing techniques for recovering bio-based materials, (c) novel and innovative manufacturing

pathways with higher yields, and (d) logistics for the feedstock. Another limiting factor for the broad adoption of bio-based polymers is providing vital contributions in every aspect presently dominated by their petroleum-sourced counterparts. This will reduce dependence on fossil fuels, and consequently, positive environmental results can be attained by reducing the CO_2 footprint. Regardless of the technological challenges being experienced, it is in a developing phase.

There are several directions the sustainability of bioprocessing can progress in based on strategies currently being investigated with potentials for optimization being considered as well. They are outlined as follows: (1) improved synthesis of water-degradable polymers that contain functional groups such as acetal, which do not rely on precise biological conditioning prior to biodegradation; (2) the incorporation of specific functional groups into the main polymeric functional group via ring-opening metathesis polymerization (R.O.M.P), which enables the production of a broad range of complex polymeric compounds; (3) investigating lignin-based polymers for methods of improving the operative temperatures of bio-based polymers, which at the moment is considered poor; and (4) the development of novel polymerization chemistry for the use of low-cost abundant feedstocks. Of note, bio-based polymers are not the sole way to attain polymer sustainability; other tools will be required. This includes mechanical and chemical recycling of synthetic polymers that enables a waste-free circular economy.

In conclusion, regardless of the enumerated challenges, bio-based polymers will play a critical role in achieving global sustainability goals and will serve as a contributor to the solution. This is because there is a clear rise in demand by consumers for inexpensive and functional bio-based polymer products. Furthermore, more laboratory innovations will invigorate the collective switch from conventional polymers to sustainable and bio-based polymers.

6. Concluding Remarks

Bio-based plastics are derived from renewable sources contrary to biodegradable plastics that can be derived from renewable or non-renewable feedstocks but can easily disintegrate and biodegrade in the environment. These materials have unique opportunities as a preferred alternative to conventional plastics. There is, however, a need to compare the sustainability impacts of the bio-based polymers, to maximize their use in functional use stage and still withhold the bio-degradation capability. This study therefore focuses on poly (lactic acid) (PLA), Poly (ε-caprolactone) (PCL), polyhydroxyalkanoates (PHA), and polyamides (PA) as biopolymers of interest due to their potential in technological applications. The review covers the processing and biodegradation pathways for each biopolymer. In addition, thermal and photodegradation are covered, and future trends and conclusions are drawn.

The processing methods for bio-based polymers can be performed based on their properties, and applications exist in native forms and blends, hybrids, and composite/nanocomposite materials with a range of natural and synthetic polymers. For preparing bio-based, value-added products, selection of fabrication or functional modification process is an important factor for industrial or biomedical applications. Therefore, the development of new bio-based materials is needed depending on the processing approach via single or in combination. Some selected bio-based polymers and their processing approaches are discussed in the various sections.

In the life cycle of material, there will always be either chemical or physical change due to varying environmental factors such as biological activity, light, heat, moisture, and chemical conditions. This process leads to polymer property change as pertains to functional deterioration because of the physical, biological, and chemical reactions that result in chemical transformations and bond scission and thus can be regarded as polymer degradation. Biodegradation research on polymers is carried out with both in vitro and in vivo studies. This literature review indicates that in vivo is preferred to in vitro because it suits an overall study of the experimental effects on a living subject.

Author Contributions: Conceptualization, J.N., O.O., A.K. and V.K.T.; methodology, O.O., A.K., V.K.T., A.O. and J.N.; formal analysis, O.O., A.K., V.K.T., A.O. and J.N.; investigation, O.O., A.K., V.K.T., A.O. and J.N.; resources, J.N., C.E., S.M., L.A.L. and V.K.T.; data curation, J.N., O.O., A.K. and V.K.T.; writing—original draft preparation, O.O., A.K., V.K.T., A.O. and J.N.; writing—review and editing, O.O., A.K., V.K.T., C.E., S.M., L.A.L., A.O. and J.N.; visualization, O.O., A.K., V.K.T., A.O. and J.N.; supervision, V.K.T. and J.N.; project administration, J.N.; funding acquisition, J.N., C.E., S.M., L.A.L., A.K. and V.K.T. All authors have read and agreed to the published version of the manuscript.

Funding: The authors acknowledge funding support by the Robert Gordon University Pump Prriming Funding support.

Data Availability Statement: No datasets were generated or analysed during the current study.

Conflicts of Interest: The authors declare no conflict of interest.

References

1. Oke, A.; Osobajo, O.; Obi, L.; Omotayo, T. Rethinking and optimising post-consumer packaging waste: A sentiment analysis of consumers' perceptions towards the introduction of a deposit refund scheme in Scotland. *Waste Manag.* **2020**, *118*, 463–470. [CrossRef] [PubMed]
2. Keshavarz, T.; Roy, I. Polyhydroxyalkanoates: Bioplastics with a green agenda. *Curr. Opin. Microbiol.* **2010**, *13*, 321–326. [CrossRef] [PubMed]
3. Lambert, S.; Wagner, M. Environmental performance of bio-based and biodegradable plastics: The road ahead. *Chem. Soc. Rev.* **2017**, *46*, 6855–6871. [CrossRef]
4. Karamanlioglu, M.; Preziosi, R.; Robson, G.D. Abiotic and biotic environmental degradation of the bioplastic polymer poly(lactic acid): A review. *Polym. Degrad. Stab.* **2017**, *137*, 122–130. [CrossRef]
5. Geissdoerfer, M.; Savaget, P.; Bocken, N.M.; Hultink, E.J. The Circular Economy–A new sustainability paradigm? *J. Clean. Prod.* **2017**, *143*, 757–768. [CrossRef]
6. Mohan, S.; Oluwafemi, O.S.; George, S.C.; Jayachandran, V.; Lewu, F.B.; Songca, S.P.; Kalarikkal, N.; Thomas, S. Completely green synthesis of dextrose reduced silver nanoparticles, its antimicrobial and sensing properties. *Carbohydr. Polym.* **2014**, *106*, 469–474. [CrossRef]
7. Benavides, P.T.; Dunn, J.B.; Han, J.; Biddy, M.; Markham, J. Exploring Comparative Energy and Environmental Benefits of Virgin, Recycled, and Bio-Derived PET Bottles. *ACS Sustain. Chem. Eng.* **2018**, *6*, 9725–9733. [CrossRef]
8. Pawar, R.P.; Tekale, S.U.; Shisodia, S.U.; Totre, J.T.; Domb, A.J. Biomedical applications of poly (lactic acid). *Recent Pat. Regen. Med.* **2014**, *4*, 40–51. [CrossRef]
9. Ren, J. Modification of PLA. In *Biodegradable Poly (Lactic Acid): Synthesis, Modification, Processing and Applications*; Springer: Berlin/Heidelberg, Germany, 2010; pp. 38–141.
10. Lim, L.T.; Cink, K.; Vanyo, T. Processing of poly (lactic acid). In *Poly (lactic acid): Synthesis, Structures, Properties, Processing and Applications*; Auras, R., Lim, L.T., Selke, S.E.M., Tsuji, H., Eds.; Wiley: Hoboken, NJ, USA; pp. 189–215.
11. Lasprilla, A.J.; Martinez, G.A.; Lunelli, B.H.; Jardini, A.L.; Maciel Filho, R. Poly (lactic acid) synthesis for application in biomedical devices—A review. *Biotechnol. Adv.* **2012**, *30*, 321–328. [CrossRef]
12. Kalia, S.; Avérous, L. *Biodegradable and Biobased Polymers for Environmental and Biomedical Applications*; John Wiley & Sons: Hoboken, NJ, USA, 2016; Volume 6, p. 171.
13. Genovese, L.; Soccio, M.; Lotti, N.; Gazzano, M.; Siracusa, V.; Salatelli, E.; Balestra, F.; Munari, A. Design of bio-based PLLA triblock copolymers for sustainable food packaging: Thermo-mechanical properties, gas barrier ability and compostability. *Eur. Polym. J.* **2017**, *95*, 289–303. [CrossRef]
14. Wang, L.; Qiu, J.; Sakai, E.; Wei, X. The relationship between microstructure and mechanical properties of carbon nanotubes/poly (lactic acid) nanocomposites prepared by twin-screw extrusion. *Compos. Part A Appl. Sci. Manuf.* **2016**, *89*, 18–25. [CrossRef]
15. Mohammad NN, B.; Arsad, A.; Choi, H.J.; Ngadi, N.; Desa MS, Z.M. Influences of pristine carbon nanotube on the rheological properties of compatibilized poly (lactic acid)/natural rubber nanocomposite. *Mater. Today Proc.* **2012**, *39*, 951–955. [CrossRef]
16. Zhou, Y.; Lei, L.; Yang, B.; Li, J.; Ren, J. Preparation and characterization of poly (lactic acid) (PLA) carbon nano-tube nanocomposites. *Polym. Test.* **2018**, *68*, 34–38. [CrossRef]
17. Liu, Y.; Wang, S.; Lan, W.; Qin, W. Fabrication of poly (lactic acid)/carbon nanotubes/chitosan composite fibers by electrospinning for strawberry preservation. *Int. J. Biol. Macromol.* **2019**, *121*, 1329–1336. [CrossRef]
18. Kian, L.K.; Saba, N.; Jawaid, M.; Sultan, M.T.H. A review on processing techniques of bast fibers nanocellulose and its poly (lactic acid) (PLA) nanocomposites. *Int. J. Biol. Macromol.* **2019**, *121*, 1314–1328. [CrossRef]
19. Li, L.; Chen, Y.; Yu, T.; Wang, N.; Wang, C.; Wang, H. Preparation of poly (lactic acid)/TEMPO-oxidized bacterial cellulose nanocomposites for 3D printing via Pickering emulsion approach. *Compos. Commun.* **2019**, *16*, 162–167. [CrossRef]
20. Geng, S.; Wloch, D.; Herrera, N.; Oksman, K. Large-scale manufacturing of ultra-strong, strain-responsive poly (lactic acid)-based nanocomposites reinforced with cellulose nanocrystals. *Compos. Sci. Technol.* **2020**, *194*, 108144. [CrossRef]

21. Wang, X.; Tang, Y.; Zhu, X.; Zhou, Y.; Hong, X. Preparation and characterization of poly (lactic acid)/polyaniline/nanocrystalline cellulose nanocomposite films. *Int. J. Biol. Macromol.* **2020**, *146*, 1069–1075. [CrossRef]
22. Wang, Y.Y.; Yu, H.Y.; Yang, L.; Abdalkarim, S.Y.H.; Chen, W.L. Enhancing long-term biodegradability and UV-shielding performances of transparent poly (lactic acid) nanocomposite films by adding cellulose nanocrystal-zinc oxide hybrids. *Int. J. Biol. Macromol.* **2019**, *141*, 893–905. [CrossRef]
23. Arjmandi, R.; Hassan, A.; Haafiz, M.K.M.; Zakaria, Z.; Islam, M.S. Effect of hydrolysed cellulose nanowhiskers on properties of montmorillonite/poly (lactic acid) nanocomposites. *Int. J. Biol. Macromol.* **2016**, *82*, 998–1010. [CrossRef]
24. Barmouz, M.; Behravesh, A.H. The role of foaming process on shape memory behavior of poly (lactic acid)-thermoplastic polyurethane-nano cellulose bio-nanocomposites. *J. Mech. Behav. Biomed. Mater.* **2019**, *91*, 266–277. [CrossRef] [PubMed]
25. Herrera, N.; Roch, H.; Salaberria, A.M.; Pino-Orellana, M.A.; Labidi, J.; Fernandes, S.C.M.; Radic, D.; Leiva, A.; Oksman, K. Functionalized blown films of plasticized poly (lactic acid)/chitin nanocomposite: Preparation and characterization. *Mater. Des.* **2016**, *92*, 846–852. [CrossRef]
26. Swaroop, C.; Shukla, M. Development of blown poly (lactic acid)-MgO nanocomposite films for food packaging. *Compos. Part A Appl. Sci. Manuf.* **2019**, *124*, 105482. [CrossRef]
27. Balakrishnan, H.; Hassan, A.; Wahit, M.U.; Yussuf, A.A.; Razak, S.B.A. Novel toughened poly (lactic acid) nanocomposite: Mechanical, thermal and morphological properties. *Mater. Des.* **2010**, *31*, 3289–3298. [CrossRef]
28. Connolly, M.; Zhang, Y.; Brown, D.M.; Ortuño, N.; Jordá-Beneyto, M.; Stone, V.; Fernandez, T.F.; Johnston, H.J. Novel poly (lactic acid) (PLA)-organoclay nanocomposite bio-packaging for the cosmetic industry; migration studies and in vitro assessment of the dermal toxicity of migration extracts. *Polym. Degrad. Stab.* **2019**, *168*, 108938. [CrossRef]
29. Nam, B.U.; Min, K.D.; Son, Y. Investigation of the nanostructure, thermal stability, and mechanical properties of poly (lactic acid)/cellulose acetate butyrate/clay nanocomposites. *Mater. Lett.* **2015**, *150*, 118–121. [CrossRef]
30. Sharma, S.; Singh, A.A.; Majumdar, A.; Butola, B.S. Harnessing the ductility of poly (lactic acid)/halloysite nano-composites by synergistic effects of impact modifier and plasticiser. *Compos. Part B Eng.* **2020**, *188*, 107845. [CrossRef]
31. Fu, Y.; Liu, L.; Zhang, J.; Hiscox, W.C. Functionalized graphenes with polymer toughener as novel interface modifier for property-tailored poly (lactic acid)/graphene nanocomposites. *Polymer* **2014**, *55*, 6381–6389. [CrossRef]
32. Najafi, N.; Heuzey, M.; Carreau, P. Polylactide (PLA)-clay nanocomposites prepared by melt compounding in the presence of a chain extender. *Compos. Sci. Technol.* **2012**, *72*, 608–615. [CrossRef]
33. Cai, X.; Tong, H.; Shen, X.; Chen, W.; Yan, J.; Hu, J. Preparation and characterization of homogeneous chitosan–poly (lactic acid)/hydroxyapatite nanocomposite for bone tissue engineering and evaluation of its mechanical properties. *Acta Biomater.* **2009**, *5*, 2693–2703. [CrossRef]
34. Davachi, S.M.; Heidari, B.S.; Hejazi, I.; Seyfi, J.; Oliaei, E.; Farzaneh, A.; Rashedi, H. Interface modified poly (lactic acid)/starch/poly ε-caprolactone antibacterial nanocomposite blends for medical applications. *Carbohydr. Polym.* **2017**, *155*, 336–344. [CrossRef] [PubMed]
35. Alam, F.; Shukla, V.R.; Varadarajan, K.M.; Kumar, S. Microarchitected 3D printed poly (lactic acid) (PLA) nano-composite scaffolds for biomedical applications. *J. Mech. Behav. Biomed. Mater.* **2020**, *103*, 103576. [CrossRef] [PubMed]
36. Alam, F.; Varadarajan, K.M.; Kumar, S. 3D printed poly (lactic acid) nanocomposite scaffolds for tissue engineering applications. *Polym. Test.* **2020**, *81*, 106203. [CrossRef]
37. Ansari, Z.; Kalantar, M.; Kharaziha, M.; Ambrosio, L.; Raucci, M.G. Poly (ε-caprolactone) /fluoride substituted-hydroxyapatite (PCL/FHA) nanocomposite coatings prepared by in-situ sol-gel process for dental implant applications. *Prog. Org. Coat.* **2020**, *147*, 105873. [CrossRef]
38. Tay, B.Y.; Zhang, S.X.; Myint, M.H.; Ng, F.L.; Chandrasekaran, M.; Tan, L.K.A. Processing of Poly (ε-caprolactone) porous structure for scaffold development. *J. Mater. Process. Technol.* **2007**, *182*, 117–121. [CrossRef]
39. Lee, S.H.; Teramoto, Y.; Endo, T. Cellulose nanofiber-reinforced Poly (ε-caprolactone)/polypropylene hybrid nanocomposite. *Compos. Part A Appl. Sci. Manuf.* **2011**, *42*, 151–156. [CrossRef]
40. Ahmadzadeh, Y.; Babaei, A.; Goudarzi, A. Assessment of localization and degradation of ZnO nano-particles in the PLA/PCL biocompatible blend through a comprehensive rheological characterization. *Polym. Degrad. Stab.* **2018**, *158*, 136–147. [CrossRef]
41. Guadagno, L.; Raimondo, M.; Longo, R.; Sarno, M.; Iuliano, M.; Mariconda, A.; Saturnino, C.; Ceramella, J.; Lacopetta, D.; Sinicropi, M.S. Development and characterization of antitumoral electrospun Poly (ε-caprolactone)/functionalized Fe_3O_4 hybrid membranes. *Mater. Today Chem.* **2020**, *17*, 100309. [CrossRef]
42. Mallakpour, S.; Nouruzi, N. Effects of citric acid-functionalized ZnO nanoparticles on the structural, mechanical, thermal and optical properties of Poly (ε-caprolactone) nanocomposite films. *Mater. Chem. Phys.* **2017**, *197*, 129–137. [CrossRef]
43. Ahmadi, T.; Monshi, A.; Mortazavi, V.; Fathi, M.H.; Sharifi, S.; Kharaziha, M.; Khazdooz, M.; Zarei, A.; Dehaghani, M.T. Fabrication and characterization of Poly (ε-caprolactone) fumarate/gelatin-based nanocomposite incorporated with silicon and magnesium co-doped fluorapatite nanoparticles using electrospinning method. *Mater. Sci. Eng. C* **2020**, *106*, 110172. [CrossRef]
44. Abdal-hay, A.; Raveendran, N.T.; Fournier, B.; Ivanovski, S. Fabrication of biocompatible and bioabsorbable Poly (ε-caprolactone) /magnesium hydroxide 3D printed scaffolds: Degradation and in vitro osteoblasts interactions. *Compos. Part B Eng.* **2020**, *197*, 108158. [CrossRef]

45. Torres, E.; Fombuena, V.; Vallés-Lluch, A.; Ellingham, T. Improvement of mechanical and biological properties of Poly (ε-caprolactone) loaded with hydroxyapatite and halloysite nanotubes. *Mater. Sci. Eng. C* **2017**, *75*, 418–424. [CrossRef] [PubMed]
46. Abdal-hay, A.; Abbasi, N.; Gwiazda, M.; Hamlet, S.; Ivanovski, S. Novel Poly (ε-caprolactone) /hydroxyapatite nanocomposite fibrous scaffolds by direct melt-electrospinning writing. *Eur. Polym. J.* **2018**, *105*, 257–264. [CrossRef]
47. Esmaeilzadeh, J.; Hesaraki, S.; Hadavi, S.M.M.; Ebrahimzadeh, M.H.; Esfandeh, M. Poly (D/L) lactide/Poly (ε-caprolactone) /bioactive glasss nanocomposites materials for anterior cruciate ligament reconstruction screws: The effect of glass surface functionalization on mechanical properties and cell behaviors. *Mater. Sci. Eng. C* **2017**, *77*, 978–989. [CrossRef]
48. Yildirim, S.; Demirtas, T.T.; Dincer, C.A.; Yildiz, N.; Karakecili, A. Preparation of Poly (ε-caprolactone)/graphene oxide scaffolds: A green route combining supercritial CO_2 technology and porogen leaching. *J. Supercrit. Fluids* **2018**, *133*, 156–162. [CrossRef]
49. Sadeghi, M.; Talakesh, M.M.; Ghalei, B.; Shafiei, M. Preparation, characterization and gas permeation properties of a Poly (ε-caprolactone) based polyurethane-silica nanocomposite membrane. *J. Membr. Sci.* **2013**, *427*, 21–29. [CrossRef]
50. Seema, K.M.; Mamba, B.B.; Njuguna, J.; Bakhtizin, R.Z.; Mishra, A.K. Removal of lead (II) from aqeouos waste using (CD-PCL-TiO2) bio-nanocomposites. *Int. J. Biol. Macromol.* **2018**, *109*, 136–142. [CrossRef]
51. Karagoz, S.; Kiremitler, N.B.; Sakir, M.; Salem, S.; Onses, M.S.; Sahmetlioglu, E.; Ceylan, A.; Yilmaz, E. Synthesis of Ag and TiO_2 modified Poly (ε-caprolactone) electrospun nanofibers (PCL/TiO_2-Ag NFs) as a multifunctional material for SERS, photocatalysis and antibacterial applications. *Ecotoxicol. Environ. Saf.* **2020**, *188*, 109856. [CrossRef]
52. Larsson, M.; Markbo, O.; Jannasch, P. Melt processability and thermomechanical properties of blends based on polyhydroxyalkanoates and poly(butylene adipate-co-terephthalate). *RSC Adv.* **2016**, *6*, 44354–44363. [CrossRef]
53. Lemoigne, M. Products of dehydration and of polymerization of β-hydroxybutyric acid. *Bull Soc. Chem. Biol* **1926**, *8*, 770–782.
54. Catara, V. *Pseudomonas corrugata*: Plant pathogen and/or biological resource? *Mol. Plant Pathol.* **2007**, *8*, 233–244. [CrossRef] [PubMed]
55. Thakur, P. Screening of Plastic Degrading Bacteria from Dumped Soil Area. Doctoral Dissertation, National Institute of Technology, Rourkela, India, 10 May 2012.
56. Lim, J.; You, M.; Li, J.; Li, Z. Emerging bone tissue engineering via Polyhydroxyalkanoate (PHA)-based scaf-folds. *Mater. Sci. Eng. C* **2017**, *79*, 917–929. [CrossRef] [PubMed]
57. Tarrahi, R.; Fathi, Z.; Seydibeyoğlu, M.Ö.; Doustkhah, E.; Khataee, A. Polyhydroxyalkanoates (PHA): From production to nanoarchitecture. *Int. J. Biol. Macromol.* **2020**, *146*, 596–619. [CrossRef] [PubMed]
58. Phukon, P.; Radhapyari, K.; Konwar, B.K.; Khan, R. Natural polyhydroxyalkanoate–gold nanocomposite based biosensor for detection of antimalarial drug artemisinin. *Mater. Sci. Eng. C* **2014**, *37*, 314–320. [CrossRef]
59. Bugnicourt, E.; Cinelli, P.; Lazzeri, A.; Alvarez, V. Polyhydroxyalkanoate (PHA): Review of synthesis, characteristics, processing and potential applications in packaging. *Express Polym. Lett.* **2014**, *8*, 791–808. [CrossRef]
60. Grassie, N.; Murray, E.J.; Holmes, P.A. The thermal degradation of poly(-(d)-β-hydroxybutyric acid): Part 2—Changes in molecular weight. *Polym. Degrad. Stabil.* **1984**, *6*, 95–103. [CrossRef]
61. Ishida, K.; Wang, Y.; Inoue, Y. Comonomer Unit Composition and Thermal Properties of Poly (3-hydroxybutyrate-co-4-hydroxybutyrate) s Biosynthesized by *Ralstonia eutropha*. *Biomacromolecules* **2001**, *2*, 1285–1293. [CrossRef]
62. Pal, A.K.; Wu, F.; Misra, M.; Mohanty, A.K. Reactive extrusion of sustainable PHBV/PBAT-based nanocompo-site films with organically modified nanoclay for packaging applications: Compression moulding vs. cast film extrusion. *Compos. Part B Eng.* **2020**, *198*, 108141. [CrossRef]
63. Perret, E.; Reifler, F.A.; Gooneie, A.; Hufenus, R. Tensile study of melt-spun poly(3-hydroxybutyrate) P3HB fibers: Reversible transformation of a highly oriented phase. *Polymer* **2019**, *180*, 121668. [CrossRef]
64. Tebaldi, M.L.; Maia, A.L.C.; Poletto, F.; de Andrade, F.V.; Soares, D.C.F. Poly (-3-hydroxybutyrate-co-3-hydroxyvalerate)(PHBV): Current advances in synthesis methodologies, antitumor applications and biocompatibility. *J. Drug Deliv. Sci. Technol.* **2019**, *51*, 115–126. [CrossRef]
65. Naderi, P.; Zarei, M.; Karbasi, S.; Salehi, H. Evaluation of the effects of keratin on physical, mechanical and bio-logical properties of poly (3-hydroxybutyrate) electrospun scaffold: Potential application in bone tissue engineering. *Eur. Polym. J.* **2020**, *124*, 109502. [CrossRef]
66. Figueroa-Lopez, K.J.; Enescu, D.; Torres-Giner, S.; Cabedo, L.; Cerqueira, M.A.; Pastrana, L.; Fuciños, P.; Lagaron, J.M. Development of electrospun active films of poly(3-hydroxybutyrate-co-3-hydroxyvalerate) by the incorporation of cyclodextrin inclusion complexes containing oregano essential oil. *Food Hydrocoll.* **2020**, *108*, 106013. [CrossRef]
67. Lee, R.E.; Azdast, T.; Wang, G.; Wang, X.; Lee, P.C.; Park, C.B. Highly expanded fine-cell foam of polylactide/polyhydroxyalkanoate/nano-fibrillated polytetrafluoroethylene composites blown with mold-opening injection molding. *Int. J. Biol. Macromol.* **2020**, *155*, 289–292. [CrossRef] [PubMed]
68. Xu, P.; Yang, W.; Niu, D.; Yu, M.; Du, M.; Dong, W.; Chen, M.; Jan Lemstra, P.; Ma, P. Multifunctional and robust polyhydroxyalkanoate nanocomposites with superior gas barrier, heat resistant and inherent antibacterial performances. *Chem. Eng. J.* **2020**, *382*, 122864. [CrossRef]
69. Jayakumar, A.; Prabhu, K.; Shah, L.; Radha, P. Biologically and environmentally benign approach for PHB-silver nanocomposite synthesis and its characterization. *Polym. Test.* **2020**, *81*, 106197. [CrossRef]
70. Castro-Mayorga, J.; Freitas, F.; Reis, M.; Prieto, M.; Lagaron, J. Biosynthesis of silver nanoparticles and polyhydroxybutyrate nanocomposites of interest in antimicrobial applications. *Int. J. Biol. Macromol.* **2018**, *108*, 426–435. [CrossRef]

71. Rivera-Briso, A.L.; Aachmann, F.L.; Moreno-Manzano, V.; Serrano-Aroca, Á. Graphene oxide nanosheets versus carbon nanofibers: Enhancement of physical and biological properties of poly (3-hydroxybutyrate-co-3-hydroxyvalerate) films for biomedical applications. *Int. J. Biol. Macromol.* **2020**, *143*, 1000–1008. [CrossRef]
72. Parvizifard, M.; Karbasi, S. Physical, mechanical and biological performance of PHB-Chitosan/MWCNTs nano-composite coating deposited on bioglass based scaffold: Potential application in bone tissue engineering. *Int. J. Biol. Macromol.* **2020**, *152*, 645–662. [CrossRef]
73. Torres, M.G. 3D-composite scaffolds from radiation-induced chitosan grafted poly (3-hydroxybutyrate) polyure-thane. *Mater. Today Commun.* **2020**, *23*, 100902. [CrossRef]
74. Ochoa-Segundo, E.I.; González-Torres, M.; Cabrera-Wrooman, A.; Sánchez-Sánchez, R.; Huerta-Martínez, B.M.; Melgarejo-Ramírez, Y.; Leyva-Gómez, G.; Rivera-Muñoz, E.M.; Cortés, H.; Velasquillo, C.; et al. Gamma radiation-induced grafting of n-hydroxyethyl acrylamide onto poly(3-hydroxybutyrate): A companion study on its polyurethane scaffolds meant for potential skin tissue engineering applications. *Mater. Sci. Eng. C* **2020**, *116*, 111176. [CrossRef]
75. Wu, C.S. Comparative assessment of the interface between poly (3-hydroxybutyrate-co-3-hydroxyvalerate) and fish scales in composites: Preparation, characterization, and applications. *Mater. Sci. Eng. C* **2019**, *104*, 109878. [CrossRef] [PubMed]
76. de Almeida Neto, G.R.; Barcelos, M.V.; Ribeiro, M.E.A.; Folly, M.M.; Rodríguez, R.J.S. Formulation and characterization of a novel PHBV nanocomposite for bone defect filling and infection treatment. *Mater. Sci. Eng. C* **2019**, *104*, 110004. [CrossRef]
77. Oprea, M.; Panaitescu, D.M.; Nicolae, C.A.; Gabor, A.R.; Frone, A.N.; Raditoiu, V.; Trusca, R.; Casarica, A. Nanocomposites from functionalized bacterial cellulose and poly(3-hydroxybutyrate-co-3-hydroxyvalerate). *Polym. Degrad. Stab.* **2020**, *179*, 109203. [CrossRef]
78. Nishida, M.; Ogura, T.; Shinzawa, H.; Nishida, M.; Kanematsu, W. Tensile properties of polyhydroxyalka-noate/Poly (ε-caprolactone) blends studied by rheo-optical near-infrared (NIR) spectroscopy. *J. Mol. Struct.* **2016**, *1124*, 92–97. [CrossRef]
79. Panaitescu, D.M.; Nicolae, C.A.; Gabor, A.R.; Trusca, R. Thermal and mechanical properties of poly(3-hydroxybutyrate) reinforced with cellulose fibers from wood waste. *Ind. Crop. Prod.* **2020**, *145*, 112071. [CrossRef]
80. Garcia-Garcia, D.; Lopez-Martinez, J.; Balart, R.; Strömberg, E.; Moriana, R. Reinforcing capability of cellulose nanocrystals obtained from pine cones in a biodegradable poly (3-hydroxybutyrate)/poly (ε-caprolactone)(PHB/PCL) thermoplastic blend. *Eur. Polym. J.* **2018**, *104*, 10–18. [CrossRef]
81. Garcia-Garcia, D.; Garcia-Sanoguera, D.; Fombuena, V.; Lopez-Martinez, J.; Balart, R. Improvement of mechanical and thermal properties of poly(3-hydroxybutyrate) (PHB) blends with surface-modified halloysite nanotubes (HNT). *Appl. Clay Sci.* **2018**, *162*, 487–498. [CrossRef]
82. Garcia-Garcia, D.; Rayón, E.; Carbonell-Verdu, A.; López-Martínez, J.; Balart, R. Improvement of the compatibility between poly (3-hydroxybutyrate) and poly (ε-caprolactone) by reactive extrusion with dicumyl peroxide. *Eur. Polym. J.* **2017**, *86*, 41–57. [CrossRef]
83. Clavería, I.; Elduque, D.; Santolaria, J.; Pina, C.; Javierre, C.; Fernandez, A. The influence of environmental conditions on the dimensional stability of components injected with PA6 and PA66. *Polym. Test.* **2016**, *50*, 15–25. [CrossRef]
84. Chavarria, F.; Paul, D. Comparison of nanocomposites based on nylon 6 and nylon 66. *Polymer* **2004**, *45*, 8501–8515. [CrossRef]
85. Ogunsona, E.O.; Codou, A.; Misra, M.; Mohanty, A.K. A critical review on the fabrication processes and performance of polyamide biocomposites from a biofiller perspective. *Mater. Today Sustain.* **2019**, *5*, 100014. [CrossRef]
86. Winnacker, M.; Rieger, B. Biobased Polyamides: Recent Advances in Basic and Applied Research. *Macromol. Rapid Commun.* **2016**, *37*, 1391–1413. [CrossRef] [PubMed]
87. Munoz-Guerra, S. Carbohydrate-based polyamides and polyesters: An overview illustrated with two selected examples. *High Perform. Polym.* **2012**, *24*, 9–23. [CrossRef]
88. Thiyagarajan, S.; Gootjes, L.; Vogelzang, W.; Wu, J.; van Haveren, J.; van Es, D.S. Chiral building blocks from biomass: 2,5-diamino-2,5-dideoxy-1,4-3,6-dianhydroiditol. *Tetrahedron* **2010**, *67*, 383–389. [CrossRef]
89. Bou, J.J.; Rodriguez-Galan, A.; Munoz-Guerra, S. Optically active polyamides derived from L-tartaric acid. *Macromolecules* **1993**, *26*, 5664–5670. [CrossRef]
90. Kiely, D.E.; Chen, L.; Lin, T.H. Synthetic polyhydroxypolyamides from galactaric, xylaric, D-glucaric, and D-mannaric acids and alkylenediamine monomers—Some comparisons. *J. Polym. Sci. Part A Polym. Chem.* **2000**, *38*, 594–603. [CrossRef]
91. Arabpour, A.; Shockravi, A.; Rezania, H.; Farahati, R. Investigation of anticorrosive properties of novel silane-functionalized polyamide/GO nanocomposite as steel coatings. *Surf. Interfaces* **2020**, *18*, 100453. [CrossRef]
92. Pant, H.R.; Risal, P.; Park, C.H.; Tijing, L.D.; Jeong, Y.J.; Kim, C.S. Synthesis, characterization, and mineralization of polyamide-6/calcium lactate composite nanofibers for bone tissue engineering. *Colloids Surf. B Biointerfaces* **2013**, *102*, 152–157. [CrossRef]
93. Vasiljević, J.; Čolović, M.; Jerman, I.; Simončič, B.; Demšar, A.; Samaki, Y.; Sobak, M.; Sest, E.; Golja, B.; Leskovsek, M.; et al. In situ prepared polyamide 6/DOPO-derivative nano-composite for melt-spinning of flame retardant textile filaments. *Polym. Degrad. Stab.* **2019**, *166*, 50–59. [CrossRef]
94. Ali, F.A.A.; Alam, J.; Shukla, A.K.; Alhoshan, M.; Khaled, J.M.; Al-Masry, W.A.; Alharby, N.S.; Alam, M. Graphene oxide-silver nanosheet-incorporated polyamide thin-film composite membranes for antifouling and antibacterial action against Escherichia coli and bovine serum albumin. *J. Ind. Eng. Chem.* **2019**, *80*, 227–238.

95. Touchaleaume, F.; Soulestin, J.; Sclavons, M.; Devaux, J.; Lacrampe, M.F.; Krawczak, P. One-step water-assisted melt-compounding of polyamide 6/pristine clay nanocomposites: An efficient way to prevent matrix degradation. *Polym. Degrad. Stab.* **2011**, *96*, 1890–1900. [CrossRef]
96. Abdelwahab, M.; Codou, A.; Anstey, A.; Mohanty, A.K.; Misra, M. Studies on the dimensional stability and mechanical properties of nanobiocomposites from polyamide 6-filled with biocarbon and nanoclay hybrid systems. *Compos. Part A Appl. Sci. Manuf.* **2020**, *129*, 105695. [CrossRef]
97. Battegazzore, D.; Salvetti, O.; Frache, A.; Peduto, N.; De Sio, A.; Marino, F. Thermo-mechanical properties enhancement of bio-polyamides (PA10. 10 and PA6. 10) by using rice husk ash and nanoclay. *Compos. Part A Appl. Sci. Manuf.* **2016**, *81*, 193–201. [CrossRef]
98. Shabanian, M.; Mirzakhanian, Z.; Basaki, N.; Khonakdar, H.A.; Faghihi, K.; Hoshyargar, F.; Wagenknecht, U. Flammability and thermal properties of novel semi aromatic polyamide/organoclay nanocomposite. *Thermochim. Acta* **2014**, *585*, 63–70. [CrossRef]
99. Shabanian, M.; Hajibeygi, M.; Roohani, M. Synthesis of a novel CNT/polyamide composite containing phosphine oxide groups and its flame retardancy and thermal properties. *New Carbon Mater.* **2015**, *30*, 397–403. [CrossRef]
100. Venkatraman, P.; Gohn, A.M.; Rhoades, A.M.; Foster, E.J. Developing high performance PA 11/cellulose nano-composites for industrial-scale melt processing. *Compos. Part B Eng.* **2019**, *174*, 106988. [CrossRef]
101. Rahimi, S.K.; Otaigbe, J.U. The role of particle surface functionality and microstructure development in isothermal and non-isothermal crystallization behavior of polyamide 6/cellulose nanocrystals nanocomposites. *Polymer* **2016**, *107*, 316–331. [CrossRef]
102. Rahimi, S.K.; Otaigbe, J.U. The effects of the interface on microstructure and rheo-mechanical properties of pol-yamide 6/cellulose nanocrystal nanocomposites prepared by in-situ ring-opening polymerization and subsequent melt extrusion. *Polymer* **2017**, *127*, 269–285. [CrossRef]
103. Panaitescu, D.M.; Frone, A.N.; Nicolae, C. Micro- and nano-mechanical characterization of polyamide 11 and its composites containing cellulose nanofibers. *Eur. Polym. J.* **2013**, *49*, 3857–3866. [CrossRef]
104. Shrestha, B.K.; Mousa, H.M.; Tiwari, A.P.; Ko, S.W.; Park, C.H.; Kim, C.S. Development of polyamide-6, 6/chitosan electrospun hybrid nanofibrous scaffolds for tissue engineering application. *Carbohydr. Polym.* **2016**, *148*, 107–114. [CrossRef]
105. Masui, A.; Ikawa, S.; Kawasaki, N.; Yamano, N.; Nakayama, A. Biodegradation control of a polyamide 4–visible-light-sensitive TiO_2 composite by a fluorescent light irradiation. *Polym. Degrad. Stab.* **2019**, *167*, 44–49. [CrossRef]
106. Zammarano, M.; Bellayer, S.; Gilman, J.W.; Franceschi, M.; Beyer, F.L.; Harris, R.H.; Meriani, S. Delamination of organo-modified layered double hydroxides in polyamide 6 by melt processing. *Polymer* **2006**, *47*, 652–662. [CrossRef]
107. Pospíšil, J.; Nešpůrek, S. Highlights in chemistry and physics of polymer stabilization. In *Macromolecular Symposia*; Hüthig & Wepf Verlag: Basel, Switzerland, 1997; Volume 115, pp. 143–163.
108. Doi, Y.; Kanesawa, Y.; Tanahashi, N.; Kumagai, Y. Biodegradation of microbial polyesters in the marine environment. *Polym. Degrad. Stab.* **1992**, *36*, 173–177. [CrossRef]
109. Guo, D.; Chen, F.; Wheeler, J.; Winder, J.; Selman, S.; Peterson, M.; Dixon, R.A. Improvement of in-rumen digestibility of alfalfa forage by genetic manipulation of lignin O-methyltransferases. *Transgenic Res.* **2001**, *10*, 457–464. [CrossRef] [PubMed]
110. Olayan, H.B.; Hami, H.S.; Owen, E.D. Photochemical and Thermal Crosslinking of Polymers. *J. Macromol. Sci. Part C Polym. Rev.* **1996**, *36*, 671–719. [CrossRef]
111. Elbanna, K.; Lütke-Eversloh, T.; Jendrossek, D.; Luftmann, H.; Steinbüchel, A. Studies on the biodegradability of polythioester copolymers and homopolymers by polyhydroxyalkanoate (PHA)-degrading bacteria and PHA depolymerases. *Arch. Microbiol.* **2004**, *182*, 212–225. [CrossRef]
112. Jendrossek, D.; Schirmer, A.; Schlegel, H.G. Biodegradation of polyhydroxyalkanoic acids. *Appl. Microbiol. Biotechnol.* **1996**, *46*, 451–463. [CrossRef]
113. Mabrouk, M.; Sabry, S.A. Degradation of poly (3-hydroxybutyrate) and its copolymer poly (3-hydroxybutyrate-co-3-hydroxyvalerate) by a marine *Streptomyces* sp. SNG9. *Microbiol. Res.* **2001**, *156*, 323–335. [CrossRef]
114. Feng, L.; Wang, Y.; Inagawa, Y.; Kasuya, K.; Saito, T.; Doi, Y.; Inoue, Y. Enzymatic degradation behavior of comonomer compositionally fractionated bacterial poly(3-hydroxybutyrate-co-3-hydroxyvalerate)s by poly(3-hydroxyalkanoate) depolymerases isolated from *Ralstonia pickettii* T1 and *Acidovorax* sp. TP4. *Polym. Degrad. Stab.* **2004**, *84*, 95–104. [CrossRef]
115. Kasuya, K.-I.; Doi, Y.; Yao, T. Enzymatic degradation of poly[(R)-3-hydroxybutyrate] by *Comamonas testosteroni* ATSU of soil bacterium. *Polym. Degrad. Stab.* **1994**, *45*, 379–386. [CrossRef]
116. Kita, K.; Mashiba, S.I.; Nagita, M.; Ishimaru, K.; Okamoto, K.; Yanase, H.; Kato, N. Cloning of poly (3-hydroxybutyrate) depolymerase from a marine bacterium, Alcaligenes faecalis AE122, and characterization of its gene product. *Biochim. Et Biophys. Acta (BBA)-Gene Struct. Expr.* **1997**, *1352*, 113–122. [CrossRef]
117. Romen, F.; Reinhardt, S.; Jendrossek, D. Thermotolerant poly(3-hydroxybutyrate)-degrading bacteria from hot compost and characterization of the PHB depolymerase of *Schlegelella* sp. KB1a. *Arch. Microbiol.* **2004**, *182*, 157–164. [CrossRef] [PubMed]
118. Abou-Zeid, D.M.; Müller, R.J.; Deckwer, W.D. Biodegradation of aliphatic homopolyesters and aliphatic−aro-matic copolyesters by anaerobic microorganisms. *Biomacromolecules* **2004**, *5*, 1687–1697. [CrossRef] [PubMed]
119. Benedict, C.V.; Cameron, J.A.; Huang, S.J. Poly (ε-caprolactone) degradation by mixed and pure cultures of bacteria and a yeast. *J. Appl. Polym. Sci.* **1983**, *28*, 335–342. [CrossRef]
120. Torres, A.; Li, S.M.; Roussos, S.; Vert, M. Poly (lactic acid) degradation in soil or under controlled conditions. *J. Appl. Polym. Sci.* **1996**, *62*, 2295–2302. [CrossRef]

121. Pranamuda, H.; Tokiwa, Y.; Tanaka, H. Polylactide Degradation by an *Amycolatopsis* sp. *Appl. Environ. Microbiol.* **1997**, *63*, 1637–1640. [CrossRef] [PubMed]
122. Pranamuda, H.; Tokiwa, Y. Degradation of poly (L-lactide) by strains belonging to genus Amycolatopsis. *Biotechnol. Lett.* **1999**, *21*, 901–905. [CrossRef]
123. Shah, A.A.; Hasan, F.; Hameed, A.; Ahmed, S. Biological degradation of plastics: A comprehensive review. *Biotechnol. Adv.* **2008**, *26*, 246–265. [CrossRef]
124. Fukuzaki, H.; Yoshida, M.; Asano, M.; Kumakura, M. Synthesis of copoly(d,l-lactic acid) with relatively low molecular weight and in vitro degradation. *Eur. Polym. J.* **1989**, *25*, 1019–1026. [CrossRef]
125. Lee, B.; Pometto, A.L.; Fratzke, A.; Bailey, T.B. Biodegradation of degradable plastic polyethylene by Phanero-chaete and Streptomyces species. *Appl. Environ. Microbiol.* **1991**, *57*, 678–685. [CrossRef]
126. Guo, B.; Glavas, L.; Albertsson, A.C. Biodegradable and electrically conducting polymers for biomedical applications. *Prog. Polym. Sci.* **2013**, *38*, 1263–1286. [CrossRef]
127. Jamshidian, M.; Tehrany, E.A.; Imran, M.; Jacquot, M.; Desobry, S. Poly-Lactic Acid: Production, applications, nanocomposites, and release studies. *Compr. Rev. Food Sci. Food Saf.* **2010**, *9*, 552–571. [CrossRef] [PubMed]
128. Lim, L.-T.; Auras, R.; Rubino, M. Processing technologies for poly(lactic acid). *Prog. Polym. Sci.* **2008**, *33*, 820–852. [CrossRef]
129. Nampoothiri, K.M.; Nair, N.R.; John, R.P. An overview of the recent developments in polylactide (PLA) research. *Bioresour. Technol.* **2010**, *101*, 8493–8501. [CrossRef]
130. Haw, T.C.; Ahmad, A.; Anuar, F.H. Synthesis and characterization of poly (D,L-lactide)-poly (ethylene glycol) multiblock poly (ether-ester-urethane)s. In *AIP Conference Proceedings*; AIP Publishing LLC: Melville, NY, USA, 2015; Volume 1678, p. 050025.
131. Drumright, R.E.; Gruber, P.R.; Henton, D.E. Poly (lactic acid) technology. *Adv. Mater.* **2000**, *12*, 1841–1846. [CrossRef]
132. Vert, M.; Li, S.M.; Garreau, H. Attempts to map the structure and degradation characteristics of aliphatic polyesters derived from lactic and glycolic acids. *J. Biomater. Sci.* **1995**, *6*, 639–649. [CrossRef]
133. Li, S.M.; Garreau, H.; Vert, M. Structure-property relationships in the case of the degradation of massive aliphatic poly-(α-hydroxy acids) in aqueous media. *J. Mater. Sci. Mater. Med.* **1990**, *1*, 123–130. [CrossRef]
134. Therin, M.; Christel, P.; Li, S.; Garreau, H.; Vert, M. In vivo degradation of massive poly (α-hydroxy acids): Validation of in vitro findings. *Biomaterials* **1992**, *13*, 594–600. [CrossRef]
135. Shimpi, N.; Borane, M.; Mishra, S.; Kadam, M.; Sonawane, S.S. Biodegradation of Isotactic Polypropylene (iPP)/Poly (lactic acid)(PLA) and iPP/PLA/Nano Calcium Carbonates Using *Phanerochaete chrysosporium*. *Adv. Polym. Technol.* **2018**, *37*, 522–530. [CrossRef]
136. Okada, M. Molecular design and syntheses of glycopolymers. *Prog. Polym. Sci.* **2001**, *26*, 67–104. [CrossRef]
137. Hudson, J.A.; Crugnola, A. The in vivo Biodegradation of Nylon 6 Utilized in a Particular IUD. *J. Biomater. Appl.* **1986**, *1*, 487–501. [CrossRef] [PubMed]
138. Smith, R.; Oliver, C.; Williams, D.F. The enzymatic degradation of polymers in vitro. *J. Biomed. Mater. Res.* **1987**, *21*, 991–1003. [CrossRef]
139. Deguchi, T.; Kitaoka, Y.; Kakezawa, M.; Nishida, T. Purification and characterization of a nylon-degrading enzyme. *Appl. Environ. Microbiol.* **1998**, *64*, 1366–1371. [CrossRef] [PubMed]
140. Nomura, I.; Narita, K.; Kurokawa, M. Mitsubishi Gas Chemical Co Inc. Molding Polyamide Resin Composition. U.S. Patent 4,822,846, 2001.
141. Yamano, N.; Nakayama, A.; Kawasaki, N.; Yamamoto, N.; Aiba, S. Mechanism and Characterization of Polyamide 4 Degradation by *Pseudomonas* sp. *J. Polym. Environ.* **2008**, *16*, 141–146. [CrossRef]
142. Wu, J.; Eduard, P.; Thiyagarajan, S.; van Haveren, J.; van Es, D.S.; Koning, C.E.; Lutz, M.; Guerra, C.F. Isohexide Derivatives from Renewable Resources as Chiral Building Blocks. *Chemsuschem* **2011**, *4*, 599–603. [CrossRef] [PubMed]
143. Díaz, E.; Sandonis, I.; Valle, M.B. In vitro degradation of poly (caprolactone)/nHA composites. *J. Nanomater.* **2014**, *2014*, 185. [CrossRef]
144. Heimowska, A.; Morawska, M.; Bocho-Janiszewska, A. Biodegradation of poly(ε-caprolactone) in natural water environments. *Pjct* **2017**, *19*, 120–126. [CrossRef]
145. Fukumura, D.; Jain, R.K. Tumor microvasculature and microenvironment: Targets for anti-angiogenesis and normalization. *Microvasc. Res.* **2007**, *74*, 72–84. [CrossRef]
146. Klun, U.; Friedrich, J.; Kržan, A. Polyamide-6 fibre degradation by a lignolytic fungus. *Polym. Degrad. Stab.* **2003**, *79*, 99–104. [CrossRef]
147. Lam Christopher, X.F.; Dietmar, W. Hutmacher, Jan-Thorsten Schantz, Maria Ann Woodruff, and Swee Hin Teoh. Evaluation of Poly (ε-caprolactone) scaffold degradation for 6 months in vitro and in vivo. *J. Biomed. Mater. Res. Part A Off. J. Soc. Biomater. Jpn. Soc. Biomater. Aust. Soc. Biomater. Korean Soc. Biomater.* **2009**, *90*, 906–919.
148. Woodward, S.C.; Brewer, P.S.; Moatamed, F.; Schindler, A.; Pitt, C.G. The intracellular degradation of poly (ε-caprolactone). *J. Biomed. Mater. Res.* **1985**, *19*, 437–444. [CrossRef]
149. Sun, H.; Mei, L.; Song, C.; Cui, X.; Wang, P. The in vivo degradation, absorption and excretion of PCL-based implant. *Biomaterials* **2006**, *27*, 1735–1740. [CrossRef] [PubMed]
150. Mohan, S.; Oluwafemi, O.S.; Kalarikkal, N.; Thomas, S.; Songca, S.P. Biopolymers–Application in Nanoscience and Nanotechnology. *Recent Adv. Biopolym.* **2016**, *1*, 47–66. [CrossRef]

151. Babu, R.P.; Oconnor, K.; Seeram, R. Current progress on bio-based polymers and their future trends. *Prog. Biomater.* **2013**, *2*, 8. [CrossRef] [PubMed]
152. Williams, S.F.; Martin, D.P.; Horowitz, D.M.; Peoples, O.P. PHA applications: Addressing the price performance issue: I. Tissue engineering. *Int. J. Biol. Macromol.* **1999**, *25*, 111–121. [CrossRef]
153. Gilmore, I.S.; Seah, M.P. Static SIMS: A study of damage using polymers. *Surf. Interface Anal. Int. J. Devoted Dev. Appl. Tech. Anal. Surf. 1996 Interfaces Thin Film.* **1996**, *24*, 746–762. [CrossRef]
154. Gilliam, K.D.; Paschke, E.E. BP Corporation North America Inc. Diisocyanate-Modified Polyesters as Hot Melt Adhesives and Coatings. U.S. Patent 4,166,873, 04 September 1979.
155. Doi, Y.; Tamaki, A.; Kunioka, M.; Soga, K. Production of copolyesters of 3-hydroxybutyrate and 3-hydroxyvalerate by Alcaligenes eutrophus from butyric and pentanoic acids. *Appl. Microbiol. Biotechnol.* **1988**, *28*, 330–334. [CrossRef]
156. Luzier, W.D. Materials derived from biomass/biodegradable materials. *Proc. Natl. Acad. Sci. USA* **1992**, *89*, 839–842. [CrossRef]
157. Scott, G. Why Degradable Polymers? In *Degradable Polymers*; Springer: Dordrecht, The Netherlands, 2002; pp. 1–15.
158. Lee, S.; Parthasarathy, R.; Botwin, K.; Kunneman, D.; Rowold, E.; Lange, G.; Klover, J.; Abegg, A.; Zobel, J.; Beck, T.; et al. Biochemical and Immunological Properties of Cytokines Conjugated to Dendritic Polymers. *Biomed. Microdevices* **2004**, *6*, 191–202. [CrossRef]
159. Shah, A.; Hasan, F.; Hameed, A.; Ahmed, S. A novel poly(3-hydroxybutyrate)-degrading *Streptoverticillium kashmirense* AF1 isolated from soil and purification of PHB-depolymerase. *Acta Biol. Hung.* **2008**, *59*, 489–499. [CrossRef]
160. Seng, W.P.; Tam, K.C.; Jenkins, R.D.; Bassett, D.R. Calorimetric studies of model hydrophobically modified alka-li-soluble emulsion polymers with varying spacer chain length in ionic surfactant solutions. *Macromolecules* **2000**, *33*, 1727–1733. [CrossRef]
161. Shah, A.A.; Hasan, F.; Hameed, A.; Ahmed, S. Isolation and characterization of poly(3-hydroxybutyrate-co-3-hydroxyvalerate) degrading bacteria and purification of PHBV depolymerase from newly isolated *Bacillus* sp. AF3. *Int. Biodeterior. Biodegradation* **2007**, *60*, 109–115. [CrossRef]
162. Molitoris, H.P.; Moss, S.T.; De Koning, G.J.M.; Jendrossek, D. Scanning electron microscopy of polyhydroxyalka-noate degradation by bacteria. *Appl. Microbiol. Biotechnol.* **1996**, *46*, 570–579. [CrossRef]
163. Whitchurch, P.C.; Bogdan, P.L.; Deak, T.E.; Trufanov, D.A. UOP LLC. Aromatic Isomerization Catalyst and a Process of Use Thereof. U.S. Patent 7939701, 10 May 2011.
164. Bachmann, B.M.; Seebach, D. Investigation of the enzymatic cleavage of diastereomeric oligo (3-hydroxybutanoates) containing two to eight HB units. A model for the stereoselectivity of PHB depolymerase from Alcali-genes faecalis T1. *Macromolecules* **1999**, *32*, 1777–1784. [CrossRef]
165. Shimamura, E.; Kasuya, K.; Kobayashi, G.; Shiotani, T.; Shima, Y.; Doi, Y. Physical properties and biodegradability of microbial poly (3-hydroxybutyrate-co-3-hydroxyhexanoate). *Macromolecules* **1994**, *27*, 878–880. [CrossRef]
166. Nakayama, K. Biological image motion processing: A review. *Vis. Res.* **1985**, *25*, 625–660. [CrossRef]
167. Mukai, K.; Yamada, K.; Doi, Y. Efficient hydrolysis of polyhydroxyalkanoates by *Pseudomonas stutzeri* YM1414 isolated from lake water. *Polym. Degrad. Stab.* **1994**, *43*, 319–327. [CrossRef]
168. Schober, B.J.; Pialet, J.W.; Pollack, R.A.; Clark, D.R. Lubrizol Corp. Polymeric Materials to Self-Regulate the Level of Polar Activators in Electrorheological Fluids. U.S. Patent 6,065,572, 23 May 2000.
169. Kalia, S.; Averous, L. *Biopolymers: Biomedical and Environmental Applications*; John Wiley & Sons: Hoboken, NJ, USA, 2011; Volume 70.
170. Abdel-Monem, M.O. Thermal Degradation of Polymers, SlideShare, Alexandria University Egypt. Available online: https://pt.slideshare.net/MohamedMahmoud443/thermal-degradation-of-polymers (accessed on 12 November 2017).
171. Kopinke, F.D.; Remmler, M.; Mackenzie, K.; Möder, M.; Wachsen, O. Thermal decomposition of biodegradable polyesters—II. Poly (lactic acid). *Polym. Degrad. Stab.* **1996**, *53*, 329–342. [CrossRef]
172. Gupta, M.; Deshmukh, V.G. Radiation effects on poly(lactic acid). *Polymer* **1983**, *24*, 827–830. [CrossRef]
173. Carrasco, F.; Pagès, P.; Gámez-Pérez, J.; Santana, O.O.; Maspoch, M.L. Processing of poly (lactic acid): Characterization of chemical structure, thermal stability and mechanical properties. *Polym. Degrad. Stab.* **2010**, *95*, 116–125. [CrossRef]
174. Hyon, S.H.; Jamshidi, K.; Ikada, Y. Effects of residual monomer on the degradation of DL-lactide poly-mer. *Polym. Int.* **1998**, *46*, 196–202. [CrossRef]
175. Wang, Y.; Steinhoff, B.; Brinkmann, C.; Alig, I. In-line monitoring of the thermal degradation of poly (l-lactic acid) during melt extrusion by UV–vis spectroscopy. *Polymer* **2008**, *49*, 1257–1265. [CrossRef]
176. McNeill, I.C.; Leiper, H.A. Degradation studies of some polyesters and polycarbonates—2. Polylactide: Degradation under isothermal conditions 1985, thermal degradation mechanism and photolysis of the polymer. *Polym. Degrad. Stab.* **1985**, *11*, 309–326. [CrossRef]
177. Jamshidi, K.; Hyon, S.-H.; Ikada, Y. Thermal characterization of polylactides. *Polymers* **1988**, *29*, 2229–2234. [CrossRef]
178. Södergård, A.; Stolt, M. Properties of lactic acid based polymers and their correlation with composition. *Prog. Polym. Sci.* **2002**, *27*, 1123–1163. [CrossRef]
179. Tsuji, H.; Fukui, I. Enhanced thermal stability of poly (lactide) s in the melt by enantiomeric polymer blending. *Polymer* **2003**, *44*, 2891–2896. [CrossRef]
180. Ohkita, T.; Lee, S.H. Thermal degradation and biodegradability of poly (lactic acid)/corn starch biocomposites. *J. Appl. Polym. Sci.* **2006**, *100*, 3009–3017. [CrossRef]

181. Persenaire, O.; Alexandre, M.; Degée, P.; Dubois, P. Mechanisms and Kinetics of Thermal Degradation of Poly(ε-caprolactone). *Biomacromolecules* **2001**, *2*, 288–294. [CrossRef]
182. Rattanapan, S.; Pasetto, P.; Pilard, J.F.; Tanrattanakul, V. Preparation and properties of bio-based polyurethane foams from natural rubber and Poly (ε-caprolactone) diol. *J. Polym. Res.* **2016**, *23*, 182. [CrossRef]
183. Saetung, A.; Kaenhin, L.; Klinpituksa, P.; Rungvichaniwat, A.; Tulyapitak, T.; Munleh, S.; Campistron, I.; Pilard, J.-F. Synthesis, characteristic, and properties of waterborne polyurethane based on natural rubber. *J. Appl. Polym. Sci.* **2012**, *124*, 2742–2752. [CrossRef]
184. Saetung, A.; Rungvichaniwat, A.; Campistron, I.; Klinpituksa, P.; Laguerre, A.; Phinyocheep, P.; Doutres, O.; Pilard, J.-F. Preparation and physico-mechanical, thermal and acoustic properties of flexible polyurethane foams based on hydroxytelechelic natural rubber. *J. Appl. Polym. Sci.* **2010**, *117*, 828–837. [CrossRef]
185. Chattopadhyay, D.K.; Webster, D.C. Thermal stability and flame retardancy of polyurethanes. *Prog. Polym. Sci.* **2009**, *34*, 1068–1133. [CrossRef]
186. Li, S.D.; He, J.D.; Yu, P.H.; Cheung, M.K. Thermal degradation of poly (3-hydroxybutyrate) and poly (3-hydroxybutyrate-co-3-hydroxyvalerate) as studied by TG, TG–FTIR, and Py–GC/MS. *J. Appl. Polym. Sci.* **2003**, *89*, 1530–1536. [CrossRef]
187. Aoyagi, Y.; Yamashita, K.; Doi, Y. Thermal degradation of poly [(R)-3-hydroxybutyrate], poly [ε-caprolactone], and poly [(S)-lactide]. *Polym. Degrad. Stab.* **2002**, *76*, 53–59. [CrossRef]
188. Melchiors, M.; Keul, H.; Höcker, H. Depolymerization of Poly[(*R*)-3-hydroxybutyrate] to Cyclic Oligomers and Polymerization of the Cyclic Trimer: An Example of Thermodynamic Recycling. *Macromolecules* **1996**, *29*, 6442–6451. [CrossRef]
189. Myung, J.; Strong, N.I.; Galega, W.M.; Sundstrom, E.R.; Flanagan, J.C.; Woo, S.G.; Waymouth, R.M.; Criddle, C.S. Disassembly and reassembly of polyhydroxyalkanoates: Recycling through abiotic depolymerization and biotic repolymerization. *Bioresour. Technol.* **2014**, *170*, 167–174. [CrossRef] [PubMed]
190. Flanagan, J.C.; Myung, J.; Criddle, C.S.; Waymouth, R.M. Poly (hydroxyalkanoate) s from waste biomass: A combined chemical–biological approach. *ChemistrySelect* **2016**, *1*, 2327–2331. [CrossRef]
191. Ariffin, H.; Nishida, H.; Hassan, M.A.; Shirai, Y. Chemical recycling of polyhydroxyalkanoates as a method towards sustainable development. *Biotechnol. J.* **2010**, *5*, 484–492. [CrossRef]
192. Hatti-Kaul, R.; Nilsson, L.J.; Zhang, B.; Rehnberg, N.; Lundmark, S. Designing Biobased Recyclable Polymers for Plastics. *Trends Biotechnol.* **2020**, *38*, 50–67. [CrossRef]
193. Otsuka, H.; Endo, T. Poly(hemiacetal ester)s: New Class of Polymers with Thermally Dissociative Units in the Main Chain. *Macromolecules* **1999**, *32*, 9059–9061. [CrossRef]
194. Morikawa, H.; Marchessault, R.H. Pyrolysis of bacterial polyalkanoates. *Can. J. Chem.* **1981**, *59*, 2306–2313. [CrossRef]
195. Kasirajan, S.; Ngouajio, M. Polyethylene and biodegradable mulches for agricultural applications: A review. *Agron. Sustain. Dev.* **2012**, *32*, 501–529. [CrossRef]
196. Jayanth, D.; Kumar, P.S.; Nayak, G.C.; Kumar, J.S.; Pal, S.K.; Rajasekar, R. A Review on Biodegradable Polymeric Materials Striving Towards the Attainment of Green Environment. *J. Polym. Environ.* **2018**, *26*, 838–865. [CrossRef]
197. Morro, A.; Catalina, F.; Sanchez-León, E.; Abrusci, C. Photodegradation and Biodegradation Under Thermophile Conditions of Mulching Films Based on Poly (Butylene Adipate-co-Terephthalate) and Its Blend with Poly (Lactic Acid). *J. Polym. Environ.* **2019**, *27*, 352–363. [CrossRef]
198. Gu, J.D.; Ford, T.E.; Mitchell, R. Microbial degradation of materials: General processes. In *Uhlig's Corrosion Handbook*; John Wiley and Sons: Hoboken, NJ, USA, 2011.
199. Schnabel, W. *Polymers and light: Fundamentals and Technical Applications*; John Wiley & Sons: Hoboken, NJ, USA, 2007.
200. Yousif, E.; Haddad, R. Photodegradation and photostabilization of polymers, especially polystyrene: Review. *Springerplus* **2013**, *2*, 1–32. [CrossRef]
201. Callao, M.P.; Larrechi, M.S. Simultaneous determination of organic dyes using second-order data. In *Data Handling in Science and Technology*; Elsevier: Amsterdam, The Netherlands, 2015; Volume 29, pp. 399–426.
202. Rauf, M.; Ashraf, S. Radiation induced degradation of dyes—An overview. *J. Hazard. Mater.* **2009**, *166*, 6–16. [CrossRef]
203. Wojnárovits, L.; Takács, E. Irradiation treatment of azo dye containing wastewater: An overview. *Radiat. Phys. Chem.* **2007**, *77*, 225–244. [CrossRef]
204. Akpan, U.G.; Hameed, B.H. Parameters affecting the photocatalytic degradation of dyes using TiO_2-based photocatalysts: A review. *J. Hazard. Mater.* **2009**, *170*, 520–529. [CrossRef]
205. Luo, Y.; Cao, Y.; Guo, G. Effects of TiO_2 nanoparticles on the photodegradation of poly(lactic acid). *J. Appl. Polym. Sci.* **2018**, *135*, 46509. [CrossRef]
206. França, D.C.; Morais, D.D.; Bezerra, E.B.; Araújo, E.M.; Wellen, R.M.R. Photodegradation Mechanisms on Poly (ε-caprolactone)(PCL). *Materials Research* **2018**, 21. [CrossRef]
207. Wellen, R.M.R.; Canedo, E.L.; Rabello, M.S.; Fechine, G.J.M. Photodegradation and Photostabilization of Poly(3-Hydroxybutyrate). *Mater. Res.* **2016**, *19*, 759–764. [CrossRef]
208. Han, W.; Luo, C.; Yang, Y.; Ren, J.; Xuan, H.; Ge, L. Free-standing poly (lactic acid)/chitosan/molybdenum disulfide films with controllable visible-light photodegradation. *Colloids Surf. A Physicochem. Eng. Asp.* **2018**, *558*, 488–494. [CrossRef]
209. Arrigo, R.; Dintcheva, N.T. Natural anti-oxidants for bio-polymeric materials. *Arch. Chem. Res.* **2017**, *1*, 1–4.

210. Pan, F.; Chen, L.; Jiang, Y.; Xiong, L.; Min, L.; Xie, J.; Qi, J.; Xiao, H.; Chen, Y.; Cornelis, F. Bio-based UV protective films prepared with poly (lactic acid) (PLA) and Phoebe zhennan extractives. *Int. J. Biol. Macromol.* **2018**, *119*, 582–587. [CrossRef] [PubMed]
211. Salač, J.; Šerá, J.; Jurča, M.; Verney, V.; Marek, A.A.; Koutný, M. Photodegradation and Biodegradation of Poly(Lactic) Acid Containing Orotic Acid as a Nucleation Agent. *Materials* **2019**, *12*, 481. [CrossRef]
212. Garrison, T.F.; Murawski, A.; Quirino, R.L. Bio-based polymers with potential for biodegradability. *Polymers* **2016**, *8*, 262. [CrossRef]
213. Artham, T.; Doble, M. Biodegradation of Aliphatic and Aromatic Polycarbonates. *Macromol. Biosci.* **2008**, *8*, 14–24. [CrossRef]
214. Business Wire. Global Biodegradable Polymers Market to 2030–End-Use, Type and Region–ResearchAndMarkets.com. [online]. 2022. Available online: https://www.businesswire.com/news/home/20220202005451/en/Global-Biodegradable-Polymers-Market-to-2030---by-End-use-Type-and-Region---ResearchAndMarkets.com (accessed on 2 November 2022).
215. Iwata, T. Biodegradable and bio-based polymers: Future prospects of eco-friendly plastics. *Angew. Chem. Int. Ed.* **2015**, *54*, 3210–3215. [CrossRef]